Materials Today Bio 14 (2022) 100249

Contents lists available at ScienceDirect

Materials Today Bio

journal homepage: www.journals.elsevier.com/materials-today-bio

Polymeric nanoparticles in the diagnosis and treatment of myocardial infarction: Challenges and future prospects

Mia Karam [a,b], Duaa Fahs [a,b], Batoul Maatouk [a,b], Brouna Safi [c], Ayad A. Jaffa [b,*], Rami Mhanna [a,**]

[a] Biomedical Engineering Program, Maroun Semaan Faculty of Engineering and Architecture, Lebanon
[b] Department of Biochemistry and Molecular Genetics, Faculty of Medicine, American University of Beirut, P.O. Box 11-0236, Beirut, Lebanon
[c] Department of Chemical Engineering, Maroun Semaan Faculty of Engineering and Architecture, Lebanon

ARTICLE INFO

Keywords:
Polymeric nanoparticles
Myocardial infarction
Diagnosis
Treatment
Theranostics
Table of contents

ABSTRACT

Myocardial infarction (MI) is the leading cause of morbidity and mortality worldwide. Despite extensive efforts to provide early diagnosis and adequate treatment regimens, detection of MI still faces major limitations and pathological MI complications continue to threaten the recovery of survivors. Polymeric nanoparticles (NPs) represent novel noninvasive drug delivery systems for the diagnosis and treatment of MI and subsequent prevention of fatal heart failure. In this review, we cover the recent advances in polymeric NP-based diagnostic and therapeutic approaches for MI and their application as multifunctional theranostic tools. We also discuss the *in vivo* behavior and toxicity profile of polymeric NPs, their application in noninvasive imaging, passive, and active drug delivery, and use in cardiac regenerative therapy. We conclude with the challenges faced with polymeric nanosystems and suggest future efforts needed for clinical translation.

1. Introduction

Myocardial infarction (MI), commonly known as a heart attack, most often arises during the unstable period of coronary atherosclerosis when the vascular wall is inflamed. It is responsible for irreversible myocardium damage including cardiomyocyte death and extracellular matrix (ECM) degradation due to prolonged ischemia [1]. It is the most prevalent type of cardiovascular diseases (CVD) and remains the leading cause of morbidity and mortality worldwide [2]. The early and accurate diagnosis of MI in patients is crucial for the initiation of adequate treatments to limit morbidity and mortality rates. The diagnosis of MI not only relies on the interpretation of the patient's history and electrocardiogram (ECG), but also on serum enzyme analysis and contrast agent-based enhanced imaging techniques. However, it is challenged by the enzyme immunoassays' low sensitivity and/or specificity and the contrast agent's rapid renal clearance and lack of tissue specificity [3]. Moreover, despite the significant progress in MI treatments, pathological ventricular remodeling continues to limit the recovery of survivors and trigger fatal heart failure. Conventional treatments aim to counteract a variety of pathological processes related to ischemia including oxidative stress, inflammation, and cardiomyocyte apoptosis to attenuate post-MI pathological remodeling and prevent heart failure [3]. These therapeutic approaches are challenged with the low bioavailability, stability, and blood circulation time of the therapeutic agents, their undesirable side-effects, and the costly procedures burdening the healthcare systems with an average of $18,953 per patient per year [4]. The above limitations and challenges can be addressed with the help of nanomedicine.

Nanomedicine is an advanced field that involves the application of biomaterials at the nanoscale, including polymeric nanoparticles (NPs), for imaging, sensing, and treatment of various diseases. NPs are evolving as potential candidates for diagnostic, therapeutic, and theranostic applications for MI. They can promote noninvasive and targeted delivery of imaging agents and/or bioactive molecules to overcome current limitations facing conventional diagnostic and therapeutic techniques for MI [5]. In this review we provide an overview of MI and polymeric NPs focusing on the development and application of polymeric NPs for the diagnosis, therapy, and theranostics of MI. We also discuss the clinical potential together with the challenges and limitations of these nanosystems and propose some needed studies required for the advancement of this field.

* Corresponding author.
** Corresponding author.
E-mail addresses: aj24@aub.edu.lb (A.A. Jaffa), rm136@aub.edu.lb (R. Mhanna).

https://doi.org/10.1016/j.mtbio.2022.100249
Received 13 January 2022; Received in revised form 28 March 2022; Accepted 30 March 2022
Available online 4 April 2022

2. Myocardial infarction and nanomedicine

2.1. Myocardial infarction: epidemiology, etiology, and pathophysiology

MI is the most severe and prevalent type of CVD and remains the leading cause of morbidity and mortality worldwide [6]. Each year, MI affects more than 7 million men and women, heavily burdening the economy with more than $450 billion spent annually due to patient hospitalizations [7]. Despite substantial improvements in patient care and lifestyle changes, MI still poses a threat to the global health accounting for 15% of the yearly worldwide mortality rate [7].

MI is most often caused by a spontaneous onset of ischemia due to partial or complete blockage in blood flow in one or more coronary arteries caused by plaque erosion and/or rupture, ulceration, or fissuring. This ultimately leads to a decreased blood supply and hence lack of oxygen in the irrigated myocardium leading to myocyte necrosis [8]. This ischemia-related MI is considered type 1 MI (Table 1) [8]. Type 2 MI also represents a spontaneous event however; the underlying cause of the observed ischemia is myocardial injury with necrosis due to an acute imbalance between oxygen supply and demand [8]. Type 3 MI represents sudden unexpected cardiac death, including cardiac arrest. It is often accompanied by signs and symptoms suggestive of myocardial ischemia or development of a fresh thrombus in a coronary artery detected by angiography and/or at autopsy [8]. On the other hand, types 4 and 5 of MI are termed periprocedural infarctions as they occur due to surgical interventions [9]. Type 4 MI is further divided into 4a and 4b, where 4a indicates an MI associated with percutaneous coronary intervention (PCI) characterized by a rise in cardiac troponin levels as well as symptoms suggestive of myocardial ischemia, new ECG changes, or new loss of viable myocardium among others. On the other hand, type 4b is related to thrombotic occlusion of a coronary stent determined by angiography or at autopsy, and accompanied by a rise and/or fall of cardiac biomarker levels [10]. Finally, type 5 MI is associated with coronary artery bypass grafting (CABG) distinguished by an elevation of cardiac biomarker values, as well as new native coronary artery occlusion, new loss of viable myocardium or new regional wall motion abnormality [10].

Immediately after MI, the ischemic insult causes severe systolic dysfunction, due to inhibition of contractile proteins, followed by ultrastructural changes in cardiomyocytes such as rapid depletion of adenosine triphosphate, reduction of cytoplasmic glycogen granules, and mitochondrial swelling [11]. These events lead to the loss of cardiomyocytes by necrosis and less often by apoptosis and autophagy, leading to the death of more than one billion cardiac cells [11]. As the adult human heart has negligible regenerative capacity, the damaged myocardium heals by forming a non-functional fibrotic tissue that replaces the normal contractile tissue to maintain the structural integrity of the left ventricle (LV). The healing process of the infarcted region follows 3 overlapping phases: acute inflammatory phase (1–7 days), proliferative/fibrotic phase (1–3 weeks), and scar maturation/ventricular remodeling phase (4 weeks or more) (Fig. 1) [11].

First, during the acute inflammatory phase, several innate immune pathways are activated by “danger signals” released by necrotic cardiomyocytes. These endogenous molecules termed alarmins trigger inflammation by activating pro-inflammatory signaling pathways such as Toll-like receptor and interleukin (IL)-1 in surviving cardiomyocytes, resident fibroblasts, endothelial cells, and leukocytes. For instance, stimulation of these pro-inflammatory signaling pathways leads to the activation of the nuclear factor kappa B which in turn promotes the transcription of pro-inflammatory cytokines and chemokines such as IL-1, IL-6, tumor necrosis factor alpha (TNF-α), and IL-8 [12]. The latter are released in the infarcted myocardium to attract and recruit neutrophils and monocytes to the injured region, and remove dead cardiomyocytes, apoptotic neutrophils, and matrix debris [12]. Moreover, CD14+/CD16-monocytes are mobilized from the bone marrow to the blood and recruited to the infarcted myocardium where they differentiate towards the “classically activated” pro-inflammatory M1 macrophages. Accordingly, they secrete pro-inflammatory cytokines as well as matrix metalloproteases (MMPs) to promote tissue digestion and necrotic debris phagocytosis [13]. The inflammatory phase is also characterized by alterations in the ECM as MMPs degrade collagen, elastin, and hyaluronan. The degradation products of these fibers can also trigger neutrophil, monocyte, and fibroblast infiltration further amplifying the inflammatory response. Matrix degradation is accompanied by provisional matrix deposition of fibrin/fibrinogen networks and platelet aggregates which provide a supportive scaffold for infiltrating immune cells and for migrating fibroblasts and endothelial cells [14]. The occurrence of these steps of the inflammatory phase in a tightly orchestrated manner is vital for the conservation of myocardial function. Defective signals leading to a prolonged inflammatory reaction or overexpansion of the inflamed area could result in the excessive death of cardiomyocytes and extreme degradation of the ECM [11].

Second, the proliferative or fibrotic phase takes place a few days after reperfusion to allow the heart to repair itself. At the beginning, the inflammatory reaction is suppressed and resolved to allow restoration of the geometrical structure and function of the injured area and reestablishment of the ECM. Accordingly, phagocytic cells are recruited to the infarct to remove all apoptotic neutrophils and remains of the ECM [15]. Moreover, M1 macrophages undergo a phenotypic switch towards the “alternatively activated” anti-inflammatory M2 macrophages. M2 cells inhibit inflammation by secreting anti-inflammatory cytokines such as IL-10 and transforming growth factor beta 1 (TGF-β1) [16,17]. Other leukocyte and lymphocyte subpopulations are also involved in this proliferative phase of repair. Dendritic cells, $CD4^+$ and $CD8^+$ T-cells, and natural killer cells contribute to the resolution of inflammation, scar tissue formation, and angiogenesis [18,19]. Resident cardiac fibroblasts are also activated to proliferate, acquire a matrix-synthetic phenotype, and transdifferentiate towards contractile myofibroblast-like cells [20]. Accordingly, myofibroblasts synthesize excessive amounts of structural and matricellular ECM proteins to provide physical support, regulate fibrinogenesis, and contribute to scar tissue formation. They also secrete anti-inflammatory molecules and pro-angiogenic factors to resolve inflammation and irrigate the ischemic regions of the infarcted myocardium, respectively [21]. The processes occurring during this phase are essential for the replacement of the necrotic cardiac tissue with a viable fibrotic scar. However, the extensive secretion and deposition of ECM proteins and the delay of its inhibition could lead to excessive

Table 1
Classification of myocardial infarction [8].

Classification		Definition
Type 1		Spontaneous MI caused by ischemia due to blood flow blockage in 1 or more coronary arteries caused by plaque erosion, rupture, ulceration, or fissuring
Type 2		Spontaneous MI caused by ischemia due to an acute imbalance between oxygen supply and demand
Type 3		Sudden unexpected cardiac death accompanied by symptoms suggestive of myocardial ischemia or development of a fresh thrombus in a coronary artery detected by angiography and/or at autopsy
Type 4	4a	MI associated with a PCI
	4b	MI associated with thrombotic occlusion of a coronary stent determined by angiography or at autopsy, accompanied by a rise and/or fall of cardiac biomarker levels
Type 5		MI associated with CABG distinguished by an elevation of cardiac biomarker values, native coronary artery occlusion, loss of viable myocardium or regional wall motion abnormality

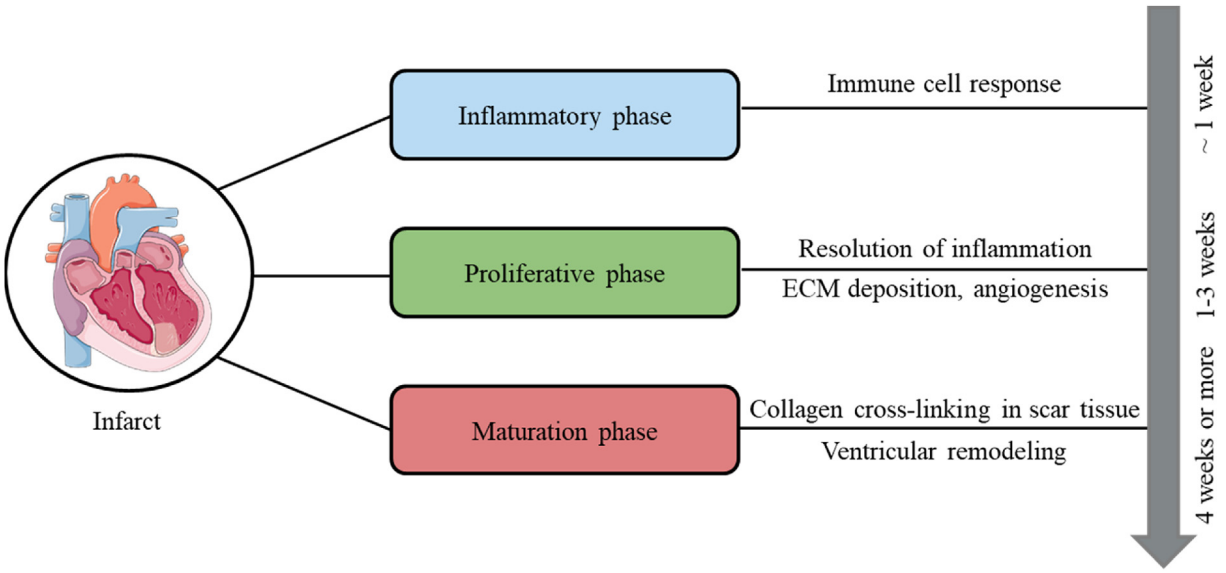

Fig. 1. Schematic representation of the temporal evolution of response to a myocardial infarct. Parts of the figure were drawn by using pictures from Servier Medical Art (http://smart.servier.com/), licensed under a Creative Commons Attribution 3.0 Unported License (https://creativecommons.org/licenses/by/3.0/).

fibrosis which risks disrupting the coordination of myocardial excitation-contraction coupling during systole and diastole, increasing the risk of heart failure [22].

Third, the scar maturation and ventricular remodeling phase concludes the healing process of the infarct by several mechanisms including regulation of ECM composition and ventricular remodeling. The ECM is reorganized by cross-linking of the newly synthesized collagen fibers and decrease of matricellular protein expression while the production of anti-fibrotic factors increases. In the scar tissue, angiogenesis is inhibited, and infarct myofibroblasts enter quiescence, undergo apoptosis, and/or stop secreting matrix proteins [11]. As the infarcted region undergoes a healing phase, the viable myocardium in remote regions of the LV undergoes dilatation to maintain an adequate cardiac output. However, the healing process overloads the non-infarcted cardiac regions with added pressure and volume promoting the re-emergence of inflammatory and fibrotic cells and causing extensive LV remodeling, which could lead to systolic dysfunction and fatal heart failure [23].

2.2. Current diagnostic and therapeutic approaches for MI and their limitations

Diagnosis of an MI by physicians typically starts by assessing the full medical history of patients and their clinical symptoms (angina pectoris, nausea, vomiting, sweating and heart palpitation). However, while medical history and physical examination of suspected MI patients is necessary for accurate patient triage and treatment, further tools are required to confer the diagnosis such as analysis of serum cardiac biomarkers like creatine kinase MB (CK-MB) and cardiac troponins (cTn). After an MI, serum levels of CK-MB, a cytosolic enzyme predominantly present in the myocardium, begin to increase at 3–6 h, reaching a peak of 5 to 20-fold their normal value at 12–24 h. Typically, serum CK-MB levels are detected by enzyme-linked immunosorbent assays, enzyme-linked fluorescent assays, chemiluminescence immunoassays, and time-resolved fluoroimmunoassays. While these methods have high sensitivity, accuracy, and clinical applicability, they remain expensive, time-consuming, and they are limited by their low analytical sensitivity and the background fluorescence interference [24]. Compared to CK-MB, cardiac troponins (cTn) are the most commonly detected enzymes as they are more sensitive and specific to acute MI [25]. The cTn group of proteins are regulatory proteins that control calcium-mediated actin--myosin interactions, resulting in contraction and relaxation of the cardiac muscle [26]. The cTn proteins are released in a biphasic manner into the serum 2–4 h after an MI reaching a peak at 24 h then maintaining elevated serum levels for up to 10 days. Their elevated concentrations in the serum are indicative of myocardial cell damage or necrosis and myofibrillar cTn degradation [27]. The most widely used assays for the detection and quantification of cTn are sandwich enzyme-linked immunosorbent assays which rely on the high specificity and affinity of specific cTn antibodies [28]. This technique however requires professional technicians, long procedures, and is limited by its detection efficiency, low analytical sensitivity, and false positives. As such, studies have been focused on developing rapid, reliable, and cost-effective tests for cTnI detection with improved detection limits and accuracy [29].

Imaging techniques are also adopted for accurate diagnosis of MI when the clinical symptoms of a suspected MI patient overlap with those of other conditions that lead to myocardial injury, risking an inadequate diagnosis. Imaging techniques include cardiovascular magnetic resonance (CMR), computed tomography (CT), and multimodal imaging. CMR offers a noninvasive approach to detect microvasculature stenosis, assess myocardial necrosis, and quantify the infarct size in acute MI. It also permits an adequate evaluation of the distinct stages of MI, post-MI LV remodeling, and other complications. CMR uses strong magnetic fields and relies on the body's natural magnetic properties to produce images of the heart. It has high spatiotemporal and contrast resolution that permits accurate and reproducible tissue characterization and multiplanar reconstruction, as well as differentiation between acute and chronic myocardial injury when coupled with delayed-enhancement technique [30]. However, CMR is associated with a high false-negative rate (~16%) which risks a misleading diagnosis [31]. Moreover, conventional contrast agents have several limitations such as low specificity, inconsistencies, and safety concerns. Due to their non-targeted nature, conventional contrast agents are passively absorbed into the damaged regions of the myocardium which translates into an enhancement that is not specific to MI but can be caused by other pathologies which may lead to misinterpretation and misdiagnosis [32]. Also, these gadolinium (Gd)-based contrast agents offer suboptimal reproducibility in the assessment and quantification of the infarct size [32]. Gd-based contrast agents are also labeled as unsafe for use in patients with renal disease as they have been linked to a rare but severe medical condition termed "nephrogenic systemic fibrosis" [33]. CMR is also a method with limited analysis of coronary artery stenosis and only allows a limited spatial coverage of the LV [34]. Another imaging modality widely requested by

physicians is CT. CT scan relies on delivering X-ray beams to the organ of interest and taking images from several angles to generate cross-sectional computerized images of the scanned bones, blood vessels, and soft tissues. Cardiac CT scan has evolved from diagnosis of coronary atherosclerosis to assessment of myocardial perfusion, ventricular function, as well as structural heart disease. When coupled with iodinated-based imaging agents, CT scan termed delayed enhancement CT can accurately diagnose both acute and chronic MI. In fact, delayed enhancement CT detects ischemic and viable myocardial regions as well as early perfusion defects which are evident by the reduced distribution of the contrast agent [35,36]. Nevertheless, CT scan is a costly procedure requiring exposure to high doses of ionizing radiation with a significant biological risk [37]. The intravenous (IV) exposure to the iodine-based contrast material has been associated with acute renal failure [38]. Moreover, CT scan has a low sensitivity for small vessels, and due to false positives, it is often associated with greater intervention rate for PCI and CABG without decreased MI [39]. Finally, multimodal imaging is adopted in MI diagnosis as it combines various techniques to simultaneously acquire different images and gather information regarding the functionality and morphology of the heart tissue [40]. For instance, single-photon emission computerized tomography (SPECT) can be combined with CT scan (SPECT-CT) to study MMP activity post-MI in the infarct and remote cardiac regions. This noninvasive technique helps track and quantify MMP activation in the injured myocardium and assess as such post-MI LV remodeling [41]. Moreover, positron emission tomography (PET)-CT and PET-MRI take advantage of PET's high sensitivity for cell tracking, MRI's excellent structural and functional tissue characterization, and CT's anatomical precision. PET-CT relying on ^{18}F- or ^{11}C-labeled molecular probes can help elucidate the pathophysiology underlying cardiac remodeling as well as study angiotensin II type I receptor expression in patients with chronic MI [42]. Moreover, PET-MRI has been adopted as a hybrid imaging technique which combines ^{18}F-fluorodeoxyglucose uptake and late gadolinium enhancement transmurality for better assessment of cardiomyocytes viability after an acute MI [43]. Multimodal imaging techniques are associated with some limitations such as low image quality, limited quantification of myocardial perfusion, exposure to high radiation dosages, limited spatial resolution, and limited visual assessment [44–46] (Table 2).

Conventional treatments for acute MI consist of reducing the risk of recurrent coronary thrombotic events and restoring vascular perfusion to the ischemic myocardium. Platelet activation, degranulation, and aggregation are important events that are complementary to the blood coagulation cascade and hence are tightly involved in thrombus formation. Antiplatelet drugs such as adenosine diphosphate P2Y12 receptor blockers and glycoprotein IIb/IIIa receptor blockers are typically prescribed to MI patients to disrupt the platelet aggregation pathway. Platelet aggregation disruption prevents thrombus formation and expansion of existing clots thus reducing the risk of a secondary ischemic event by 32% [47]. However, P2Y12 and glycoprotein IIb/IIIa receptor blockers are both costly medications with several limitations. The former shows a relatively slow onset of action following initiation of therapy [48]. Also, certain agents such as Cangrelor have a short half-life leading to the immediate abrogation of their inhibitory effects within minutes following IV administration [49]. These drugs have also been associated with a significant increase in the incidence of fatal or major bleeding [50]. Glycoprotein IIb/IIIa receptor blockers have also been associated with increased risk of minor and major bleeding as well as adverse reactions affecting the cardiovascular system by inducing hypotension and bradycardia, and the circulatory system by causing thrombocytopenia [51]. As patients having experienced an MI event are likely to experience a secondary MI even after antiplatelet treatment, a dual treatment of antiplatelet and anticoagulant drugs has been recommended for secondary prevention [52]. Oral anticoagulants target different mediators in the coagulation cascade, and they include vitamin K antagonists, direct factor Xa inhibitors, and direct thrombin inhibitors. However, anticoagulants have limited therapeutic potential due to their many disadvantages such as their narrow therapeutic window, low bioavailability, and associated side effects. Warfarin, a vitamin K antagonist, has a narrow therapeutic window requiring regular coagulation monitoring. It has been associated with several drug and food interactions, as well as an increased risk of bleeding [53], bruising, fatigue, and gastrointestinal adverse effects [54]. Direct factor Xa inhibitors such as Apixaban have been associated with dose-dependent increase in bleeding including bruising and hematoma [55]. Rivaroxaban has also been linked to some adverse reactions including hepatobiliary disorders, allergy and hypersensitivity reactions [56]. Direct thrombin inhibitors were also shown to increase hepatic enzyme levels which could be potentially harmful to patients. They are also limited by relatively low bioavailability, suboptimal pharmacokinetic properties, and inapplicability to patients with severe renal insufficiencies [57–59]. Other traditional pharmacological

Table 2
Major limitations of MI diagnostic imaging techniques.

Imaging technique	Limitations	Ref.
Creatine kinase MB assays	Expensive Time-consuming Low analytical sensitivity Background fluorescence interference	[24]
Cardiac troponin enzyme-linked immunosorbent assays	Professional technicians Long procedure Limited detection efficiency Low analytical sensitivity Risk of false positive results	[29]
Cardiovascular magnetic resonance	High false-negative rate Untargeted conventional contrast agents Suboptimal reproducibility of Gd-based contrast agents Toxicity of Gd contrast agents Limited analysis of coronary artery stenosis Limited spatial coverage of the left ventricle	[31–34]
Computed tomography	Costly procedure Exposure to high radiation dose Association of contrast material with acute renal failure Low sensitivity for small vessels Association of CT with greater intervention rate for PCI and CABG without decreased MI	[37–39]
Multimodal imaging	Low image quality Limited quantification of myocardial perfusion Exposure to high radiation dose Limited spatial resolution Limited visual assessment	[44–46]

approaches adopted to treat MI patients include β-blockers, angiotensin converting enzyme (ACE) inhibitors, and statins. Beta-blockers decrease myocardial oxygen consumption by lowering blood pressure and heart rate and reduce the infarct size and arrhythmogenesis by diminishing the neural and humoral sympathetic systems. They can also exert beneficial actions on the remote myocardium by reducing ventricular remodeling due to their anti-apoptotic, anti-inflammatory, and anti-fibrotic properties [60,61]. β-blockers' therapeutic effects are restricted by their low bioavailability, relatively short half-life, poor permeability, and adverse reactions which include irregular heart rate, bronchitis, and hepatitis [62,63]. Moreover, ACE inhibitors can reverse post-MI ventricular remodeling, decrease blood pressure, reduce cardiac hypertrophy and interstitial fibrosis, and overall decrease the mortality rate. Their beneficial effects are mediated by the decreased degradation of the potent vasodilator bradykinin and the decreased conversion of angiotensin I into angiotensin II, which further help attenuate their pro-apoptotic and pro-inflammatory activities [11]. Furthermore, statins mediate their effects mainly by reducing the production of low-density lipoproteins, which helps to prevent plaque formation and reduce mortality in MI patients. Statins also mediate their cardioprotective effects through attenuation of inflammation and suppression of MMP expression [64,65]. The use of ACE inhibitors and statins is however limited by several inconveniences. Ace inhibitors were found to be poorly tolerated by patients and linked to several side effects including angioedema, renal failure, and hypotension [66]. Statins exhibit limited water solubility and low bioavailability as they undergo extensive first-pass metabolism in the liver [67]. Studies also showed that treatment regimens with statins increase the risk of developing myopathy, type 2 diabetes mellitus, and hemorrhagic stroke. Statins also have several side effects such as memory loss, neuropathy, and an overall decrease of the quality of life [68].

Additionally, there are therapeutic strategies adopted to provide rapid and sustained restoration of blood flow in the coronary artery irrigating the ischemic myocardium to restore cardiac function and viability and relieve anginal symptoms. Thrombolytic therapy, also termed as fibrinolysis, has revolutionized the way patients with ST-elevation MI (STEMI) are treated and has been linked to a significant decrease in cardiovascular mortality. Thrombolytics including streptokinase and urokinase can rapidly lyse blood clots by cleaving plasminogen into the serine protease plasmin, which in turn cleaves the fibrin cross-links into soluble degradation products leading to complete thrombi dissolution [69,70]. Thrombolytic therapy is contraindicated however to 10.3% of patients who have been subjects of recent cardiopulmonary resuscitation, prior stroke or transient ischemic attack, or trauma. Moreover, certain fibrinolytic agents such as Lanetoplase and Saruplase have been linked to an increased risk of hemorrhagic strokes as well as increased reinfarction rates [69]. PCI, also known as coronary angioplasty, is a nonsurgical procedure which requires cardiac catheterization, where a guide catheter is introduced into the coronary artery in which a contrast agent is injected to visualize the blockage. Another catheter is then introduced with a balloon at its tip which is inflated to unclog the narrowed artery and restore blood flow. A stent implantation may also be required in order to relieve stenosis for a longer time [71]. PCI has become the preferred treatment modality for STEMI patients however, for patients whose coronary anatomy renders them ineligible for such an intervention, CABG surgery is adopted as the primary reperfusion modality [72]. CABG is a surgical intervention which involves bypassing an atheromatous blockage in coronary arteries with harvested arterial or venous conduits [73]. PCI and CABG are associated with several drawbacks. PCI is limited by its high costs, high in-hospital mortality, and lack of trained personnel [74]. Moreover, PCI is associated with severe post-surgical complications such as restenosis and stent thrombosis [75,76]. CABG is a costly procedure with several post-operative complications [77] such as atrial fibrillation, secondary surgical site infection, and neuropsychiatric complications [78–81] (Table 3).

2.3. Polymeric NPs: synthesis, in vivo behavior, and toxicity

Nanomedicine, defined as the application of nanotechnology in the healthcare system, has emerged to address unmet medical needs with a focus on cancer and CVDs. NPs, nanoemulsions, nanovesicles among others, have proven to be effective nanosystems for the safe and efficient treatment of CVDs such as MI as they help overcome limitations encountered in conventional drug delivery systems such as low drug bioavailability, undesired side effects, and systemic drug exposure. Accordingly, nanomedicine is proving to be the new solution for age-old problems [5].

NPs are solid colloidal particles with a size range of 10–1000 nm. They can be engineered with different compositions, sizes, shapes, and surface chemistries to enable their use in drug delivery applications, diagnostics, and imaging techniques. Active molecules such as pharmacological and imaging agents can be encapsulated or adsorbed onto the NPs' matrix. The advantage of designing NPs as delivery systems emerges from the ability to control their morphology, surface chemistry, pharmacokinetic and release properties [82–84]. NPs' characteristic small size helps them evade the immune system, reach specific tissues by size-dependent passive targeting, and extend their retention times within biological tissues [85].

Polymeric NPs are typically composed of biocompatible and/or biodegradable or inert materials such that the end-products are harmonious with the human body in terms of adaptability, lack of toxicity, carcinogenicity, and immunogenicity [86]. In general, polymeric NPs are characterized by their small size at the nanoscale, their relatively simple synthesis, and their high stability. They are also known for their ability to increase the stability of any volatile pharmaceutical agent with minimal alteration to its chemical composition and protect the carried drug as they are less reactive to enzymatic degradation [87]. Polymeric NPs are classified as nanospheres or nanocapsules based on their structure and preparation technique (Fig. 2). Nanospheres are matrix particles meaning that their entire mass is solid and molecules such as drugs or dyes can be covalently conjugated or adsorbed on their surface or uniformly dispersed within the NP. They tend to have a spherical shape however; "nanospheres" with an aspherical shape have also been described in the literature [88]. Nanocapsules on the other hand are vesicular systems with a core-shell structure. They consist of either oil or aqueous liquid cavity or "core" which can entrap the molecules of choice and a solid polymeric membrane or "shell" surrounding the core. As such, they act as "reservoirs" for the embedded molecules and serve as drug delivery systems (DDS) [89]. The term "polymeric nanoparticles" is also used to refer to polymeric micelles, drug-polymer conjugates, dendrimers (dendritic or branched NPs), polymersomes, and polyplexes, all of which are most often prepared from synthetic polymers [90].

Polymeric materials utilized to formulate NPs are either natural (extracted from bacteria, algae, plants, or animals) or synthetic (prepared by polymerization reactions beginning with monomeric units). Different polymers have been used to form polymeric NPs utilizing several synthesis techniques based on their application and the physicochemical attributes of the encapsulated agent [89]. The preparation techniques can be divided into two categories, namely, the bottom-up approach and the top-down approach [89]. The first category includes emulsion polymerization (1), mini- (2) and micro-emulsion polymerization (3), interfacial polymerization (4), and controlled radical polymerization (5) [91]. In the first method, water is used as a dispersion medium which is advantageous in terms of safety and heat removal control during the polymerization process. This general method is sub-categorized into conventional (1a) or surfactant-free (1b) emulsion polymerization [92]. (1a) involves the use of a continuous aqueous phase, monomers with low water-solubility which represent the reactive organic phase, a hydrophilic initiator typically an ion or a free radical, and an ionic surfactant. The synthesis process occurs by the initial formation of large monomer droplets upon dispersion of the monomers with the surfactant and water solution. Simultaneously, the excessive amounts of surfactant form

Table 3
Major limitations of MI therapeutic modalities.

Therapeutic modality		Limitations	Ref.
Antiplatelet drugs	P2Y12 receptor blockers	Costly medications Slow onset of action Short half-life following IV administration Increased incidence in fatal or major bleeding	[48–51]
	Glycoprotein IIb/IIIa receptor blockers	Increased risk of minor and major bleeding Adverse effects on cardiovascular, circulatory systems	
Anticoagulant drugs	Vitamin K antagonists	Narrow therapeutic window Drug and food interactions Increased risk of bleeding Side effects (bruising, fatigue …)	[53–59]
	Direct factor Xa inhibitors	Dose-dependent increase in bleeding events Adverse reactions (hepatobiliary disorders, allergy …)	
	Direct thrombin inhibitors	Increase hepatic enzymes levels Low bioavailability Suboptimal pharmacokinetic properties Inapplicability to patients with renal insufficiencies	
Beta-blockers		Low bioavailability Short half-life Poor permeability Adverse reactions (irregular heart rate, bronchitis …)	[62,63]
ACE inhibitors		Poorly tolerated by patients Side effects (angioedema, renal failure …)	[66]
Statins		Limited water solubility Low bioavailability Increased risk of myopathy, type 2 diabetes mellitus … Side effects (memory loss, neuropathy …) Decreased quality of life	[67,68]
Thrombolysis/fibrinolysis		Contraindicated to 10.3% of patients Increased risk of hemorrhagic strokes Increased reinfarction rates	[69]
PCI		High costs High in-hospital mortality Lack of trained personnel Limitation of mortality benefits to high-risk patients Severe complications (restenosis, stent thrombosis)	[74–76]
CABG		Costly procedure Postoperative complications (atrial fibrillation, secondary surgical site infection ….)	[78–81]

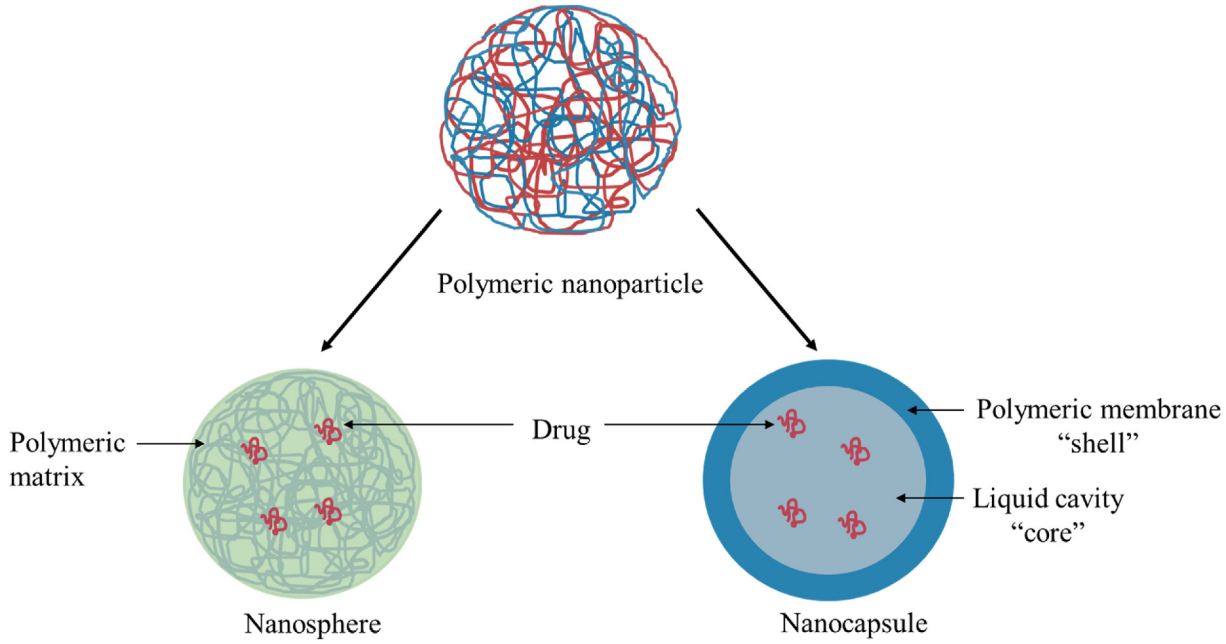

Fig. 2. Schematic representations of the two types of polymeric nanoparticles: nanospheres and nanocapsules. Parts of the figure were drawn by using pictures from Servier Medical Art (http://smart.servier.com/), licensed under a Creative Commons Attribution 3.0 Unported License (https://creativecommons.org/licenses/by/3.0/).

micelles in water. The polymerization reaction starts by diffusion of monomers from the large droplets to the micelles and by collision of the initiator molecule with these monomers in the micelles. This step of nucleation occurs within the self-organized monomer-swollen micelles and is then repeated continuously as more monomers migrate into the micelles. This promotes particle growth until formation of NPs which can then be phase-separated to obtain solid particles (Fig. 3) [92]. The size of the NPs is controlled by the choice of the surfactant. For instance, the use of nonionic surfactants such as Poloxamer 188, vitamin E TPGS, and Tween 80, typically leads to smaller NPs of 300 nm [93]. Technique (1b) emerged as a greener, faster, and simpler method for emulsion polymerization without the use of a surfactant. Accordingly, the stability of the emulsion is maintained by the use of ionizable initiators or ionic co-monomers. However, this technique still faces challenges regarding the preparation of monodisperse particles with a precisely controlled size [94].

The formation of mini-emulsions (2) is similar to the previous techniques in that it requires the use of water, monomers, a hydrophobic initiator, a surfactant, and a co-stabilizer. The main difference relies in the employment of a hydrophobic co-stabilizer with a low molecular mass and the use of a high-shear device such as ultrasound to ensure the emulsification (Fig. 4). This technique is versatile and allows the formation of core-shell NPs and nanotubes [95].

Micro-emulsion polymerization (3) consists of adding a water-soluble initiator molecule to vinyl monomers in a thermodynamically stable aqueous phase of micro-emulsions and relies on high quantities of surfactant which completely cover the formed particles and form an interfacial film. This leads to the formation of stable colloidal NPs termed "latex" with a size less than 100 nm (Fig. 5) [96].

Other hetero-phase polymerization techniques are less often employed for the preparation of polymeric NPs. Method (4) consists of step polymerization of two reactive monomers which are dissolved respectively in continuous and dispersed phases. Polymerization takes place at the interface of these two immiscible liquids and allows the formation of nanocapsules. A membrane reactor can be used during this process to promote size control and facilitate the separation of products from reaction mixtures (Fig. 6) [97].

Method (5) is an environmentally friendly technique that controls the characteristics of the obtained NPs in terms of molar mass distribution, architecture, and function. It involves 3 steps: polymerization reaction initiation, propagation of the growing polymer chain, and termination of the reaction. The end-product is then subject to a disproportionation reaction whereby it converts to two separate compounds, one of higher and one of lower oxidation state. Otherwise, the polymer undergoes a combination reaction whereby it is combined with other polymers to form a new single compound (Fig. 7) [98].

The top-down approach for synthesizing polymeric NPs involves dispersion of premade polymers to form nanostructures. It is performed via different techniques including solvent-evaporation (1), salting-out (2), nanoprecipitation (3), dialysis (4), and supercritical fluid technology (SCF) (5). Technique (1) is the most widely used for synthesis of polymeric NPs. It consists of forming single (oil-in-water or water-in-oil) or double emulsions ((water-in-oil)-in-water or (oil-in-water)-in-oil) where the polymer of choice is often dissolved in an organic solvent to form the oil phase. Homogenization of the immiscible phases is attained by high-speed homogenization or ultrasonication which breaks the emulsions into smaller ones. Then the organic solvent is left to evaporate and reach a point of insolubility to promote NPs solidification (Fig. 8). The NPs are collected by ultracentrifugation, washed to remove any residual surfactant, and lyophilized. The concentration of the polymer,

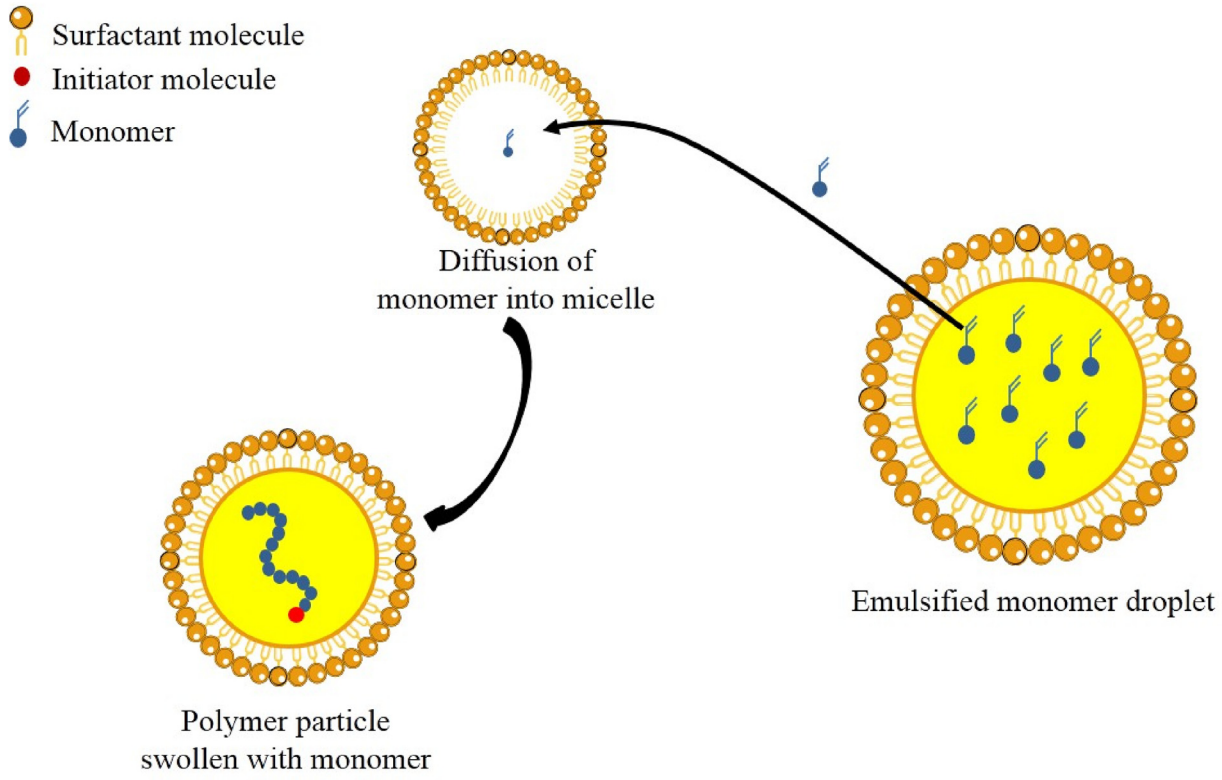

Fig. 3. Schematic representation of the preparation of polymeric nanoparticles by the emulsion polymerization technique. Dispersion of monomers with the surfactant and water solution leads to the formation of large monomer droplets. The excessive amounts of surfactant also form micelles in water. Polymerization starts by diffusion of monomers from the large monomer droplets to the micelles. Afterwards, nucleation occurs by collision of the initiator molecule with the monomers within the micelles and is repeated continuously as more monomers migrate into the micelles to form a polymer particle. Parts of the figure were drawn by using pictures from Servier Medical Art (http://smart.servier.com/), licensed under a Creative Commons Attribution 3.0 Unported License (https://creativecommons.org/licenses/by/3.0/).

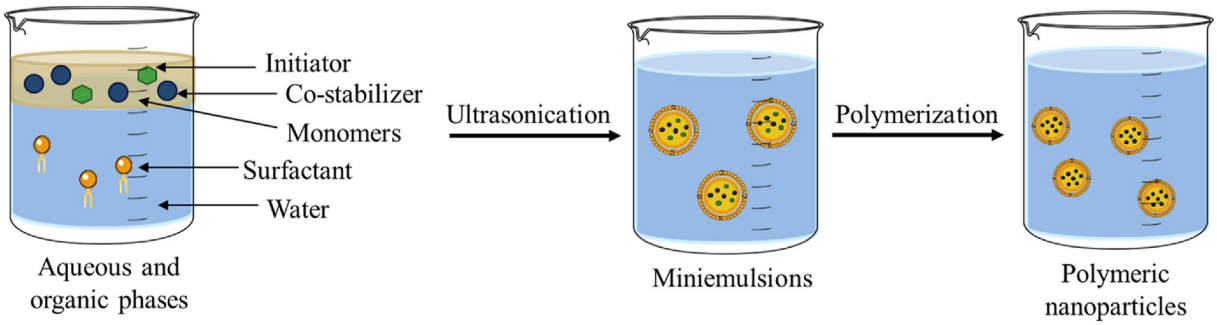

Fig. 4. Schematic representation of the preparation of polymeric nanoparticles by the mini-emulsion polymerization technique. The reaction mixture consisting of monomers, surfactant, co-stabilizer, and initiator, is miniemulsified by ultrasonication to form stable monomer droplets. Nucleation occurs by collision of the initiator with the monomers within the droplets and is repeated continuously throughout polymerization. Parts of the figure were drawn by using pictures from Servier Medical Art (http://smart.servier.com/), licensed under a Creative Commons Attribution 3.0 Unported License (https://creativecommons.org/licenses/by/3.0/).

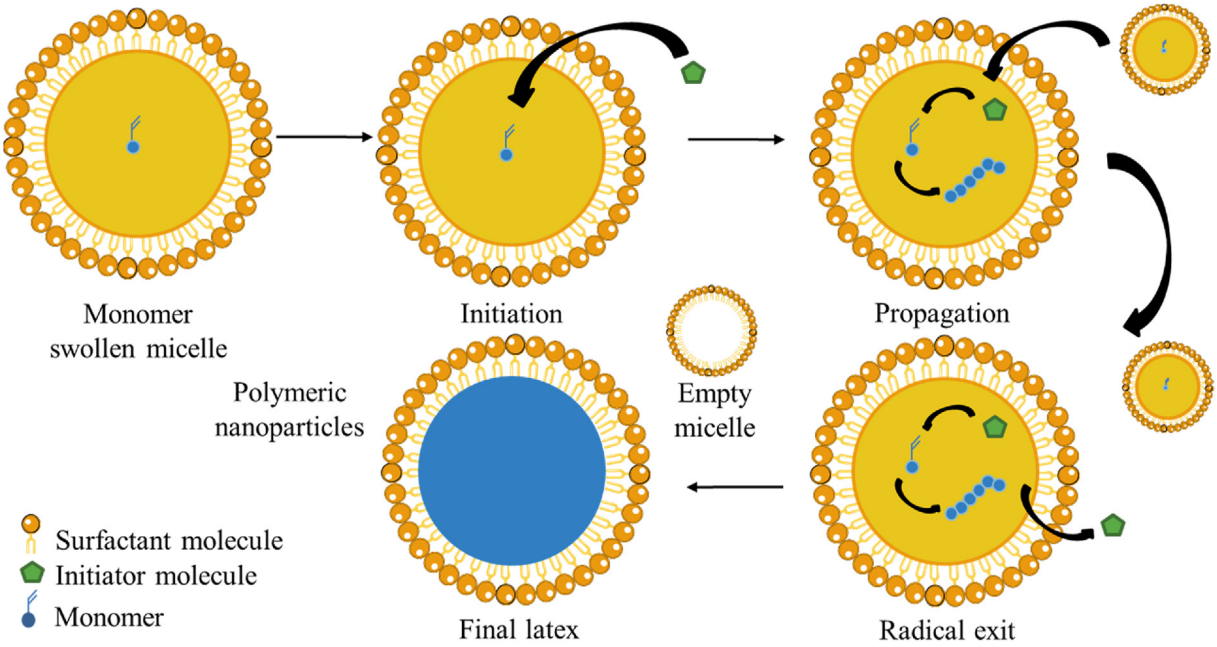

Fig. 5. Schematic representation of the preparation of polymeric nanoparticles by the micro-emulsion polymerization technique. The reaction mixture of vinyl monomers and surfactant is microemulsified to form micelles. Initiators collide with the monomers to start the nucleation and form polymer particles. The nucleated particles continue to grow by diffusion of monomers from other inactive micelles. The polymer particles continue growing until depletion of the micelle reservoir and formation of the final latex. Parts of the figure were drawn by using pictures from Servier Medical Art (http://smart.servier.com/), licensed under a Creative Commons Attribution 3.0 Unported License (https://creativecommons.org/licenses/by/3.0/).

organic solvent, and surfactant as well as sonication parameters affect the NPs size distribution [93].

As organic solvents are often associated with some degree of toxicity, an alternative method was developed which eliminates the use of chlorinated solvents. This method termed "salting-out" (2) requires emulsifying an organic phase, containing the polymer and solvent of choice, and an aqueous phase, containing a stabilizer and a salting-out agent, without the use of high-shear forces. Emulsion of the two phases occurs by the action of high concentrations of the salting-out agent. To precipitate the formed NPs, a reverse salting-out technique is used whereby the oil-in-water emulsion is dissolved in an excessive volume of water. Upon addition of water, the salting-out agent's concentration decreases inducing the migration of the solvent from the emulsion droplets to the aqueous phase and hence complete removal of the solvent (Fig. 9). Small size (<500 nm) and spherical polymeric NPs can be obtained by this method and they include poly (lactic acid) and poly (lactic-co-glycolic acid) (PLGA) [99].

Nanoprecipitation (3) involves the formation of an oil-in-water or water-in-oil emulsion under moderate magnetic stirring followed by removal of the solvent under reduced pressure. In an oil-in-water emulsion, a lipophilic solution consisting of a polymer and a semi-polar organic solvent is slowly added dropwise under magnetic stirring to an aqueous solution containing a stabilizing agent (Fig. 10). NPs are formed instantaneously by the Marangoni effect [100]. The characteristics of the obtained NPs are influenced by the aqueous phase agitation rate, organic phase injection rate, and the organic phase/aqueous phase ratio. Overall, this is a relatively easy and rapid technique that produces NPs with narrow size distribution [101].

The dialysis technique (4) is another simple and fast method for producing polymeric NPs. It is based on the dissolution of a lipophilic polymer in a water miscible organic solvent followed by transfer of this solution to a dialysis membrane with adequate molecular weight cut-off. This semi-permeable membrane is placed in a beaker containing an aqueous solution that is miscible with the organic solvent but not with the polymer. The organic solvent diffuses into the aqueous solution by osmosis leading to progressive polymer aggregation due to loss of solubility and hence formation of NPs (Fig. 11). The choice of organic solvent affects the NPs' size and morphology. Dimethylsulfoxide often allows the

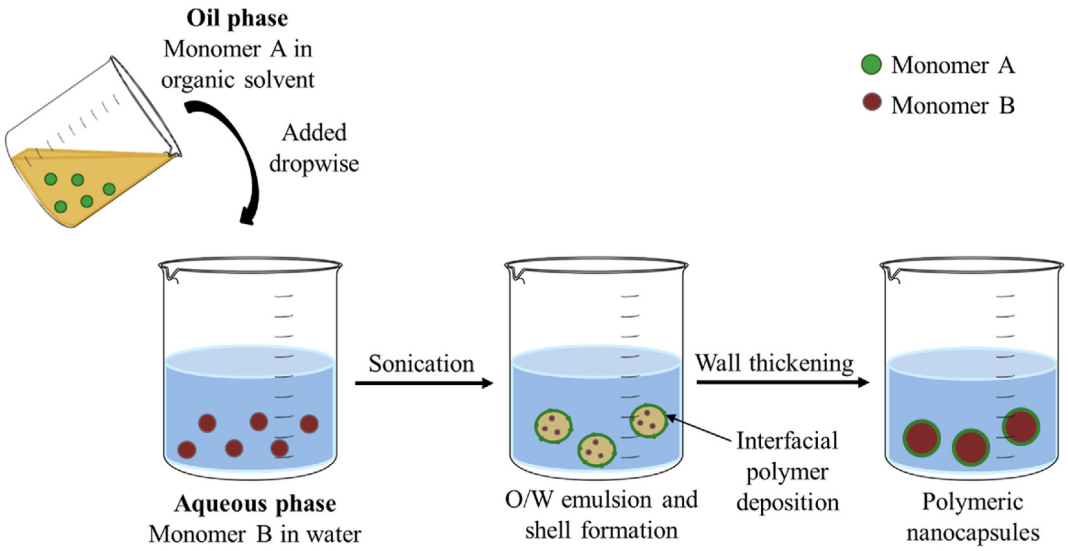

Fig. 6. Schematic representation of the preparation of polymeric nanoparticles by the interfacial polymerization technique. Two reactive monomers dissolved respectively in organic and aqueous solutions are emulsified by sonication to form O/W emulsions. The polymerization reaction takes place at the interface of the two immiscible liquids, promotes wall thickening and allows the formation of nanocapsules. Parts of the figure were drawn by using pictures from Servier Medical Art (http://smart.servier.com/), licensed under a Creative Commons Attribution 3.0 Unported License (https://creativecommons.org/licenses/by/3.0/).

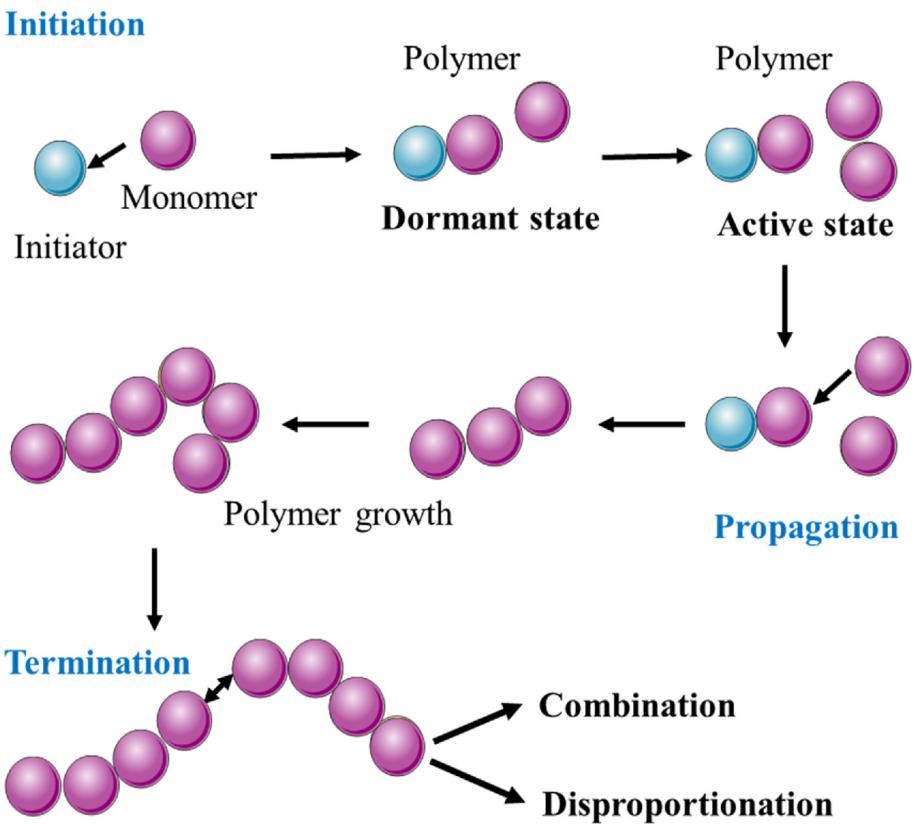

Fig. 7. Schematic representation of the preparation of polymeric nanoparticles by the controlled radical polymerization technique. Initiation begins as cleavage of the initiator generates a reactive free radical which reacts with the monomer. The monomer is hence activated from its dormant state. During the propagation phase additional molecules of monomer are added in a sequential manner to produce a growing polymer chain. Termination occurs when two free radicals react to form a stable non-radical adduct. The end-product is then subject to a combination or disproportionation reaction. Parts of the figure were drawn by using pictures from Servier Medical Art (http://smart.servier.com/), licensed under a Creative Commons Attribution 3.0 Unported License (https://creativecommons.org/licenses/by/3.0/).

formation of spherical particles with a size less than 450 nm [102,103].

Finally, SCF technology (5) is divided into 2 subtypes: rapid expansion of supercritical solution (RESS) and rapid expansion of supercritical solution into a liquid solvent (RESOLV). SCF technology is based on the use of supercritical fluids as safer and more environmentally friendly solvents. Supercritical fluids combine favorable properties of liquids and gases such as liquid-like density and gas-like viscosity and they include water, carbon dioxide (CO_2), and ammonia [104]. RESS involves pumping supercritical fluids such as CO_2 to a high-pressure stainless steel mixing cell containing the polymer of choice. SCF-CO_2 dissolves the polymer, and the resulting solution is pushed via a syringe pump to a pre-expansion unit where it is heated isobarically to the desired supercritical temperature. The solution is then depressurized through a heated capillary nozzle at supersonic speed from which it can expand at ambient temperature into an expansion vessel. This rapid pressure reduction during expansion causes a high degree of polymer supersaturation and leads to the formation of well-dispersed particles by nucleation (Fig. 12a). Particle size and morphology are affected by polymer's

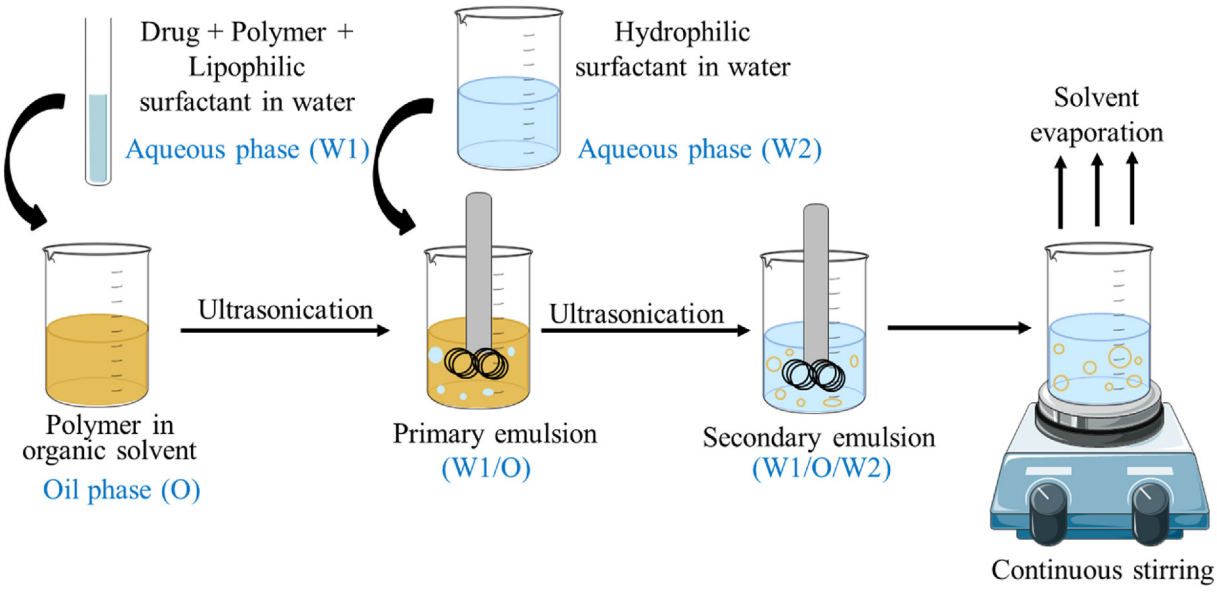

Fig. 8. Schematic representation of the preparation of w/o/w double emulsion nanoparticles by the solvent evaporation technique. An aqueous phase (W1) consisting of the drug, polymer, and lipophilic surfactant is emulsified by ultrasonicaton with an oil phase (O) containing a polymer dissolved in an organic solvent. A second aqueous phase (W2) containing a hydrophilic surfactant is then added dropwise to the primary emulsion and further emulsified by ultrasonication. The obtained double emulsion is left on a stirrer to allow solvent evaporation and solidification of the polymeric NPs. Parts of the figure were drawn by using pictures from Servier Medical Art (http://smart.servier.com/), licensed under a Creative Commons Attribution 3.0 Unported License (https://creativecommons.org/licenses/by/3.0/).

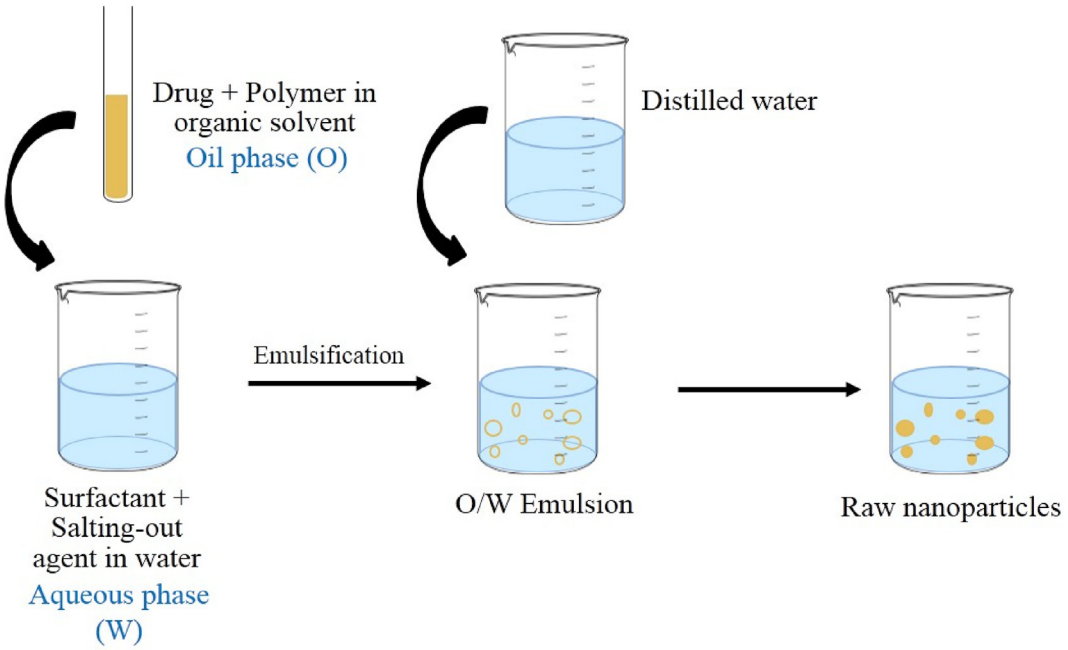

Fig. 9. Schematic representation of the preparation of o/w emulsion nanoparticles by the salting-out technique. An oil phase (O) containing the drug and polymer of choice is emulsified with an aqueous phase (W) consisting of a surfactant and salting-out agent added at high concentration. An excessive volume of distilled water is added to the O/W emulsion to precipitate the NPs. Parts of the figure were drawn by using pictures from Servier Medical Art (http://smart.servier.com/), licensed under a Creative Commons Attribution 3.0 Unported License (https://creativecommons.org/licenses/by/3.0/).

concentration and degree of saturation [105]. RESOLV is a variation of the above technique where the supercritical solution is expanded into a liquid solvent instead of ambient air. The liquid solvent is placed in a chamber at ambient temperature and is carefully chosen such that it is immiscible with the polymer used to allow precipitation of the NPs (Fig. 12b) [106].

NPs intended for treatment of MI during the early stages of remodeling can be administered via intracoronary, intramyocardial, or IV injections, depending on their cargo, blood circulation time, and targeting ligands. Intramyocardial injection of polymeric NPs proved to be the most effective route to ensure localization of NPs to the site of injury with minimal systemic side effects. However, its invasive nature renders it unlikely to translate to clinical applications since it is associated with the risk of systemic embolization, tissue perforation at the injection sites inside the LV, and tissue irritation which could lead to cardiac arrhythmias [107]. Conversely, IV injection of NPs was proven to be the ultimate

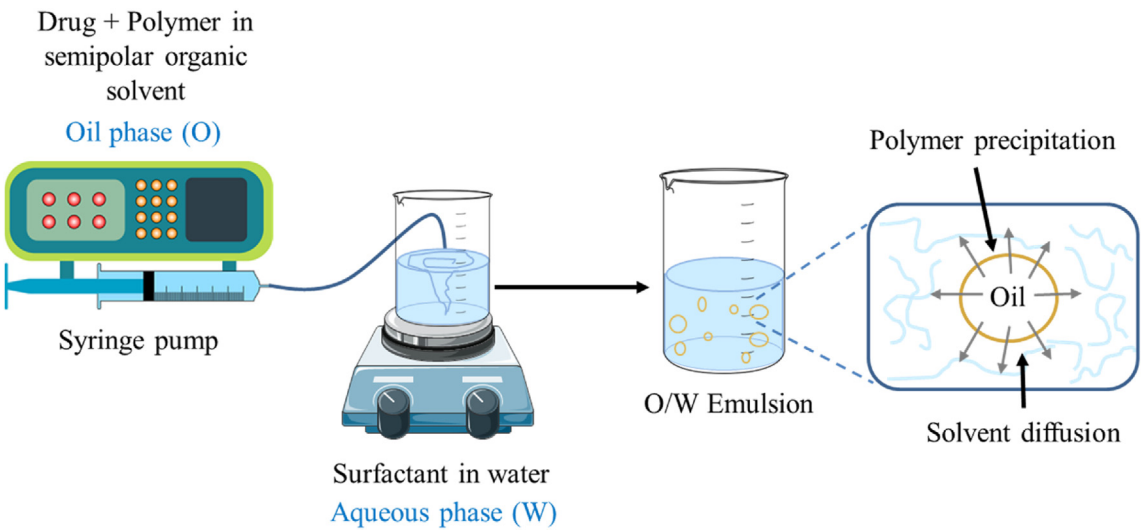

Fig. 10. Schematic representation of the preparation of o/w emulsion nanoparticles by the nanoprecipitation technique. An oil phase (O) consisting of the drug and polymer dissolvent in a semipolar organic solvent is slowly added via a syringe pump to an aqueous solution (W) containing a surfactant. NPs are formed upon precipitation of the polymer and diffusion of the organic solvent. Parts of the figure were drawn by using pictures from Servier Medical Art (http://smart.servier.com/), licensed under a Creative Commons Attribution 3.0 Unported License (https://creativecommons.org/licenses/by/3.0/).

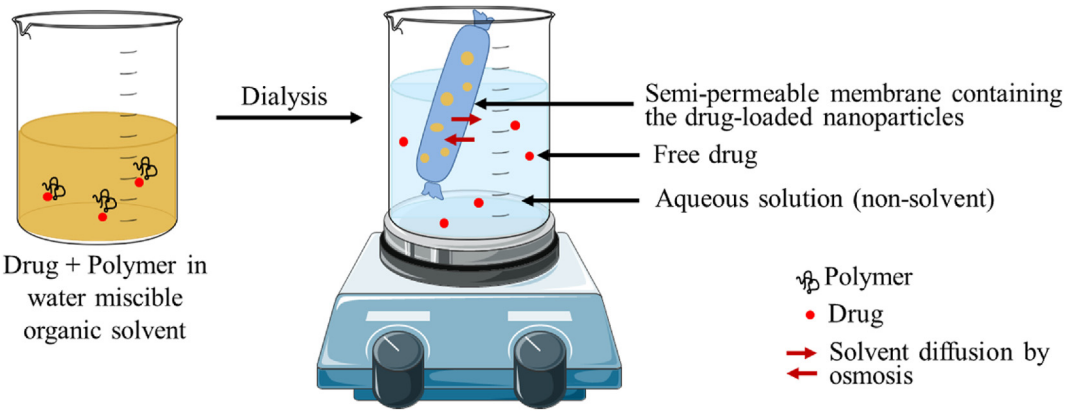

Fig. 11. Schematic representation of the preparation of polymeric nanoparticles by the dialysis technique. A lipophilic polymer is dissolved along with the drug of choice in a water miscible organic solvent. The solution is then transferred to a semi-permeable dialysis tubing which is placed in an aqueous solution non-miscible with the polymer. Upon diffusion of the organic solvent to the aqueous phase by osmosis, the polymer aggregates and allows the formation of NPs. Parts of the figure were drawn by using pictures from Servier Medical Art (http://smart.servier.com/), licensed under a Creative Commons Attribution 3.0 Unported License (https://creativecommons.org/licenses/by/3.0/).

minimally invasive technique that promotes passive targeting of nanomaterials to the injured myocardium. Passive targeting is feasible due to the increased vascular permeability in the post-MI myocardium, reduced microvascular flow, loss of cardiomyocytes, and cross-linking of ECM components. These mechanisms promote an enhanced permeability and retention (EPR) effect. Consequently, polymeric NPs take advantage of their small size (20–200 nm) to accumulate preferentially in the infarcted myocardium where they are retained for a longer period compared to other organs. Accordingly, systemic distribution and internalization of NPs is size-dependent and organ-specific in inflammatory conditions confirming the EPR effect in MI [108–110]. Similarly, intracoronary infusion of nanomaterials exploits the EPR effect and allows passive targeting towards the injured heart. While this administration route has proven to be effective, it remains an invasive technique that requires the use of catheters and is therefore less favorable than IV injections [107].

After IV or intracoronary infusion, polymeric NPs are transported in blood vessels to reach their target. Studies have shown that NPs interact with blood components including red blood cells, platelets, plasma proteins, and white blood cells while migrating. Unlike inorganic NPs, polymeric NPs do not significantly influence red blood cells interaction [111]. However, plasma proteins such as albumin, fibrinogen, complement proteins, and immunoglobulins tend to bind to polymeric NPs and have distinct effects on their *in vivo* fate. Binding of albumin to NPs' surface shields them from leukocyte recognition and decreases their uptake, while binding of other proteins to NPs promotes their opsonization, phagocytic uptake, and induces inflammatory reactions [112]. While binding of NPs to albumin helps them evade the immune system, certain polymeric NPs activate immune cells. Chitosan NPs induce leukocyte secretion of pro-inflammatory cytokines such as IL-18 and IL-1β, while PLGA NPs induce neutrophils activation and degranulation [113,114]. Upon systemic administration, polymeric NPs tend to accumulate preferentially within inflammatory tissues with leaky vasculature such as the case post-MI by EPR-mediated passive targeting. NPs biodistribution is not limited however to the target tissue as many get distributed to the immune system [115]. Moreover, a study on ischemia/reperfusion (I/R) murine model of MI demonstrated that IV injected poly (ethylene glycol) (PEG) coated polystyrene NPs of 20–200 nm rapidly accumulate within the infarcted LV with significantly higher

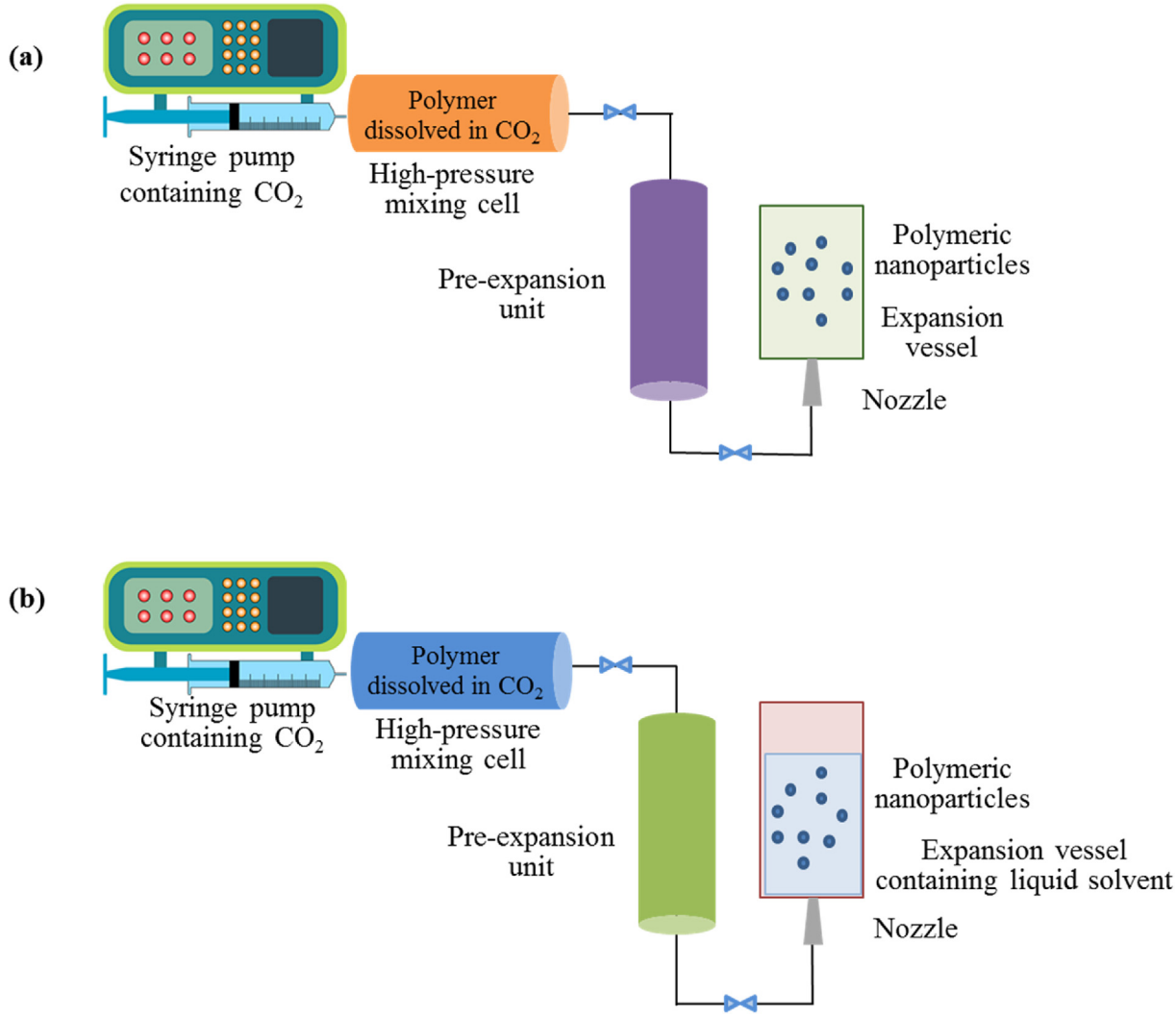

Fig. 12. Schematic representation of the preparation of polymeric nanoparticles by the supercritical fluid technique: RESS (a) and RESOLV (b). (a) An SCF such as CO_2 is pumped to a high-pressure mixing cell containing the polymer of choice. SCF-CO_2 dissolves the polymer, and the solution is pushed to a pre-expansion unit where it is heated isobarically to the supercritical temperature. The solution is then depressurized through a nozzle from which it can expand into an expansion vessel and promote formation of NPs by nucleation. (b) An SCF such as CO_2 is pumped to a high-pressure mixing cell containing the polymer of choice. SCF-CO_2 dissolves the polymer, and the solution is pushed to a pre-expansion unit where it is heated isobarically to the supercritical temperature. SCF is expanded into a liquid solvent immiscible with the polymer which promotes precipitation of the NPs. Parts of the figure were drawn by using pictures from Servier Medical Art (http://smart.servier.com/), licensed under a Creative Commons Attribution 3.0 Unported License (https://creativecommons.org/licenses/by/3.0/).

retention rate compared to sham-operated controls. Expectedly, low NPs concentration was detected in the brain due to the blood-brain barrier. High concentrations of NPs were retained in the spleen, liver, lungs, and kidneys, especially larger NPs (≥200 nm). This further proves that NPs with an average size less than 200 nm are ideal for passive targeting to the heart with minimal systemic distribution [108]. As a final step, polymeric NPs that evaded the mononuclear phagocytic system in the liver and spleen are excreted by the kidneys. They are then taken up by the glomerular or peritubular capillaries and finally eliminated from the body by renal clearance [116].

Despite the high potential of polymeric NPs in drug delivery applications, it is crucial to take into consideration their possible toxic effects. Many factors could influence nanomaterial's toxicity and biocompatibility and they should be studied before applying nanomaterials in biomedicine. These factors include the size of NPs, their shape, and their surface properties such as surface charge and surface energy (hydrophobicity/hydrophilicity) [117]. Due to their small size that is comparable to the size of globular proteins, NPs can penetrate capillaries and reach different tissues that are normally inaccessible to larger particles, which could result in increased interaction with resident cells and potential cytotoxic effects. Also, their nanosize provides them with higher surface area to volume ratio which translates to an enhanced reactivity and cytotoxicity as more chemical compounds can be adsorbed onto their surface. Xu et al. developed NPs out of block copolymers (monomethoxy (polyethylene glycol)-*b*-P (D,L-lactic-*co*-glycolic acid)-*b*-P (L-glutamic acid)) (mPEG-PLGA-PGlu) for the delivery of Doxorubicin, a chemotherapeutic agent with known cardiotoxicity. They found that mPEG-PLGA-PGlu NPs of 100–200 nm did not exhibit any cardiac or hepatic toxicity [118]. On the contrary, smaller PLGA NPs of 60 nm were found to disrupt cytosolic calcium homeostasis and trigger an inflammatory response [119]. NPs' morphology also affects their cytotoxicity. Elongated rod- and needle-shaped PLGA-PEG NPs were found to induce significant toxicity in human cell lines by disrupting the lysosomes after endocytosis-mediated internalization and leading eventually to DNA damage and apoptosis. On the other hand, spherical NPs safely entered cells without causing any damage indicating their safe usage [120]. NPs

surface charge is another important factor to be considered. Cationic NPs are more likely to activate the immune system and cause damage to the cell membrane than their anionic counterparts due to the electrostatic interaction between the positively charged NPs and the negatively charged cell membrane. Anionic and neutral NPs are more likely to enter cells in a safe manner by clathrin- or caveolae-mediated endocytosis without disrupting the cell membrane. Also, NPs with a neutral surface charge are less prone to opsonization than charged NPs [117]. Other important factors include the NPs' surface topography, crystallinity, concentration, coating, and level of degradation products [117]. The overall desired characteristics of NPs which confer minimal to no toxicity are summarized in Fig. 13. Overall, bare and small NPs have higher toxicity than modified and bulk materials, respectively. Also, NPs with a spherical morphology are less toxic than the ones with a rod or elongated shape [117]. Coating NPs with hydrophilic and biocompatible polymers such as PEG and chitosan, or with natural proteins such as albumin, can attenuate cytotoxicity by "hiding" the NPs from the immune system [82, 121].

The size of polymeric NPs strongly determines the mechanism by which they enter cells. NPs with a size of 200 nm or less enter cells by clathrin- and caveolae-mediated endocytosis while larger particles typically rely on macropinocytosis or phagocytosis [122]. Moreover, smaller NPs of <25 nm penetrate cells and reach perinuclear regions via a cholesterol-independent pathway instead of the conventional endosomal/lysosomal pathway [123]. However, positively charged polymeric NPs most often penetrate cells in a more disruptive way by damaging the phospholipid bilayer of the cell membrane and inducing nanoscale holes that can enhance conductance through the membrane [124]. Studies also showed that NPs used at high concentrations may disrupt cellular organelles causing malfunctions in the mitochondria and lysosomes leading to disturbances in normal cellular metabolism and autophagy, respectively; inducing damages in the structure of the actin network compromising the cytoskeleton integrity and normal cell division, or inhibiting DNA transcription and inducing oxidative damage [125–128]. Cationic polymeric NPs such as amino-modified polystyrene NPs disrupt the glutathione metabolism and damage the cell membrane which may then lead to cell apoptosis [128]. Although polymeric NPs are widely used for the delivery of anti-inflammatory drugs, some cationic polymers such as poly (ethylene imine) (PEI) elicit an inflammatory response by activating toll like receptor 5-mediated cytokines release and upregulating IL-8 [129]. Importantly, NPs can be exploited for their toxic effects on bacteria whereby they were found to interact with proteins and induce their inactivation, modify their target ligands, or even eliminate infectious proteins [130]. All the mentioned mechanisms of NPs cytotoxic effects are summarized in Fig. 14.

3. Polymeric NPs for the diagnosis of MI

Early detection and diagnosis of MI are crucial for the establishment of an adequate therapeutic strategy, reduction of myocardial damage and salvation of cardiac function. Different cardiac imaging techniques are adopted for the diagnosis of MI however; contrast agents essential for the accurate differentiation of the myocardium tissue from the cardiac lumen remain a major area for improvement. To enhance diagnostic accuracy and specificity, various molecular and cellular imaging techniques based on polymeric NPs have been shown to provide promising results (Table 4).

3.1. Polymeric NPs-mediated delivery of cardiac biomarkers for MI diagnosis

Immunoassays for the detection of serum CK-MB and cTnI are still

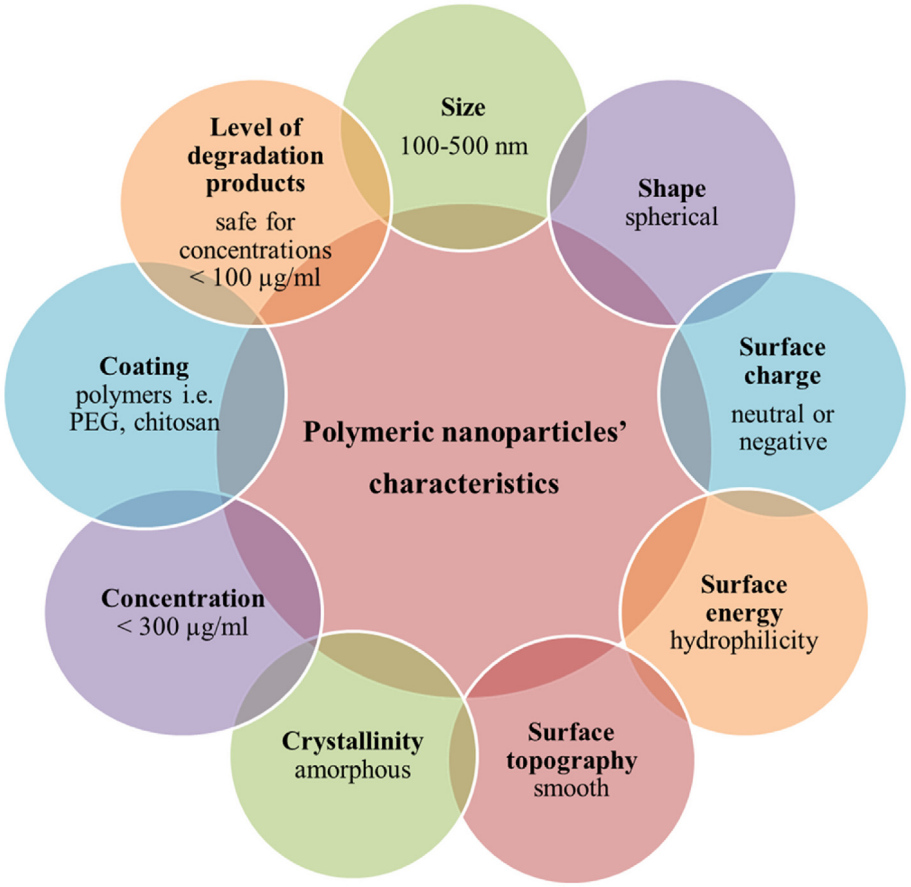

Fig. 13. Scheme summarizing the desired physico-chemical characteristics of polymeric nanoparticles for minimal toxicity and good biocompatibility [230–233].

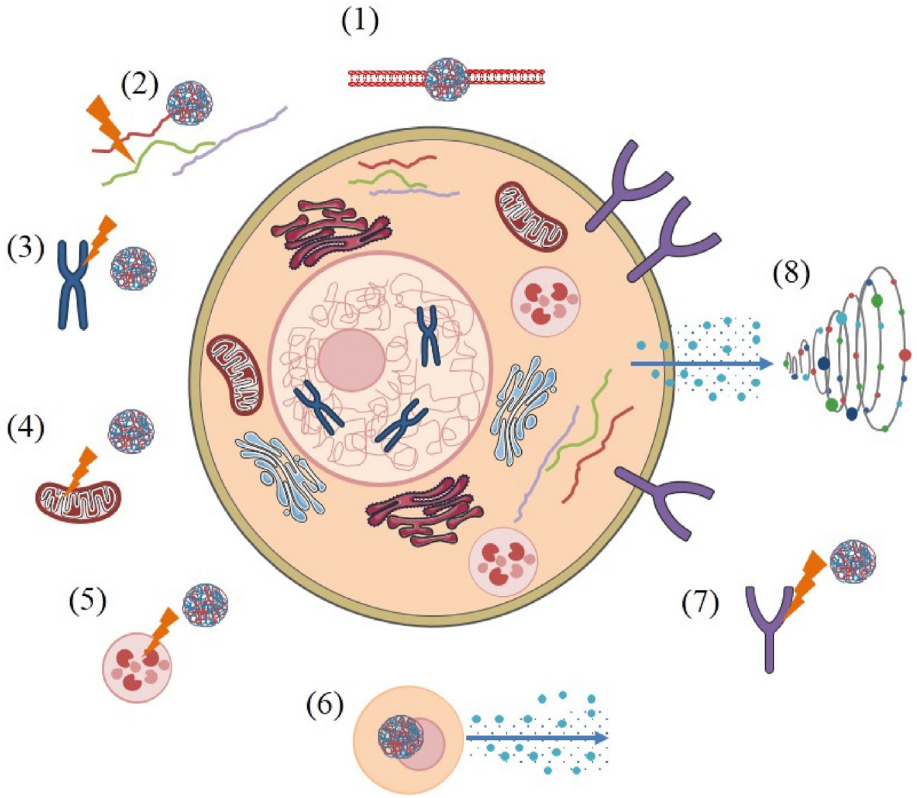

Fig. 14. Scheme summarizing the mechanisms of cellular damage induced by polymeric nanoparticles. Physical damage of cell membrane (1), structural changes in cytoskeleton (2), disturbance of transcription and DNA damage (3), damage of mitochondria (4), disturbance of lysosomal function (5), generation of ROS (6), disturbance of membrane receptor function (7), and synthesis of inflammatory factors (8). Parts of the figure were drawn by using pictures from Servier Medical Art (http://smart.servier.com/), licensed under a Creative Commons Attribution 3.0 Unported License (https://creativecommons.org/licenses/by/3.0/).

limited by their cost and low specificity. Accordingly, studies have been focused on developing rapid, reliable, and cost-effective tests for the detection of serum cardiac biomarkers with improved detection limits and accuracy. Most studies adopt metal-based NPs for the detection of CK-MB serum levels and only a few modified the surface of these NPs with polymers such as chitosan, dextran, and poly (maleic anhydride-alt-1-octadecene) due to their good adhesion quality and high permeability [131–133]. Alternatively, Lai et al. developed a rapid and relatively simple fluorescence immunochromatographic assay based on Europium (III) chelate carboxylate-modified polystyrene microparticles for the detection of serum CK-MB levels. The developed test strip allowed the quantitative detection of CK-MB levels in small volumes of serum with a range of detection of 0.85–100.29 ng/mL and a limit of detection as low as 0.029 ng/mL [24]. As this study showed promising results, it is vital to explore polymeric NPs in the future for the detection of CK-MB serum levels for rapid MI diagnosis. Cai et al. developed fluorescent core-shell NPs to establish a new point-of-care test for the detection of cTnI. The NPs of 500 nm consisted of a polystyrene core which efficiently entrapped 400 μM of the fluorescent dye "Nile Red", and a poly (acrylic acid) (PAA) shell which was functionalized with carboxyl groups to allow covalent binding of anti-cTnI antibodies. The NPs were then tested on a lateral flow immunoassay strip coated with capture antibodies. Their results proved that this method can rapidly and accurately detect cTnI levels as low as 0.016 ng/mL. This technique holds great promise as it allows proper detection of cTnI levels in plasma samples based on an inexpensive, simple, and reproducible method that only takes 15 min to provide an accurate result [29]. Another study opted to improve the sensitivity of cTnI immunoassay based on upconverting NPs (UCNP). UCNPs are inorganic NPs containing lanthanide ions as optical luminescent centers and serve as reporters in immunoassays. However, non-specific binding of cTnI antibody-UCNP conjugates on protein-coated support leads to background signals which limit the immunoassay sensitivity. Accordingly, UCNP were coated with PAA and mixed with free PAA prior to adding them to cTnI antibody-coated wells. This resulted in a significant decrease of the detection limit from 2.1 to 0.48 ng/L, which provides highly sensitive and accurate detection of cTnI [134].

3.2. Polymeric NPs-mediated delivery of CMR and CT imaging agents for MI diagnosis

CMR is widely used in the detection and diagnosis of MI as it provides detailed information about myocardial anatomy, function, and flow and permits proper delineation of the injured tissue from the normal myocardium. One of its limitations however is caused by the contrast agent Gd which exhibits rapid clearance from the body and lacks tissue specificity. This has incentivized researchers to develop Gd-loaded NPs to overcome these limitations.

Human serum albumin NPs were coupled to Gd-diethylenetriaminepentaacetic acid (Gd-DTPA) by chemical conjugation [135]. The NPs were also coated with transferrin to achieve targeted imaging. The obtained NPs had a spherical morphology, a size of 200 nm, and a highly negative zeta potential indicating good colloidal stability. The transferrin-coated and non-coated human serum albumin NPs were visualized by MRI after injection into healthy mice and their *in vivo* biodistribution was assessed. Both types of NPs provided good contrast enhancement at lower doses of Gd-DTPA as compared to the contrast agent injected alone, implicating the role of NPs in entrapping Gd-DTPA and prolonging its circulation time. They also yielded contrast enhancement in the cardiac muscle among other tissues, whereby the transferrin-coated NPs provided significantly higher contrast enhancement than their non-coated counterparts, suggesting their potential uptake by cardiomyocytes expressing transferrin receptors on their surface. This study offers great potential for the employment of transferrin-coated human serum albumin NPs as heart-specific contrast agents for the noninvasive diagnosis of cardiac diseases by CMR [135]. Wang et al. also sought to overcome the disadvantages of small-molecule Gd chelates, such as their poor selectivity and inability to distinguish infarcted tissue from edema regions, by exploiting the acidic environment within the infarcted myocardium [136]. They developed low pH-sensitive bovine

Table 4
Diagnostic applications of polymeric NPs.

Diagnostic tool	Type of nanosystem	Entrapped cargo	Surface modification	Diagnostic effect	Ref.
CK-MB immunochromatographic assay	Polystyrene microparticles	Europium (III) chelate	Carboxylate	Rapid simple quantitative detection of CK-MB levels No requirement for large volumes of serum Range of detection: 0.85–100.29 ng/mL Limit of detection: 0.029 ng/mL	[24]
cTnI immunoassay	Polystyrene/Poly (acrylic acid) core-shell NPs	Red fluorescent dye "Nile Red" Anti-cTnI antibodies	–	Effective for early screening and diagnosis of acute MI Inexpensive, accurate rapid detection of cTnI levels Range of detection: 0–40 ng/mL Limit of detection: 0.016 ng/mL	[29]
	Upconverting NPs	Lanthanide ions Anti-cTnI antibodies	Poly (acrylic acid)	Effective for diagnosis of MI Sensitive detection of cTnI levels Range of detection: 0–100 ng/mL Limit of detection: 0.00048 ng/mL	[134]
Cardiac magnetic resonance	Human serum albumin NPs	Gadolinium-diethylenetriamine-pentaacetic acid	Transferrin	Allowed loading of lower doses of Gadolinium Improved Gadolinium enhancement and circulation time Enhanced imaging of cardiac muscle via transferrin-mediated targeting	[135]
	Bovine serum albumin NPs	MnO_2 motifs	Low pH-sensitive motifs	Enhanced T1 relaxivity Induced rapid NPs accumulation, increased contrast enhancement in infarcted myocardium of MI rabbits Improved diagnostic accuracy compared to Gd-DTPA	[136]
	Polymeric nanoreactor	Acid phosphatase Glucose-1-phosphate Gadolinium chloride	Polyguanylic acid	Induced precipitation of gadolinium phosphate NPs within nanoreactor Induced selective uptake by macrophages	[137]
Computed tomography	N1177 (poloxamer 338/poly (ethylene glycol) NPs)	Iodinated aroyloxy ester	–	Effective for detection of high-risk atherosclerotic plaques Promoted selective uptake of NPs by macrophages Promoted high iodine concentration in macrophage-rich tissues Prolonged iodine's half-life Allowed delayed enhanced imaging	[139]
	Poly (styrene)-block-poly (acrylic acid) NPs	Radio-opaque organometallic iodine atoms	–	Entrapped high iodine payload Promoted homing of NPs to vascular targets Prolonged iodine's half-life Allowed enhanced imaging of LV and intra vena cava	[140]
	Polylysine/poly (ethylene glycol) dendrimer	Triiodophthalamide moieties	–	Entrapped high iodine content Increased NPs' molecular weight and water solubility Prolonged iodine's circulation half-life Allowed CT enhancement of inferior vena cava and hepatic veins Applicable for CT angiography and quantitative microvascular studies	[141]
	ExiTron MyoC 8000 (polymeric nanocapsules)	Iodine atoms	–	Entrapped high iodine content Prolonged iodine's circulation half-life Delayed blood elimination Allowed signal enhancement in blood and healthy myocardium Allowed longitudinal monitoring of cardiac functions and quantification of infarct size in small animal MI models	[142]
	Dextran NPs for PET		–	Entrapped high yield of ^{89}Zr	[143]

(*continued on next page*)

Table 4 (*continued*)

Diagnostic tool	Type of nanosystem	Entrapped cargo	Surface modification	Diagnostic effect	Ref.
Other diagnostic techniques and multimodal imaging		Radio-isotope [^{89}Zr]-Zr oxalate		Enhanced PET imaging of inflammatory macrophages Applicable for selective macrophage imaging and quantification	
	Chitosan NPs for PET	^{89}Zr or^{64}Cu	–	^{89}Zr NPs induced highest radiolabeling efficiency and retention of radioactivity with human leukocytes	[144]
	Poly (methyl methacrylate)/ poly (ethylene glycol) NPs for PET	DOTA radiometal chelators ^{64}Cu	C-type atrial natriuretic factor targeting moieties	Enhanced circulatory retention, decreased accumulation in liver and spleen, reduced renal clearance Increased radiotracer accumulation within atherosclerotic and angiogenic regions	[146, 234]
	Dendritic poly (ethylene oxide) NPs for PET	Radiohalogens	Cyclic arginine–glycine–aspartic acid motifs	Enhanced endocytosis by cells expressing $\alpha_v\beta_3$ integrins Enhanced PET imaging of angiogenic muscles in ischemic conditions	[147]
	Carboxymethylated polyglucose/lysine NPs for PET-MR	^{18}F	–	Increased cell uptake by cardiac and plaque macrophages Enhanced detection and quantification of macrophages in MI and atherosclerosis models	[148]
	Porphysome NPs for PET-CT and FMT	Porphysome ^{64}Cu	Folate	Promoted detection of macrophages Allowed discrimination of different macrophage phenotypes	[149]

serum albumin NPs with manganese oxide motifs for improved T1-weighted CMR imaging of acute MI. *In vitro* studies demonstrated the safety of the NPs and their efficient uptake by macrophages which lead to increased T1 relaxivity due to low pH-triggered release of Mn^{2+} within macrophages (pH = 5.0). Moreover, upon their IV administration to rabbit MI models, the NPs were found to accumulate rapidly and preferentially in the infarcted myocardium (pH = 6.5) and increase contrast enhancement. Overall, the authors demonstrated a promising alternative approach to conventional Gd-DTPA which has great implication for specific imaging of acute MI for early and accurate diagnosis [136]. Nano-sized self-assembled polymeric vesicles can serve as bioreactors with chemically modifiable surfaces. Broz et al. used water-soluble enzyme nanoreactors self-assembled from amphiphilic triblock copolymers to entrap acid phosphatase enzyme, its substrate glucose-1-phosphate, and Gd chloride [137]. Upon hydrolysis of the substrate by acid phosphatase, phosphoric acid is produced. The latter reacts with Gd chloride and results in the precipitation of the water insoluble hydrated Gd phosphate. These enzyme nanoreactors were then rendered macrophage-specific by surface functionalization with polyguanylic acid, a macrophage scavenger receptor A1 ligand; they were also fluorescently labeled with Streptavidin-Alexa Fluor. As a result, the developed nanoreactor was successfully applied in MRI and fluorescent imaging whereby the vesicles were effectively and selectively taken up by macrophages and allowed local and temporal control of Gd precipitation. This study holds great potential for imaging macrophages and detecting inflammation within the infarcted myocardium in MI patients [137].

CT is yet another widely used noninvasive imaging technique for the detection and diagnosis of acute MI. However, like CMR, it is still facing some limitations which require new technology for overcoming them. Early and accurate imaging of macrophages is vital for the detection of post-MI inflammatory phase and for the detection of high macrophage densities, characteristic of vulnerable atherosclerotic plaques whose rupture can lead to thrombus formation and subsequent acute type 1 MI [138]. Hyafil et al. designed an iodinated nanoparticulate contrast agent, N1177, for the selective detection of macrophages. N1177 consisted of an iodinated aroyloxy ester combined with poloxamer 338 as the surfactant agent and PEG as the polymer of choice for stabilizing the NP size. The NPs entrapped 67 mg/mL of iodine which were concentrated in the electron-dense granules. Their small size of 259 nm allowed the NPs to be taken up by macrophages *in vitro* after only 1 h of incubation. *In vivo* studies conducted in non-atherosclerotic rabbits showed that densities measured by CT were significantly higher in macrophage-rich tissues (i.e. liver and spleen) 2 h after N1177 IV injection as compared to pre-injection, and were not detected upon injection of the conventional contrast agent or in organs devoid of macrophages. This study successfully proved that iodinated nanoparticulate contrast agents can selectively infiltrate macrophages and prolong the imaging agent's half-life permitting delayed enhanced imaging. Accordingly, N1177 may be useful for the clinical evaluation of inflamed coronary arteries during MI [139]. Moreover, Pan et al. developed novel polymeric NPs for the targeted delivery of imaging agents towards the vasculature. The NPs consisted of radio-opaque organometallic imaging elements entrapped within a colloidal poly (styrene)-block-poly (acrylic acid) copolymer which self-assembles due to its amphiphilic nature. This di-block copolymer had a double function of encapsulating high payloads of the metals reaching 96% efficiency and permitting homing of the NPs to vascular targets while preventing them from extravasating into tissues. By subjecting the formed NPs to carbodiimide, the NPs were intramolecularly cross-linked which enhanced their shelf-life stability and integrity. Furthermore, upon IV administration of the NPs in a rat model, CT imaging showed that they had a half-life up to 6 times longer than commercial iodinated agents and allowed enhanced imaging of the LV and intra vena cava for 3.5 h, suggesting their potential application for the detection and diagnosis of MI [140]. Moreover, Fu et al. developed novel macromolecular CT contrast agents for microvasculature imaging. The NPs consisted of a hydrophilic and biocompatible PEG core from which two symmetrical polylysine dendrimers were initiated, generating several free amino groups on the NPs surface. These groups were used to conjugate highly soluble and stable reactive triiodophthalamide moieties, representing the contrast agent of choice. The generated iodinated NPs had a large molecular weight (>30 kDa), high iodine content (>27%), and high-water solubility (>550 mg/mL at 25 °C). *In vivo* CT

contrast enhancement in normal rats showed that the NPs possessed a prolonged blood circulation half-life of 35 min compared to the conventional small-molecular contrast media that only allows vascular enhancement for 5 min. These intravenously-injected NPs also demonstrated strong and persistent intravascular enhancement of the inferior vena cava and hepatic veins within the liver, suggesting their potential application in angiography and quantitative microvascular characterization of ischemic cardiac injury such as MI [141]. Finally, a novel micro-CT technique was developed for longitudinal monitoring of cardiac functions and quantification of infarct size in *in vivo* MI murine models. This technique involved a new blood pool agent designated as ExiTron MyoC 8000 which consists of polymeric biocompatible nanocapsules of 300 nm with high iodine content of 210 mg/mL. Kinetic studies showed that it had prolonged blood circulation half-life and delayed elimination, suggesting that it can be used for extended imaging of the LV. Moreover, ExiTron MyoC 8000 not only allowed signal enhancement in the blood, but also in the myocardium even when administered at a low dose of 420 mg of iodine/kg. Moreover, it was found that the NPs were specifically taken up by healthy intact cardiac cells but not by injured ones, which allowed an accurate quantification of the infarct size. Accordingly, this low-dose microCT method allowed the construction of images with superior spatiotemporal resolution, extended cardiac imaging time, and quantification of the infarct size in small animal MI models [142].

3.3. Polymeric NPs in other MI diagnostic techniques and multimodal imaging

While diagnosis of MI is most often achieved by detection of serum cardiac biomarkers levels, and cardiac anatomical and functional characteristics by CMR and CT, other imaging techniques such as PET scan and fluorescence molecular tomography (FMT) are also employed by physicians. PET scan helps estimate the infarct size and detect markers of inflammation and angiogenesis within unstable atherosclerotic plaques and the infarcted region of the myocardium. However, there is still critical need for specific PET imaging agents that allow quantitative and specific detection of biomarkers within the desired tissue.

Keliher et al. developed cross-linked dextran NPs radiolabeled with ^{89}Zr–Zr oxalate for imaging of inflammatory macrophages. The NPs were highly stable and entrapped a high yield of ^{89}Zr. *In vivo* studies showed that the NPs had a long half-life of 3.9 h and accumulated primarily within the lymph nodes where macrophages are known to reside. The NPs were then tested in a mouse xenograft cancer model by applying PET-CT imaging where they were detected in macrophages within the tumor tissue and delineated as such the inflammatory region. These NPs can later be tested on a murine MI model to visualize the inflammatory region within the myocardium [143]. Leukocytes are also important immune cells involved in the inflammatory phase occurring after a cardiac infarct and represent crucial cells for imaging and diagnosis of MI. Fairclough et al. synthesized spherical chitosan NPs radiolabeled with either ^{89}Zr or ^{64}Cu to allow PET imaging of leukocytes. Their results showed that the highest radiolabeling efficiency and retention of radioactivity over 24 h of incubation with mixed human leukocytes were obtained with ^{89}Zr-labeled NPs. These NPs can later be applied in *in vivo* inflammatory models to test their potential to enhance the signaling for PET imaging and promote precise quantification of inflammation [144]. Other studies aimed at providing targeted imaging of atherosclerotic and angiogenic lesions by using NPs labeled with C-type atrial natriuretic factor (CANF) fragment for detecting the upregulation of CANF receptor termed as natriuretic peptide clearance receptor (NPRC). The core-shell comb NPs consisted of DOTA radiometal chelators attached to a poly (methyl methacrylate) core, and CANF-targeting moieties linked to PEG chains in the NPs' shell. To render them specific for NPRC PET imaging, they were labeled with ^{64}Cu. The obtained NPs demonstrated an improved biodistribution profile as compared to their non-targeted counterparts whereby they showed improved circulatory retention, minimal accumulation within the liver and spleen, and reduced renal clearance. Furthermore, when the NPs were administered in murine models of atherosclerosis and hind limb ischemia–induced angiogenesis, PET imaging showed higher radiotracer accumulation and confirmed the high specificity and sensitivity of the NPs towards tissues with high expression of NPRC. As such, ^{64}Cu-DOTA-CANF-comb NPs seem promising PET imaging agents for the detection of atherosclerosis and angiogenesis [145,146]. In a similar fashion, Almutairi et al. aimed at imaging angiogenesis by PET scan using dendritic NPs to target $\alpha_v\beta_3$ integrin, a known marker of angiogenesis. The nanoprobe consisted of a dendritic core labeled with radiohalogens and functionalized with polyethylene oxide (PEO) which formed a protective outer shell. Cyclic arginine–glycine–aspartic acid (RGD) motifs were linked to PEO chains to ensure their specific binding to the $\alpha_v\beta_3$ integrin receptors. Both *in vitro* and *in vivo* studies showed that the labeled and targeted nanoprobes increased NPs' uptake by $\alpha_v\beta_3$-positive cells by 6-fold and enhanced selective PET imaging of angiogenic muscles in a hind limb ischemia model, demonstrating the role of the targeted NPs for selective imaging of angiogenesis in ischemic conditions [147].

Multimodal imaging has been applied as well for the diagnosis of MI as it combines the unique and complementary strengths of distinct imaging techniques to provide more curated diagnosis. Accordingly, PET-CT, FMT-CT, and PET-MR among others have been adopted for these mentioned purposes. However, studies are ongoing for the development of imaging agents that can promote enhanced and targeted signaling of events leading towards MI and occurring post-MI such as atherosclerosis and inflammation, respectively.

Polymeric NPs consisting of carboxymethylated polyglucose and lysine were synthesized for the entrapment of the radiotracer ^{18}F for enhanced PET-MR imaging of inflammatory diseases. Indeed, the NPs were specifically taken up by cardiac and plaque macrophages and promoted the detection and quantification of macrophages by PET-MR in animal MI and atherosclerosis models [148]. Finally, porphysome NPs were developed for the noninvasive multimodal imaging and detection of macrophages behavior at different stages post-MI. The NPs consisted of porphysome, which can emit near infrared fluorescence, and ^{64}Cu for concomitant nuclear and fluorescent imaging. The NPs were also conjugated to folate to ensure macrophage-specific targeting. Indeed, upon administering the NPs in a murine model of MI, macrophages were easily detected by PET-CT and FMT whereby inflammatory macrophages were found to reside in the entire LV area at day 1 post-MI while anti-inflammatory cells were dominant in the scar tissue at day 7. Accordingly, folate-conjugated porphysome NPs are suitable nano-imaging agents for the detection of macrophages in an infarcted heart [149].

4. Polymeric NPs for the treatment of MI

Discovering a drug and introducing it into the market is a laborious and expensive process where often one out of thousands of initially considered compounds gets approved. Therefore, exploiting existing drugs and increasing their bioavailability by shielding them using adequate DDS can enhance their efficacy and mitigate their accumulation in off-target sites [150]. MI harbors niche microenvironments that vary with time and dictate as such the drug targeting method. Drug-containing NPs avail their small size and enter the damaged myocardium passively via the EPR effect. However, the EPR effect starts diminishing 48 h post-infarction where active targeting should override [151–153]. Active targeting can be based on the elevated and tissue-specific expression of cell receptors, pro-inflammatory cytokines, matrix proteins, and MMPs that can be targeted using ligands [154–156].

4.1. Polymeric NPs as drug delivery agents

Targeting the ischemic tissue passively requires the drug vehicle to possess specific physicochemical properties with respect to size, shape,

and surface modification and to be administered shortly after the infarction occurs. Treating MI is most effective 24 h after its occurrence where cell apoptosis reaches its peak. Importantly, prolonged circulation of certain growth factors can lead to undesirable effects, hence their immediate release is required [157,158]. For instance, insulin-like growth factor-1 (IGF-I) protects cardiomyocytes from apoptosis but can reduce cardiac functional recovery when overexpressed. Therefore, negatively charged IGF-I was conjugated to negatively charged PLGA NPs, of different sizes, after modifying them with positively charged PEI to create the necessary electrostatic binding and preserve IGF-I. PLGA NPs were only detected in the damaged tissue, unlike when IGF-I was administered freely. The 60 nm NPs showed the highest IGF-I binding affinity and retention after 24 h which resulted in preserving cardiac function, reducing the infarct size while preventing ventricular remodeling [158].

Angiogenesis is crucial to retrieve normal blood flow to the ischemic tissue. Proangiogenic cytokines, e.g., vascular endothelial growth factor (VEGF), have dose-dependent effects; thus, controlled, and sustained delivery from a DDS is required. VEGF was encapsulated in PLGA NPs and as a result, the vasculature density increased and the infarct size decreased accompanied by improved LV contractile force [159,160]. PLGA NPs were also used for the encapsulation of a novel angiogenic peptide, adrenomedullin-2 (ADM-2), to promote angiogenesis. The developed NPs containing ADM-2 were able to significantly induce proliferation in endothelial cells compared to freely administered ADM-2 [161].

Alleviating persistent inflammation in the infarcted heart can help abrogate cardiomyocytes apoptosis. Indeed, delivery of pitavastatin passively in PLGA NPs successfully activated the phosphatidylinositol 3-kinase/protein kinase B pathway and prevented as such cell death in hypoxic cells and subsequently in reoxygenated cells [162,163]. Reactive oxygen species (ROS) generated during I/R injuries are yet another factor of the niche microenvironment of an ischemic tissue [164–166]. Nicotinamide adenine dinucleotide phosphate (NADPH) oxidases also impose oxidative stresses during inflammation and are elevated in MI. Accordingly, lysine-based NPs encapsulating NADPH oxidase 2 (NOX2)-targeting small interfering ribonucleic acid (siRNA) were developed. When locally delivered in an *in vivo* atherosclerotic model, ROS production was decreased and neointimal hyperplasia was inhibited [167]. Moreover, alginate/chitosan NPs protected placental growth factor from degradation while delivering it to the ischemic myocardium and promoting its release in a sustained manner. Treatment with placental growth factor-loaded NPs was able to increase capillary and arteriole densities, enhance the release of anti-inflammatory cytokine IL-10, and decrease that of pro-inflammatory cytokines TNF-α and IL-6 [168].

Additionally, dendrimers have been used as DDS since their high charge density grants them the ability to cross membranes and barriers to deliver drugs effectively. PAMAM dendrimers embedded with a PEG cross-linker to ensure biocompatibility were further modified with cell penetrating peptides (R9 and TAT) for the delivery of angiotensin II type 1 receptor (AT1R) siRNA. AT1R is upregulated in MI and enhances the ischemic injury thus, suppressing its expression using siRNA is more effective for preserving cardiac function than receptor blockers that might increase AT1 release. R9-modified dendrimers induced significantly higher internalization compared to TAT-modified NPs due to TAT's smaller size and higher arginine content. Accordingly, R9-modified

Table 5
Therapeutic applications of drug-loaded polymeric NPs for passively-targeted therapy.

Type of nanosystem	Entrapped cargo	Surface modifications	Therapeutic effect	Ref.
Poly (lactic-co-glycolic acid) NPs	IGF-I	Polyethylene-imine	**In vivo MI model** Induced NPs cardiac retention Preserved cardiac function Prevented LV remodeling Reduced infarct size	[158]
	VEGF	–	**In vivo MI model** Increased vascular density Reduced infarct size Improved LV contractile force	[159,160]
	Adrenomedullin-2	–	**In vitro** Induced proliferation of endothelial cells	[161]
	Pitavastatin	–	**In vitro** Activated PI3K/AKT pathway Reduced the rate of cardiomyocytes apoptosis	[162,163]
Lysine-based NPs	NOX2 siRNA	–	**In vivo atherosclerotic model** Decreased ROS production Inhibited neointimal hyperplasia	[167]
Alginate NPs	PlGF	Chitosan coating	**In vivo MI model** Increased capillary and arteriole densities Decreased pro-inflammatory cytokines release Increased anti-inflammatory cytokines release	[168]
PAMAM dendrimers	AT1R siRNA	Poly (ethylene glycol) cross-linker	**In vitro** Induced AT1R silencing in cardiomyoblasts **In vivo MI model** Decreased infarct size	[169]
Hyaluronan-sulfate NPs	miRNA-21 mimic	–	**In vivo MI model** Switched pro-inflammatory macrophages into reparative phenotype Enhanced angiogenesis Limited fibrosis, cell apoptosis, cardiac hypertrophy	[170]
Polyethylene-imine	SHP-1 siRNA	Deoxycholic acid	**In vitro** Silenced SHP1 gene expression Inhibited cardiomyocytes apoptosis **In vivo I/R model** Inhibited apoptosis Reduced infarct size	[171]
Poly (glycidyl methacrylate)	Curcumin AID targeting peptide	Polyethylene-imine	**Ex vivo I/R model** Reduced muscle damage Reduced oxidative stress Decreased ROS levels in cardiomyocytes	[172]

dendrimers loaded with AT1R siRNA promoted a decrease in the infarct size [169]. Beside dendrimers, other polymeric NPs were utilized to deliver small RNA molecules to reduce inflammation and inhibit apoptosis within the damaged myocardium. As a method to switch the macrophages phenotype from pro- to anti-inflammatory in the infarct region, Bejerano et al. aimed to boost the levels of microRNA-21 (miRNA-21), typically expressed in macrophage-rich areas with peak levels at day 7 post-MI. Accordingly, they delivered self-assembled NPs of miRNA-21 mimic complexed with hyaluronan-sulfate and calcium bridges to the injured area where they were able to enhance angiogenesis, limit fibrosis and cell apoptosis, and ultimately reduced cardiac hypertrophy [170]. Genetic material can also be delivered to inhibit cardiomyocytes hypoxia-induced apoptosis in an infarcted heart. Low molecular weight PEI modified with deoxycholic acid for enhanced cellular uptake was employed to electrostatically conjugate siRNA targeting Src homology region 2 domain-containing tyrosine phosphatase-1 (SHP-1), a gene involved in cell apoptosis. After successfully silencing the corresponding gene and inhibiting apoptosis of cardiomyocytes *in vitro*, the effects of these NPs were assessed in a rat model of I/R. SHP-1 loaded NPs were found to significantly reduce apoptosis which in turn decreased the infarct size [171].

Finally, as the characteristics of an infarcted heart microenvironment are governed by intertwined factors, it is of great interest to load nanocarriers with multiple bioactive agents to effectively eliminate these synergistic repercussions. Poly (glycidyl methacrylate) NPs were synthesized for the simultaneous delivery of the antioxidant agent curcumin and a peptide targeting the alpha interacting domain L-type Ca^{2+} channel (AID) to decrease ROS and prevent their generation through mitochondrial activity. The NPs entrapped curcumin within their core and were modified with PEI to promote electrostatic adsorption to the AID peptide. The resulting NPs were able to reduce muscle damage, oxidative stress, and ROS levels in cardiomyocytes of an *ex vivo* I/R model [172] (Table 5).

4.2. Polymeric NPs for the targeted treatment of MI

Smart drug delivery can be achieved by active targeting that guides the DDS to the target using biological moieties such as receptors overexpressed on target cells or by the aid of external magnetic fields that can guide iron-containing carriers within the body [173,174]. DDS modified with ligands that bind to cell-specific receptors or moieties overexpressed in pathophysiological conditions initially employ EPR-mediated passive targeting to enter the tissue. Subsequently, they exploit ligands including sugars, peptides, folic acid, and antibodies, to improve their residence time and cellular internalization [175–177].

Myocardium-specific molecules such as fibrin and atrial natriuretic peptide (ANP) have been commonly exploited for MI targeting applications. Fibrin is a target molecule in MI due to its rare presence in healthy myocardium and the instant formation of fibrin matrices post-MI [178–181]. The Cys-Arg-Glu-Lys-Ala (CREKA) peptide sequence was covalently conjugated onto PEG/PLLA NPs to target MI fibrin. The CREKA modified NPs loaded with thymosin beta-4 had high localization in the damaged heart and were able to improve cardiac function and survival, enhance angiogenesis, and revitalize the dormant adult epicardium [178]. Another myocardium-specific molecule is ANP produced by the myocardium to stimulate repair within the infarct. Besides, ANP communicates paracrine signals by binding to natriuretic peptide receptors (NPRs) expressed on cardiomyocytes and fibroblasts [182]. Multifunctional PEGylated porous silicone NPs modified with ANP and a metal chelator were used to deliver the cardioprotective novel molecule, trisubstituted-3,4,5-isoxazole, to the damaged myocardium. The targeting ligand increased the NPs infiltration into the heart by 3-fold, whereby they effectively attenuated extracellular signal-regulated kinases' phosphorylation which play a key role in cardiac hypertrophy [182–184].

AT1R is highly expressed in the infarcted heart, as mentioned earlier, as a result of hypoxic conditions accompanying the ischemic tissue [164]. PEG-modified dendri-grafted poly-l-lysine (PLL) dendrimer conjugated to AT1R targeting ligand had significantly higher accumulation in the infarcted heart compared to bare NPs. This drug carrier was utilized to deliver microRNA-1 inhibitor that exerts anti-apoptotic effects. Accordingly, it reduced apoptotic cell death significantly across the infarcted border and decreased the infarct size [164].

Active targeting also comprises stimuli-responsive carriers governed by endogenous or exogenous factors that can precipitate, degrade, swell, or change the carriers' shape to release the encapsulated molecules [185,186]. Since MI has its distinct microenvironments, and different treatments are merely effective at specific stages, active targeting and triggered release can be employed to release the desired drug when necessary and attain sustained release.

Cardiac hypertrophy post-MI can be induced by NOX2-NADPH which contributes to ROS generation in the infarcted heart. Therefore, silencing NOX2-NADPH expression in neutrophils, macrophages, and myocytes can mitigate their effects on cardiac function [187,188]. Heffernan et al. developed pH-responsive polyketal NPs to enhance the transfection efficiency of siRNAs and promote their internalization into lysosomes where the acidic pH promotes NPs degradation. Accordingly, NOX2 levels were downregulated within the infarct which aided in retrieving cardiac function [188,189]. Polyketal NPs can be further modified by sugars such as N-acetylglucosamine (GlcNAc) to facilitate cellular uptake. GlcNAc-coated poly (cyclohexane-1,4-diyl acetone dimethylene ketal) NPs were used to encapsulate p38 MAPK inhibitor to reduce apoptotic events post-MI. The decorated NPs showed significant uptake accompanied by p38 inhibition when tested *in vitro* on cardiomyocytes. Accordingly, they were tested in an *in vivo* MI model to confirm their therapeutic effect where they decreased apoptosis, reduced infarct size, and improved cardiac function [190].

The reductive environment of the cytoplasm represents an ideal arena for responsive bioreducible carriers to release their genetic content. Many genes are implicated in cardiomyocytes apoptosis following MI including the cell surface death receptor Fas gene. In order to downregulate its expression, Fas siRNA were delivered in poly (cystamine bisacrylamide-diaminohexane) NPs, decorated with primary cardiomyocyte-specific targeting peptide, to hypoxic cardiomyocytes in order to evaluate their effectiveness. The polyplexes were found to induce significantly higher transfection efficiency in hypoxia-induced cardiomyocytes as compared to fibroblasts. Consequently, the viability of transfected cardiomyocytes was significantly higher than non-transfected ones as they were protected from hypoxia-induced apoptosis [191].

Overproduction of ROS, as indicated earlier, is a distinct feature of severe inflammation. Therefore, besides targeting ROS to eliminate its detrimental effects, an infarcted myocardium rich in ROS, namely H_2O_2, can act as a stimulating environment that prompts H_2O_2-responsive nanocarriers to release their content. Copolyxalate NPs were loaded with the bioactive agent vanillyl alcohol and conjugated to H_2O_2-responsive peroxalate ester linkages to render the NPs degradable in the presence of H_2O_2. The vanillyl alcohol-loaded NPs reduced ROS generation, exhibited anti-inflammatory and anti-apoptotic activities, and thus reduced cellular damage in hind-limb and liver I/R models [192].

Another endogenous factor is the upregulation of MMP-2/9 in the infarcted heart. MMP-specific recognition peptide sequences were conjugated to polymer amphiphiles with poly (norbornene) backbone forming peptide-polymer amphiphile NPs. When the NPs were internalized by the myocardium via the EPR effect, they transformed into a mesh-like scaffold, upon MMP recognition, that was retained in the myocardium for 7 days post-treatment unlike non-responsive NPs. This study encourages further researchers to entrap drugs within these peptide-polymer amphiphile NPs for active targeting of the heart post-MI [189] (Table 6).

Table 6
Therapeutic applications of drug-loaded polymeric NPs for actively targeted therapy.

Type of nanosystem	Entrapped cargo	Surface modifications	Therapeutic effect	Ref.
Poly (ethylene glycol)/poly-L-lactic acid	Thymosine β4	Poly (ethylene glycol) CREKA peptide sequence	**In vivo ischemic model** Improved cardiac function, survival Enhanced angiogenesis Revitalized dormant epicardium	[178]
Porous silicone NPs	Trisubstituted-3,4,5-isoxazole	Poly (ethylene glycol) ANP peptide Metal chelator	**In vivo MI model** Infiltrated into the heart Attenuated ERK1/2 phosphorylation	[182–184]
Dendri-grafted poly-l-lysine NPs	microRNA-1 inhibitor (AMO-1)	Poly (ethylene glycol) AT1R targeting ligand	**In vivo MI model** Reduced apoptotic cell death Decreased infarct size	[164]
Polyketal NPs	NOX2 siRNA	pH-responsive linkages	**In vivo MI model** Downregulated NOX2 expression Retrieved cardiac function	[188,189]
	p38 MAPK inhibitor	N-acetylglucos-amine	**In vitro** Increased uptake by cardiomyocytes Induced p38 inhibition **In vivo MI model** Reduced apoptosis Decreased infarct size Improved cardiac function	[190]
Poly (cystamine bisacrylamide diaminohexane NPs	Fas siRNA	Primary cardiomyocyte specific peptide Redox responsive bonds	**In vitro** Increased cardiomyocytes' uptake and transfection efficiency Inhibited cardiomyocytes' apoptosis under hypoxia	[191]
Copolyxalate NPs	Vanillyl alcohol	H_2O_2-responsive peroxalate ester linkages	**In vivo hind-limb and liver I/R model** Reduced ROS generation Exhibited anti-inflammatory and anti-apoptotic effects Reduced cellular damages	[192]
Peptide-polymer amphiphile NPs	–	MMPs recognition peptide sequence	**In vivo MI model** Enhanced accumulation of NPs within infarcted myocardium Transformed from discrete spheres into a scaffold upon MMP recognition	[189]

4.3. Polymeric NPs for the regeneration of the infarcted heart

Upon injury of the myocardium post-MI, and because of the limited regenerative capacity of the heart, the infarcted tissue is replaced by a non-contractile scar tissue [193]. Accordingly, researchers have opted for regenerative therapy based on the delivery of stem cells to the infarcted myocardium with the help of tissue engineering approaches to restore cardiac function and prevent heart failure. Stem cells have the ability to self-renew and differentiate towards specialized cell lineages under the appropriate environmental cues. However, their direct delivery to the injured tissue is limited by their low retention and survival rate and limited differentiation potential [193]. Accordingly, nanotechnology has paved the way for delivering stem cells and their progenitors within biocompatible NPs and scaffolds.

PLGA NPs conjugated to Simvastatin were found to be internalized by adipose-derived stem cells (ASCs) *in vitro*, promote ASCs migration in response to gradual drug release from degrading PLGA NPs, induce the expression of pro-angiogenic and anti-apoptotic factors, and enhance their differentiation towards smooth muscle and endothelial cells. These results were translated *in vivo* in a murine MI model whereby Simvastatin-NPs treated stem cells were recruited and retained in the ischemic region, improved cardiac function, and induced regeneration of the infarcted heart [194]. Moreover, core-shell NPs of 270 nm consisting of lecithin/VEGF core and Pluronic F-127 shell were prepared for the regeneration of the MI heart. The NPs were able to release VEGF in a sustained manner over a period of 42 days. *In vivo*, the NPs significantly enhanced capillary density and improved the overall cardiac function. NPs gelation was achieved by adding Capryol 90, a non-ionic water--insoluble surfactant, which resulted in the formation of a gel network containing VEGF-loaded NPs. The hydrogel was found to have more significant effects on restoring cardiac function as compared to the loaded NPs, suggesting the advantage of the hydrogel in improving NPs' localization within the ischemic heart [195].

Transdifferentiation of cardiac fibroblasts towards cardiomyocyte-like cells is yet another way to regenerate the infarcted heart. PEG-coated and ANP-modified acetylated dextran NPs were synthesized for the delivery of two small water-insoluble drugs involved in the direct reprogramming of fibroblasts into cardiomyocytes (SB431542 and CHIR99021). *In vitro* studies revealed that the NPs promoted triggered release of both drugs in an acidic environment and allowed sustained release over 24 h. The NPs also enhanced the drugs' reprogramming activity as evident by the stabilization of β-catenin and prevention of Smad3 translocation to the nucleus of myofibroblasts [196]. Similarly, PEI-coated carboxymethylcellulose NPs encapsulating cardiomyocyte-specific transcription factors (GATA4, MEF2C, and TBX5) along with 5-azacytidine, a nucleoside that inhibits proliferation and promotes differentiation, were found to induce transdifferentiation of dermal fibroblasts into cardiomyocyte-like cells. Indeed, the reprogrammed cells expressed cardiac markers (cTnI and α-actinin) and exhibited cardiac beating properties upon transplantation into murine hearts [197]. Moreover, various hydrogels synthesized from naphthalene molecules and β-galactose caged nitric oxide (NO) donors (NapFF-NO), gelatin methacrylate (GelMA) complexed with nanosilicates, and agarose supplemented with integrin-binding proteins, were all used to encapsulate ASCs, mesenchymal stem cells-derived secretome, and cardiac stem cells (CSC), respectively. NapFF-NO hydrogel improved stem cell survival and enhanced cardiac function upon NO-stimulated expression of pro-angiogenic factors. Also, the secretome-rich nanocomposite hydrogel of GelMA/nanosilicates played pro-angiogenic and cardioprotective roles and enhanced cardiomyocytes' survival upon hypoxia-induced apoptosis. Lastly the CSC-encapsulated agarose hydrogel retained the cells' viability under hypoxic conditions, promoted the production of pro-angiogenic and cardioprotective cytokines, and restored cardiac structure and function post-MI [198–200]. Overall, hydrogels made from

Table 7
Therapeutic applications of polymeric NPs for cardiac regeneration.

Type of nanosystem	Entrapped cargo	Surface modification	Therapeutic effect	Ref.
Poly (lactic-co-glycolic acid) NPs	Adipose-derived stem cells Simvastatin	–	**In vitro** Promoted cells' migration Promoted cells' expression of pro-angiogenic and anti-apoptotic factors Promoted cells' differentiation towards smooth muscle and endothelial cells **In vivo MI model** Retained cells in ischemic region Improved cardiac function Induced endogenous cardiac regeneration	[194]
Lecithin/Pluronic F-127 core-shell NPs	VEGF	–	**In vitro** Sustained release of VEGF over 42 days **In vivo MI model** Enhanced capillary density Improved cardiac function	[195]
Acetylated dextran NPs	SB431542 CHIR99021	Poly (ethylene glycol) ANP peptide	**In vitro** Induced pH-triggered release of drugs over 24 h Enhanced the drugs' reprogramming activities	[196]
Carboxymethyl-cellulose NPs	GMT plasmid DNA (GATA4, MEF2C, TBX5) 5-azacytidine	Poly (ethylene imine)	**In vitro** Transdifferentiated dermal fibroblasts into cardiomyocyte-like cells **In vivo MI model** Promoted beating properties of cardiomyocyte-like cells at injection site	[197]
Naphthalene/Nitric oxide donor hydrogel	Adipose-derived stem cells	–	**In vitro** Induced expression of pro-angiogenic factors **In vivo MI model** Enhanced stem cells' survival Improved cardiac function	[198]
Gelatin methacrylate/ nanosilicates hydrogel	Mesenchymal stem cell-derived secretome	–	**In vitro** Increased endothelial cells' proliferation Protected cardiomyocytes from hypoxia-induced apoptosis	[199]
Agarose hydrogel	Cardiac stem cells	Integrin-binding proteins	**In vivo MI model** Retained cells' viability Induced production of pro-angiogenic and cardioprotective cytokines Restored cardiac structure and function	[200]

biocompatible polymers which mimic the ECM are adequate candidates for the delivery, retention, and differentiation of stem cells and their progenitor and hold great promise for cardiac tissue regeneration post-MI (Table 7). Polymeric NPs are widely used in tissue engineering scaffolds for their ability to fine-tune the scaffolds' mechanical strength as well as entrap and deliver stem cells, growth factors, and other bioactive agents required for the regeneration of the infarcted myocardium post-MI and for the endothelialization of synthetic scaffolds [201].

Self-assembled polymeric NPs consisting of heparin and chitosan were developed for the sustained release of VEGF and were immobilized to the nanofibers of decellularized buffalo bovine jugular vein scaffolds to accelerate their vascularization. Indeed, the NPs successfully promoted higher fibroblast infiltration, ECM production, and new capillary formation in a mouse subcutaneous implantation model *in vivo*, showing promising results for future MI applications [202]. Moreover, bilayered NPs composed of a PLGA core and PLLA shell were found to induce sequential release of platelet-derived growth factor following co-release of VEGF and bFGF. Upon incorporation in a fibrin matrix, they were found to promote angiogenesis in an *ex vivo* rat aortic ring assay, suggesting their potential application within scaffolds for MI repair [203]. Furthermore, Wang et al. used an H_2O_2-sensitive injectable hydrogel strengthened with the self-assembled nanodrug tanshinone IIA. The NPs were coated with polydopamine to ensure their entrapment within the hydrogel through chemical cross-linking. The hydrogel exhibited slow degradation upon injection in a rat MI model which prompted the sustained release of the drug within the infarct and resulted in increased LV ejection fraction, decreased infarct size, and inhibition of inflammatory factors [204]. Another injectable hydrogel with shear-thinning properties was synthesized for the localization of miRNA-loaded polymeric NPs. The miR-199a-3p is a microRNA that had already demonstrated a potential for treating CVDs. Accordingly, it was entrapped in core-shell NPs of poly (9,9-dioctylfluorene-alt-benzothiadiazole)/PEG. The NPs showed great potential in inducing proliferation of cardiac and endothelial cells, as well as promoting angiogenesis in hypoxic conditions. *In vivo*, the NPs/hydrogel system successfully improved cardiac function and enhanced capillary density in the infarct border zone [205].

Other researchers focused on synthesizing polymeric NPs to functionalize conductive engineered cardiac patches (ECP) as substitutes for the infarcted tissue since they can bridge electrical signals of healthy myocardium across the scar obstacle and activate living cardiomyocytes. Conductive NPs made of gelatin methacrylate/polypyrrole (GelMA/Ppy) were cross-linked on an electrospun-GelMA/polycaprolactone nanofibrous membrane via a mussel-inspired cross-linker. Upon transplantation of this biocompatible ECP in a rat MI model for 4 weeks, the infarcted myocardium was repaired by enhancing cardiac function and promoting revascularization [206]. Similarly, Wang et al. developed Ppy NPs and incorporated them into a GelMA/PEG cryogel using a mussel-inspired cross-linker to obtain optimal mechanical and superelastic properties for the ECP. In an *in vivo* rat MI model, the GelMA/PEG NPs were shown to migrate from the ECP, fuse to the surface of cardiomyocytes, and promote their synchronous contraction which resulted in improved cardiac function [207]. Overall, polymeric NPs have shown to be adequate DDS for the delivery of drugs and/or growth factors within various scaffolds for the treatment of the injured heart after MI (Table 8).

5. Implication of polymeric NPs in theranostic approaches for MI

Theranostics is an emerging scientific discipline that combines diagnostic techniques and targeted therapy to achieve a personalized clinical approach for every patient. Polymeric biodegradable NPs have been used for the past two decades in nanotheranostics as they represent optimal

Table 8
Therapeutic applications of polymeric NPs in cardiac scaffolds.

Type of nanosystem	Entrapped cargo	Therapeutic effect	Ref.
Heparin/Chitosan NPs - immobilized decellularized buffalo bovine jugular vein scaffold	VEGF	**In vitro** Promoted effective localization and sustained release of VEGF over several weeks **In vivo subcutaneous implantation** Promoted higher fibroblast infiltration Enhanced ECM production Induced new capillary formation	[202]
Poly (lactic-co-glycolic acid)/Poly-L-lactic acid NPs incorporated in a fibrin matrix	PDGF VEGF bFGF	**In vitro** Promoted sequential release of PDGF following co-release of VEGF and bFGF **Ex vivo rat aortic ring assay** Promoted angiogenesis	[203]
Tanshinone IIA NPs - immobilized H_2O_2-sensitive injectable hydrogel	Tanshinone IIA	**In vivo I/R model** Promoted retention of hydrogel within rat hearts for 4 weeks Sustained release of Tanshinone IIA within the infarct Inhibition of inflammation Decreased infarct size Improved cardiac function	[204]
Poly (9,9-dioctylfluorene-alt-benzothiadiazole)/poly (ethylene glycol) NPs – immobilized in shear-thinning injectable hydrogel	miR-199a-3p	**In vitro** Induced proliferation of cardiac and endothelial cells Promoted angiogenesis in hypoxic conditions **In vivo MI model** Improved cardiac function Doubled capillary density in the border zone	[205]
Gelatin methacrylate/Polypyrrole NPs - crosslinked Gelatin methacrylate/ Polycaprolactone membrane	GelMA/Ppy NPs	**In vitro** NPs produced high conductivity of ECP **In vivo MI model** Improved cardiac function Promoted revascularization	[206]
Polypyrrole NPs - crosslinked Gelatin methacrylate/Poly (ethylene glycole) cryogel	Ppy NPs	**In vivo MI model** Promoted NPs' migration to cardiomyocytes and induced their synchronous contraction Improved cardiac function	[207]

candidates for the simultaneous delivery of therapeutic and imaging agents to promote monitoring of drug release and to evaluate in real time its therapeutic efficacy for various diseases (Fig. 15) [208].

Stem cell transplantation is a novel approach for regenerating the lost myocardium after MI and restoring proper cardiac function within the infarct. However, as mentioned earlier, it remains challenging to maintain stem cells' viability after transplantation and increase their retention rate within the myocardium which is currently no more than 0.1–15%. Accordingly, Gomez-Mauricio et al. developed a new theranostic approach to promote cardiac repair post-MI by delivering and tracking ASCs encapsulated within magnetic resonance-labeled microcapsules. The particles consisted of a mixture of alginate solution, Endorem (commercially available superparamagnetic iron oxide NPs), and ASCs cell pellet, extruded into a calcium chloride solution to form magnetic alginate beads. The magnetic alginate beads were then cross-linked with solutions of PLL followed by another alginate solution to obtain the final particles of magnetic resonance-labeled alginate-PLL-alginate microcapsules termed as "magnetocapsules". These capsules were able to maintain high cellular viability of ASCs for 21 days in culture and the magnetic labeling did not affect their viability. *In vivo* MRI imaging showed that ASCs-encapsulated magnetocapsules were detected within the infarcted myocardium of a porcine MI model up to 30 days post-injection without any loss of the iron oxide label intensity, indicating that ASCs were efficiently retained within the myocardium. Furthermore, these stem cells-laden magnetocapsules were able to improve cardiac function by decreasing the infarct size and increasing the LV ejection fraction as determined by MRI [209]. Another study also utilized polymeric NPs in a theranostic approach for cardiac regeneration. A lipid-based copolymer of DSPE-PEG-Maleimide was synthesized for the entrapment of a semiconductor polymeric contrast agent (PCPDTBT). The NPs were further functionalized with cell-penetrating peptides which increased their labeling efficiency for human embryonic stem cell-derived cardiomyocytes. Upon transplantation of the labeled cells into living murine hearts, both ultrasound and photoacoustic imaging permitted real-time monitoring of the delivery, engraftment, and localization of the labeled cells with high spatial resolution. This study highlighted the advantages of integrating polymeric NPs for photoacoustic imaging as a method to monitor the fate of transplanted cardiac cells in regenerative therapies [210].

Theranostic nanosystems can also be applied for the controlled delivery of therapeutic agents as well as accurate imaging and diagnosis of I/R diseases. Kang et al. developed micellar NPs from near-infrared fluorescent dye-conjugated H_2O_2-scavenging boronate polymers for imaging obstructive thrombus and inhibiting further thrombus formation. Not only does boronate scavenge H_2O_2 but it releases the antioxidant agent hydroxybenzyl alcohol (HBA) upon H_2O_2-mediated oxidation. As fibrin is one of the most important and abundant components of thrombi, the NPs were further decorated with fibrin-targeting lipopeptides on their surface to achieve site specific delivery and minimize off-target effects. These NPs, termed fibrin-targeted imaging and antithrombotic nanomedicine (FTIAN), used at 100 μg/mL were able to suppress cytotoxicity and exert antioxidant and anti-inflammatory activities in H_2O_2-stimulated macrophages and arterial endothelial cells. They also exhibited antiplatelet activities by significantly suppressing the expression of soluble CD40 ligand (sCD40L) on activated platelets. Importantly, all these mentioned effects were significantly higher upon using FTIAN as compared to HBA alone. Moreover, *in vivo* studies conducted on murine carotid thrombosis model injected with FTIAN NPs demonstrated significant reduction of inflammation and platelet activation as evidenced by the decrease in the levels of TNF-α and sCD40L, respectively. Also, upon loading these NPs with the anti-thrombotic drug tirofiban, they were able to remarkably inhibit thrombus formation and suppress ROS generation at a reduced dose of the drug. Lastly, the NPs also served as dual imaging agents as they enhanced the fluorescence and photoacoustic intensity of fibrin-rich clots obstructing arteries. Overall, these novel NPs represent promising thrombus-specific theranostic agents that could be applied for different CVDs caused primarily by thrombosis such as type 1 MI [211]. Another study also applied polymeric NPs for the entrapment of therapeutic agents and monitoring their delivery and dosage via imaging techniques. Chitosan hydrogel NPs radiolabeled with

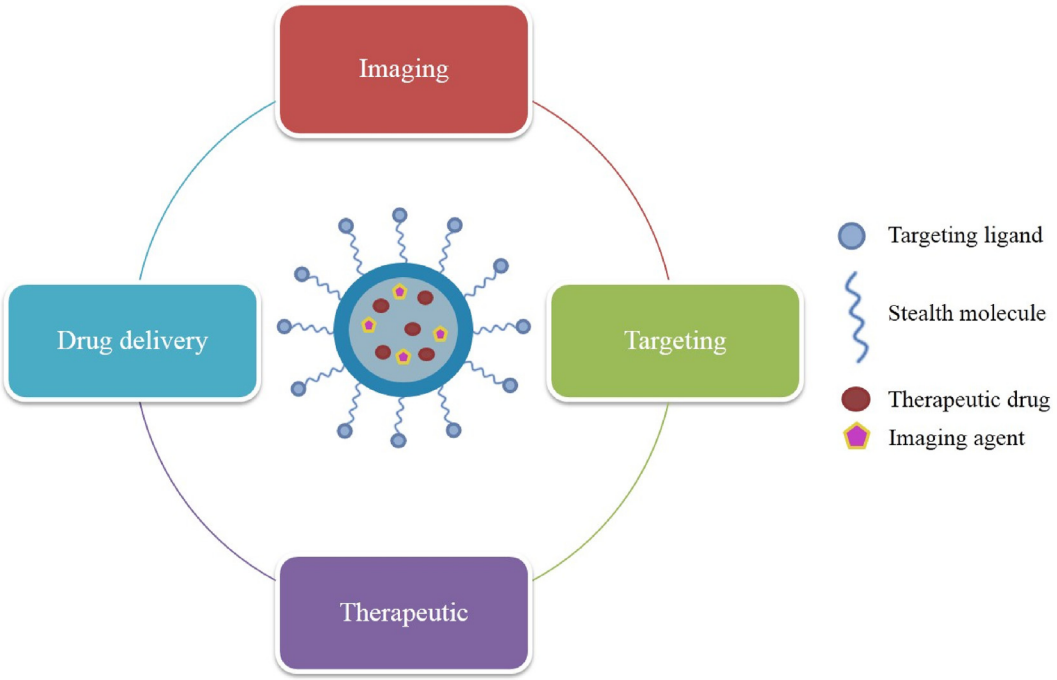

Fig. 15. Scheme summarizing the functions of polymeric NPs as nanotheranostic agents.

Table 9
Theranostic applications of polymeric NPs.

Type of nanosystem	Entrapped bioactive agents	Entrapped imaging agents	Surface modification	Theranostic effect	Ref.
Alginate/poly-L-lysine NPs	Adipose-derived stem cells VEGF	Endorem (Iron oxide NPs)	–	**In vitro** Maintained high cell viability of stem cells **In vivo MI model** Retained stem cells within infarcted myocardium Maintained high magnetic labeling intensity Improved cardiac function	[209]
DSPE-poly (ethylene glycol)-Maleimide NPs	–	Semiconductor polymeric contrast agent (PCPDTBT)	Cell-penetrating peptides	**In vitro** Provided efficient labeling of human embryonic stem cells-derived cardiomyocytes **In vivo mouse model** Allowed tracking and monitoring of transplanted human embryonic stem cells-derived cardiomyocytes with high spatial resolution	[210]
Boronate NPs	Tirofiban	Near-infrared fluorescent dye (IR820)	Fibrin-targeting lipopeptides	**In vitro** Inhibited cytotoxicity, inflammation, and ROS generation in H_2O_2–stimulated cells Exhibited antiplatelet activities **In vivo carotid thrombosis model** Reduced inflammation and platelet activation Inhibited thrombus formation and ROS generation Enhanced fluorescence and photoacoustic intensity of fibrin-rich clots	[211]
Chitosan hydrogel NPs	VEGF peptides	Radionuclide technetium 99 m	–	**In vivo I/R model** Reduced perfusion defects Induced angiogenesis Retained radionuclide and allowed image-guided drug dosage control	[212]

technetium 99 m and entrapping $VEGF_{81–91}$ peptides were tested in a murine model of cardiac I/R. They were found to reduce perfusion defects and increase vascular density in the ischemic region of the myocardium and promote retention of the radionuclide of up to 9.2% as evidenced by SPECT. Accordingly, these NPs are good candidates for the controlled delivery of VEGF peptides as well as for quantitative radionuclide imaging which can help customize treatment of myocardial ischemia [212]. In conclusion, studies have demonstrated the feasibility of applying polymeric NPs for the concomitant delivery of drugs and imaging agents for theranostic applications in MI (Table 9).

6. Discussion, conclusion, and future prospects

Polymeric NPs have been explored extensively in the past decades for their ability to entrap and deliver imaging agents and therapeutic molecules to diseased tissues. They most often achieve this delivery via EPR-

mediated passive targeting whereby they tend to accumulate preferentially in an inflamed region with leaky vasculature such as in a tumor and MI microenvironment. While the small size of polymeric NPs is the most important property driving this EPR effect, their synthesis must be achieved meticulously as sizes less than 10 nm will inevitably lead to rapid and undesired renal clearance. Accordingly, coating NPs with biocompatible polymers and proteins is advantageous to increase their size and molecular weight and promote prolonged circulation in the blood and delayed clearance. Also, the extremely small size of NPs causes them to enter non-specifically into different cell types or lengthen their circulation time without reaching their specific target [110,213,214]. Therefore, releasing NPs from larger particles or different carriers like hydrogels and scaffolds may increase the probability of margination and adhesion to endothelial walls. Another way to overcome non-specific cell targeting is by adding targeting ligands to the surface of NPs.

Research has been ongoing towards active targeted delivery of NPs to ensure higher accumulation within the infarcted myocardium, prolonged retention time, and enhanced imaging and/or therapeutic effect. To achieve active targeting, it is vital to uncover proteins, receptors, and glycosaminoglycans among others that are highly expressed on the surface of targeted cells. For diagnosis, detection, and monitoring of MI, enhanced imaging is advised for CT, CMR, and other imaging techniques following ECG and troponin level analysis [215]. Accordingly, contrast agents entrapped in appropriate polymeric NPs with optical and magnetic properties can provide better assessment of myocardial pathophysiological changes and quantification of infarct size. To promote selective uptake of these NPs by cardiac-specific inflammatory cells and viable cardiomyocytes, NPs must be coated with ligands that can recognize receptors exclusive to the damaged area and highly expressed during the time of administration. Scavenger receptor A1, C-reactive protein, and fibrin are molecules widely expressed on the surface of macrophages and in the inflammatory MI microenvironment. Hence, their appropriate ligands can be adsorbed onto the surface of NPs to promote active targeting and accurate detection of myocarditis. Similarly, ANP, AT1R, GlcNAc receptor, and $\alpha_v\beta_3$ integrin are some of the molecules highly expressed and secreted within the infarcted myocardium to stimulate cardiac repair and angiogenesis. Accordingly, adsorbing their ligands to NPs' surface can be exploited to achieve targeted imaging of the infarct size and neoangiogenesis. In a similar fashion, active targeting can be employed to deliver drug-loaded polymeric NPs to the injured myocardium, avoiding NPs distribution in non-specific tissues. Endogenous factors can also be exploited to induce triggered release of the bioactive agents from the NPs once present in the targeted infarct region. Accordingly, polymeric NPs can be engineered to possess stimuli-responsive properties. Hence, they can be stimulated to degrade and release the entrapped drug upon the presence of MI-specific factors such as low pH, redox and hypoxic environment, or the overexpression of MMP-2/9.

Various types of NPs, made from natural or synthetic polymers, were explored for their potential as diagnostic, therapeutic, and theranostic tools for MI. Biodegradable polymers have hydrolytically or enzymatically labile bonds that break and exhibit a triggered functionality in a physiologic environment, and they are ideal in the field of drug delivery [216]. Indeed, we found that PLGA is the most commonly used polymer involved in the synthesis of NPs as it promotes biodegradability, biocompatibility, and sustained release of the entrapped drug. While PEG is non-biodegradable, it is also widely used in NPs, mostly due to its high hydrophilicity, high molecular size, and low immunogenicity and antigenicity. Accordingly, PEGylation of NPs increases their solubility, extends their half-life, and shields them from recognition by antibodies and proteases. Natural polymers such as polysaccharides (alginate, chitosan, dextran, hyaluronan, β-cyclodextrin) and proteins (serum albumin, PLL) are also implicated in NPs synthesis. They are often utilized to deliver drugs, sequester inflammatory factors, and promote signaling in the infarcted area due to their favorable biocompatibility and biodegradability properties [217,218]. They are also more susceptible to be translated into biological mimics that serve as ECM entities or signaling molecules [219,220]. Moreover, dendrimers, which strongly resemble proteins in their structure, have proved to be successful NPs for imaging of MI as they formed macromolecular contrast enhancement agents which allowed them to overcome the rapid clearance of conventional low molecular weight imaging dyes. Also, these NPs can be versatile; by modifying their dendritic branching and PEO length, they can adsorb different radiotracers as well as therapeutic agents and hence may have great potential for theranostic applications [221].

The studies covered in this review highlight the great potential of polymeric NPs to provide personalized and accurate detection, diagnosis, and treatment for MI patients. However, there are several limitations and challenges which need to be addressed. As a consequence of the NPs small size and large surface area, particle-particle aggregation brings about difficulties in the physical handling of the NPs in liquid and dry form [222]. Coating NPs with positively or negatively charged polymers is widely used to enhance the NPs biocompatibility, cellular uptake, or adsorption to genetic material; however, their concentration must be well thought-out to avoid undesired effects. PAA-coated upconverting NPs were shown to be good candidates for reducing background signals in cTnI immunoassays. However, the highly negative charge of PAA may lead to non-specific binding and reduced stability of UCNPs which compromises the sensitivity of the immunoassay. Conjugation of PEG along with PAA to UCNPs may be considered as a solution to reduce undesired non-specific binding [223]. Also, coating NPs with PEI is favorable for adsorption of cell-reprogramming genes in regenerative therapy. However, as previously mentioned, PEI must be used with caution as it can trigger an inflammatory response and as such further studies are needed to confirm the inertness of the NPs. In this case replacing PEI coating with positively charged natural polymers such as chitosan or polymers made from natural amino acids such as PLL may be a safer approach [224,225]. Moreover, regarding nuclear imaging of MI, most studies focused on providing accurate delivery of the contrast agent-loaded NPs to the injured myocardium but did not attempt to reduce radiation exposure. This can be achieved by inducing modifications to the NPs such as using ^{68}Ga tracer instead of ^{89}Zr. Also, the NPs can be further modified to prolong their human blood half-life by modification of residuals amines with alternative capping agents. Moreover, while several studies indicated that imaging agent-loaded polymeric NPs can produce higher contrast enhancement in murine heart muscle compared to other organs, additional NPs surface modification and further studies in CVD models are required to evaluate the NPs potential to promote selective targeting to the injured area and hence, produce infarct-specific contrast enhancement by CMR to allow proper MI diagnosis.

Furthermore, regarding therapeutic approaches, we found that polymeric hydrogels hold great potential in delivering and maintaining cardiac stem cells viability and retaining them within the ischemic myocardium. However, significant numbers of transplanted stem cells were progressively lost which underlines the need for improving the hydrogel constituents. This can be achieved by supplementing polymeric hydrogels with ECM constituents to help enhance CSC proliferation and impregnating the hydrogel with supportive cytokines to pre-condition CSC for survival and promote indirect cardiac repair. Polymeric NPs were also involved within various scaffolds to promote sustained delivery of growth factors and other biological molecules. Importantly, they showed great potential to incorporate 3D patterned hydrogels and achieve spatiotemporal control of the entrapped bioactive agents, which is vital for the treatment of MI. However, certain studies showed discrepancies between the *in vitro* and *in vivo* hydrogel degradation rate, and hence it is important to seriously consider these distinct behaviors when designing polymeric hydrogels intended for human use in MI patients. Another limitation worth mentioning is that most studies did not investigate the possible immunomodulatory effects of the utilized polymeric NPs. While macrophage recruitment to the implanted scaffolds is required to promote their biological degradation and their replacement

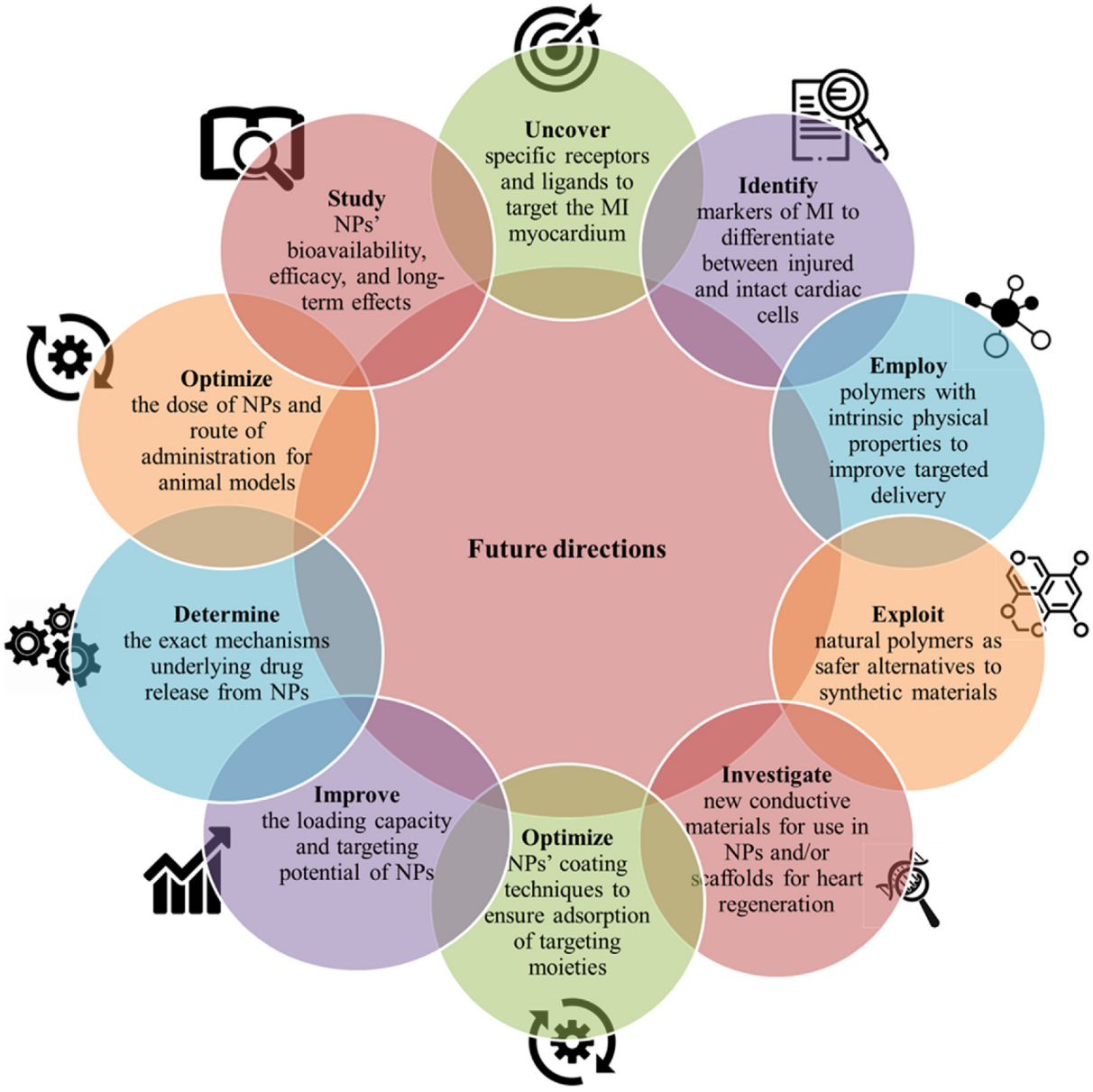

Fig. 16. Scheme summarizing the main suggested future directions.

with endogenous ECM, extensive immune cell infiltration should be avoided as it can prevent, delay, or complicate adequate cardiac repair post-MI. Furthermore, while polymeric NPs designed as theranostic tools allowed monitoring and tracking of the entrapped cells' delivery and engraftment, they did not provide information on cells fate such as cell death by necrosis or apoptosis. This is important to monitor the survival and differentiation of transplanted stem cells and their progenitors and keep track of their fate *in vivo*.

In conclusion, current advances in nanomedicine have paved the way for rapid diagnosis and treatment of MI which is crucial for the recovery and survival of patients. The development of these versatile polymeric NPs and new theranostic strategies possess great potential in enhancing and personalizing imaging and treatment of MI patients. Further works are however needed to allow the evolution of polymeric NPs towards clinical applications. Future studies should focus more on active and triggered targeting approaches and accordingly more research is needed to: (1) identify markers of MI to differentiate between injured and intact cardiomyocytes, (2) uncover polymers with intrinsic optical, magnetic, and conductive properties as well as thermal-, enzymatic-, and pH-sensitivities to improve targeted delivery, and (3) optimize the coating techniques of NPs to ensure proper adsorption of the targeting moieties without overloading the NPs and creating steric hindrance. Also, more research should be focused on exploiting natural polymers as they are more biocompatible than their synthetic counterparts, more likely to be biodegradable and cause fewer toxic effects. Moreover, further studies should investigate new conductive materials for use within NPs and/or scaffolds for the regeneration of the heart post-MI since the loss of electric unification between the infarcted tissue and the remote myocardium is known to lead to ventricular dysfunction as well as heart failure [226]. The electroactive polymers presently used such as polypyrrole, polyaniline, and polythiophene are limited by their poor electrical conductivity especially in neutral and high pH environments [227,228].

While various polymeric NPs for cancer therapy are already in clinical trial phases, those applied for CVD in general, and for MI in particular, are still far behind [229]. Further studies are needed before their translation to clinical applications. Additional *in vitro* studies need to be carried out to determine the stability of NPs with time and environmental factors such as temperature and humidity and their effect on the

entrapped cargo as well as on the overall physicochemical properties of the NPs. These stability studies are especially required when NPs are developed in one center and then transported to a different one where *in vitro* and *in vivo* studies are carried out as this might affect the results and cause discrepancies. Also, further works are required to help improve the loading capacity and targeting potential of NPs, as well as determine the exact mechanisms underlying their drug release. Moreover, preclinical research is required to determine the optimal formulation, pharmacology, safety profile, and the full range of diagnostic/therapeutic applications of polymeric NPs. Besides, the concentration of administered NPs and the route of administration are important parameters that need to be optimized on animal models. Long-term studies with a prolonged follow-up period are also needed to determine the bioavailability of NPs in plasma, their entrapment in other non-targeted tissues, their efficacy, as well as potential toxic effects on the tissue, cellular, and molecular level (Fig. 16).

Polymeric NPs are promising delivery systems for overcoming the limitations of current diagnostic and therapeutic approaches of MI. These versatile NPs hold great potential in providing rapid and personalized imaging and treatment of not only MI, but any given disease. Research on polymeric NPs is continuously growing and shaping the field of nanomedicine and we anticipate that in the near future polymeric NPs will be used extensively in the clinic, improving the quality of life of the population.

Declaration of competing interest

The authors declare that they have no known competing financial interests or personal relationships that could have appeared to influence the work reported in this paper.

Acknowledgement

This work was made possible by grants from the AUB Medical Practice Plan (MPP), University Research Board (URB) and National Council for Scientific Research (CNRS). All statements made here are the sole responsibility of the authors.

References

[1] M. Smit, A.R. Coetzee, A. Lochner, The pathophysiology of myocardial ischemia and perioperative myocardial infarction, J. Cardiothorac. Vasc. Anesth. 34 (2020) 2501–2512, https://doi.org/10.1053/j.jvca.2019.10.005.
[2] A.S. Go, et al., Heart disease and stroke statistics–2014 update: a report from the American Heart Association, Circulation 129 (2014) 280–292, https://doi.org/10.1161/01.cir.0000441139.02102.80.
[3] G.S. Wagner, et al., The importance of identification of the myocardial-specific isoenzyme of creatine phosphokinase (MB form) in the diagnosis of acute myocardial infarction, Circulation 47 (1973) 263–269, https://doi.org/10.1161/01.cir.47.2.263.
[4] Gregory A. Nichols, et al., Medical care costs among patients with established cardiovascular disease, Am. J. Manag. Care 16 (2010) 86–93.
[5] V.M. Martin Gimenez, D.E. Kassuha, W. Manucha, Nanomedicine applied to cardiovascular diseases: latest developments, Ther Adv Cardiovasc Dis 11 (2017) 133–142, https://doi.org/10.1177/1753944717692293.
[6] K. Thygesen, et al., Third universal definition of myocardial infarction, J. Am. Coll. Cardiol. 60 (2012) 1581–1598, https://doi.org/10.1016/j.jacc.2012.08.001.
[7] Joshua Chadwick Jayaraj, et al., Epidemiology of myocardial infarction Intech, (2018), pp. e707102, 10.5772/intechopen.74768.
[8] K. Thygesen, et al., Universal definition of myocardial infarction, Eur. Heart J. 28 (2007) 2525–2538, https://doi.org/10.1093/eurheartj/ehm355.
[9] Jagdish C. Mohan, J. Narula, New universal definition of myocardial infarction, Glob. Implicat. Appl. Need Glob. Heart 7 (2012) 377–380.
[10] Kristian Thygesen, et al., Third universal definition of myocardial infarction Nat, Rev. Cardiol. (2012) 2020–2035.
[11] N.G. Frangogiannis, Pathophysiology of myocardial infarction, Compr. Physiol. 5 (2015) 1841–1875, https://doi.org/10.1002/cphy.c150006.
[12] P. Christia, et al., Systematic characterization of myocardial inflammation, repair, and remodeling in a mouse model of reperfused myocardial infarction, J. Histochem. Cytochem. 61 (2013) 555–570, https://doi.org/10.1369/0022155413493912.
[13] M. Nahrendorf, M.J. Pittet, F.K. Swirski, Monocytes: protagonists of infarct inflammation and repair after myocardial infarction, Circulation 121 (2010) 2437–2445, https://doi.org/10.1161/CIRCULATIONAHA.109.916346.
[14] A.C. Silva, et al., Bearing my heart: the role of extracellular matrix on cardiac development, homeostasis, and injury response, Front. Cell Dev. Biol. 8 (2021) e621644, https://doi.org/10.3389/fcell.2020.621644.
[15] E. Wan, et al., Enhanced efferocytosis of apoptotic cardiomyocytes through myeloid-epithelial-reproductive tyrosine kinase links acute inflammation resolution to cardiac repair after infarction Circ, Res. 113 (2013) 1004–1012, https://doi.org/10.1161/CIRCRESAHA.113.301198.
[16] S.D. Prabhu, N.G. Frangogiannis, The biological basis for cardiac repair after myocardial infarction: from inflammation to fibrosis, Circ. Res. 119 (2016) 91–112, https://doi.org/10.1161/CIRCRESAHA.116.303577.
[17] M.L. Lindsey, J.J. Saucerman, K.Y. DeLeon-Pennell, Knowledge gaps to understanding cardiac macrophage polarization following myocardial infarction, Biochim. Biophys. Acta 1862 (2016) 2288–2292, https://doi.org/10.1016/j.bbadis.2016.05.013.
[18] A. Anzai, et al., Regulatory role of dendritic cells in postinfarction healing and left ventricular remodeling, Circulation 125 (2012) 1234–1245, https://doi.org/10.1161/CIRCULATIONAHA.111.052126.
[19] U. Hofmann, et al., Activation of CD4+ T lymphocytes improves wound healing and survival after experimental myocardial infarction in mice, Circulation 125 (2012) 1652–1663, https://doi.org/10.1161/CIRCULATIONAHA.111.044164.
[20] A.V. Shinde, N.G. Frangogiannis, Fibroblasts in myocardial infarction: a role in inflammation and repair, J. Mol. Cell. Cardiol. 70 (2014) 74–82, https://doi.org/10.1016/j.yjmcc.2013.11.015.
[21] A.V. Shinde, C. Humeres, N.G. Frangogiannis, The role of alpha-smooth muscle actin in fibroblast-mediated matrix contraction and remodeling Biochim Biophys, Acta. Mol. Basis Dis. 1863 (2017) 298–309, https://doi.org/10.1016/j.bbadis.2016.11.006.
[22] P. Kong, P. Christia, N.G. Frangogiannis, The pathogenesis of cardiac fibrosis Cell, Mol. Life Sci. 71 (2014) 549–574, https://doi.org/10.1007/s00018-013-1349-6.
[23] N.G. Frangogiannis, Cardiac fibrosis: cell biological mechanisms, molecular pathways and therapeutic opportunities, Mol. Aspect. Med. 65 (2019) 70–99, https://doi.org/10.1016/j.mam.2018.07.001.
[24] Xiao-Hong Lai, et al., A fluorescence immunochromatographic assay using Europium (III) chelate microparticles for rapid, quantitative and sensitive detection of creatine kinase, J. Fluorescen. 26 (2016) 987–996.
[25] R. Aloe, et al., Improved efficiency and cost reduction in the emergency department by replacing contemporary sensitive with high-sensitivity cardiac troponin immunoassay, Acta Biomed. 90 (2019) 614–620, https://doi.org/10.23750/abm.v90i4.8769.
[26] M.A. Daubert, A. Jeremias, The utility of troponin measurement to detect myocardial infarction: review of the current findings, Vasc. Health Risk Manag. 6 (2010) 691–699, https://doi.org/10.2147/vhrm.s5306.
[27] S. Aydin, et al., Biomarkers in acute myocardial infarction: current perspectives, Vasc. Health Risk Manag. 15 (2019) 1–10, https://doi.org/10.2147/Vhrm.S166157.
[28] Gregory Lee, S. Liu, Monoclonal antibodies against human cardiac troponin I for immunoassays II, Monoclon. Antibodies Immunodiagn. Immunother. 34 (2015) 169–173, https://doi.org/10.1089/mab.2014.0088.
[29] Y. Cai, et al., Rapid and sensitive detection of cardiac troponin I for point-of-care tests based on red fluorescent microspheres, Molecules 23 (2018) 1102–1114, https://doi.org/10.3390/molecules23051102.
[30] P. Rajiah, et al., MR imaging of myocardial infarction, Radiographics 33 (2013) 1383–1412, https://doi.org/10.1148/rg.335125722.
[31] A. Kidambi, et al., Factors associated with false-negative cardiovascular magnetic resonance perfusion studies: a Clinical evaluation of magnetic resonance imaging in coronary artery disease (CE-MARC) substudy, J. Magn. Reson. Imag. 43 (2016) 566–573, https://doi.org/10.1002/jmri.25032.
[32] M.M. Meloni, et al., Contrast agents for cardiovascular magnetic resonance imaging: an overview, J. Mater. Chem. B 5 (2017) 5714–5725, https://doi.org/10.1039/c7tb01241a.
[33] J.S. McDonald, R.J. McDonald, MR imaging safety considerations of gadolinium-based contrast agents gadolinium retention and nephrogenic systemic fibrosis magnetic resonance imaging, Clin. North Am. 28 (2020) 497–507, https://doi.org/10.1016/j.mric.2020.06.001.
[34] R. Manka, et al., Multicenter evaluation of dynamic three-dimensional magnetic resonance myocardial perfusion imaging for the detection of coronary artery disease defined by fractional flow reserve Circ, Cardiovasc. Imag. 8 (2015) e003061, https://doi.org/10.1161/CIRCIMAGING.114.003061.
[35] L. La Grutta, et al., Infarct characterization using CT Cardiovasc Diagn Ther 7 (2017) 171–188, https://doi.org/10.21037/cdt.2017.03.18.
[36] G.A. Rodriguez-Granillo, Delayed enhancement cardiac computed tomography for the assessment of myocardial infarction: from bench to bedside, Cardiovasc. Diagn. Ther. 7 (2017) 159–170, https://doi.org/10.21037/cdt.2017.03.16.
[37] G.P. Perna, Preventing myocardial infarction: use and limitation of non-invasive imaging modalities, Eur. Heart J. Suppl. 22 (2020) E110–E112, https://doi.org/10.1093/eurheartj/suaa073.
[38] M.S. Davenport, et al., Use of intravenous iodinated contrast media in patients with kidney disease: consensus statements from the, American College of Radiology and the National Kidney Foundation Radiology 294 (2020) 660–668, https://doi.org/10.1148/radiol.2019192094.
[39] R.J. Han, et al., Diagnostic accuracy of coronary CT angiography combined with dual-energy myocardial perfusion imaging for detection of myocardial infarction, Exp. Ther. Med. 14 (2017) 207–213, https://doi.org/10.3892/etm.2017.4485.
[40] L. Marti-Bonmati, et al., Multimodality imaging techniques Contrast Media Mol Imaging 5 (2010) 180–189, https://doi.org/10.1002/cmmi.393.

[41] S.L. Thorn, et al., Application of hybrid matrix metalloproteinase-targeted and dynamic (201)Tl single-photon emission computed tomography/computed tomography imaging for evaluation of early post-myocardial infarction remodeling, Circ Cardiovasc Imaging 12 (2019) e009055, https://doi.org/10.1161/CIRCIMAGING.119.009055.
[42] K. Fukushima, et al., Molecular hybrid positron emission tomography/computed tomography imaging of cardiac angiotensin II type 1 receptors, J. Am. Coll. Cardiol. 60 (2012) 2527–2534, https://doi.org/10.1016/j.jacc.2012.09.023.
[43] C. Rischpler, et al., PET/MRI early after myocardial infarction: evaluation of viability with late gadolinium enhancement transmurality vs. 18F-FDG uptake, Eur. Heart J Cardiovasc. Imag. 16 (2015) 661–669, https://doi.org/10.1093/ehjci/jeu317.
[44] D. Agostini, et al., Performance of cardiac cadmium-zinc-telluride gamma camera imaging in coronary artery disease: a review from the cardiovascular committee of the European Association of Nuclear Medicine (EANM), Eur. J. Nucl. Med. Mol. Imag. 43 (2016) 2423–2432, https://doi.org/10.1007/s00259-016-3467-5.
[45] H.J. Harms, et al., Comparison of clinical non-commercial tools for automated quantification of myocardial blood flow using oxygen-15-labelled water PET/CT, Eur. Heart J Cardiovasc. Imag. 15 (2014) 431–441, https://doi.org/10.1093/ehjci/jet177.
[46] R.S. Driessen, et al., Measurement of LV volumes and function using oxygen-15 water-gated PET and comparison with CMR imaging, JACC Cardiovasc Imaging 9 (2016) 1472–1474, https://doi.org/10.1016/j.jcmg.2016.01.014.
[47] A. Komosa, et al., Significance of antiplatelet therapy in emergency myocardial infarction treatment Postepy Kardiol, Interwencyjnej 10 (2014) 32–39, https://doi.org/10.5114/pwki.2014.41466.
[48] U. Schilling, J. Dingemanse, M. Ufer, Pharmacokinetics and pharmacodynamics of approved and investigational P2Y12 receptor antagonists, Clin. Pharmacokinet. 59 (2020) 545–566, https://doi.org/10.1007/s40262-020-00864-4.
[49] D.E. Baker, K.T. Ingram, Cangrelor Hosp Pharm 50 (2015) 922–929, https://doi.org/10.1310/hpj5010-922.
[50] M.P. Bonaca, M.S. Sabatine, Antiplatelet therapy for long-term secondary prevention after myocardial infarction, Jama Cardiology 1 (2016) 627–628, https://doi.org/10.1001/jamacardio.2016.2110.
[51] R. Tummala, M.P. Rai, Glycoprotein IIb/IIIa inhibitors, in: StatPearls, 2022. Treasure Island (FL.
[52] D. Atar, et al., Anticoagulants for secondary prevention after acute myocardial infarction: lessons from the past decade, Fundam. Clin. Pharmacol. 28 (2014) 353–363, https://doi.org/10.1111/fcp.12063.
[53] E. Uygungul, et al., Determining risk factors of bleeding in patients on warfarin treatment, Adv Hematol 2014 (2014) 369084, https://doi.org/10.1155/2014/369084.
[54] W. Shuaib, et al., Warfarin therapy: survey of patients' knowledge of their drug regimen malays, J. Med. Sci. 21 (2014) 37–41.
[55] A. Budovich, O. Zargarova, A. Nogid, Role of apixaban (eliquis) in the treatment and prevention of thromboembolic disease, P T 38 (2013) 206–231.
[56] E.C. Christopoulou, T.D. Filippatos, M.S. Elisaf, Non-hemorrhage-related adverse effects of rivaroxaban, Arch Med Sci Atheroscler Dis 2 (2017) 108–112, https://doi.org/10.5114/amsad.2017.72533.
[57] B. Burstein, et al., Anticoagulation with direct thrombin inhibitors during extracorporeal membrane oxygenation World, J Crit Care Med 8 (2019) 87–98, https://doi.org/10.5492/wjccm.v8.i6.87.
[58] M. Linder, et al., Assessing safety of direct thrombin inhibitors, direct factor Xa inhibitors and vitamin K antagonists in patients with atrial fibrillation: a nation-wide propensity score matched cohort from Sweden, Clin. Epidemiol. 12 (2020) 1029–1038, https://doi.org/10.2147/CLEP.S258373.
[59] V. Andersson, et al., Macrocyclic prodrugs of a selective nonpeptidic direct thrombin inhibitor display high permeability, Efficient Bioconversion but Low Bioavailability Journal of Medicinal Chemistry 59 (2016) 6658–6670, https://doi.org/10.1021/acs.jmedchem.5b01871.
[60] V. Roolvink, et al., Early intravenous beta-blockers in patients with ST-segment elevation myocardial infarction before primary percutaneous coronary intervention, J. Am. Coll. Cardiol. 67 (2016) 2705–2715, https://doi.org/10.1016/j.jacc.2016.03.522.
[61] C.C. Zhang, et al., Bisoprolol protects myocardium cells against ischemia/reperfusion injury by attenuating unfolded protein response in rats, Sci. Rep. 7 (2017) e11859, https://doi.org/10.1038/s41598-017-12366-8.
[62] S.S. Nagargoje, P.R.R., An overview on formulation and development of nanoparticulate matrix tablets for beta blockers, J. Drug Deliv. Therapeut. 9 (2019) 1078–1084, https://doi.org/10.22270/jddt.v9i3-s.2932.
[63] A.J. Barron, et al., Systematic review of genuine versus spurious side-effects of beta-blockers in heart failure using placebo control: recommendations for patient information, Int. J. Cardiol. 168 (2013) 3572–3579, https://doi.org/10.1016/j.ijcard.2013.05.068.
[64] R.N. Horodinschi, et al., Treatment with statins in elderly patients, Medicina-Lithuania 55 (2019) e721, https://doi.org/10.3390/medicina55110721.
[65] K.Y. DeLeon-Pennell, et al., Matrix metalloproteinases in myocardial infarction and heart failure progress in molecular biology and, Translational Science 147 (2017) 75–100, https://doi.org/10.1016/bs.pmbts.2017.02.001.
[66] L.L. Herman, et al., Angiotensin converting enzyme inhibitors (ACEI), in: StatPearls, 2021. Treasure Island (FL).
[67] S. Korani, et al., Application of nanotechnology to improve the therapeutic benefits of statins, Drug Discov. Today 24 (2019) 567–574, https://doi.org/10.1016/j.drudis.2018.09.023.
[68] I. Pinal-Fernandez, M. Casal-Dominguez, A.L. Mammen, Statins: pros and cons Med, Clin (Barc) 150 (2018) 398–402, https://doi.org/10.1016/j.medcli.2017.11.030.
[69] V. Kunadian, C.M. Gibson, Thrombolytics and myocardial infarction, Cardiovasc Ther 30 (2012) e81–88, https://doi.org/10.1111/j.1755-5922.2010.00239.x.
[70] M.R. Ali, et al., Aspect of thrombolytic therapy: a review, Sci. World J. 2014 (2014) 1–8, https://doi.org/10.1155/2014/586510.
[71] M. Ahmad, et al., Percutaneous coronary intervention, in: In StatPearls, 2021. Treasure Island (FL).
[72] Y.L. Gu, et al., Role of coronary artery bypass grafting during the acute and subacute phase of ST-elevation myocardial infarction, Neth. Heart J. 18 (2010) 348–354, https://doi.org/10.1007/BF03091790.
[73] B.J. Bachar, B. Manna, Coronary artery bypass graft, in: StatPearls, 2020. Treasure Island (FL).
[74] A. Doost Hosseiny, et al., Mortality pattern and cause of death in a long-term follow-up of patients with STEMI treated with primary PCI Open, Heart 3 (2016) e000405, https://doi.org/10.1136/openhrt-2016-000405.
[75] K. Modi, M.P. Soos, K. Mahajan, Stent Thrombosis, in StatPearls, 2020. Treasure Island (FL.
[76] D. Buccheri, et al., Understanding and managing in-stent restenosis: a review of clinical data, from pathogenesis to treatment, J. Thorac. Dis. 8 (2016) 1150–1162, https://doi.org/10.21037/jtd.2016.10.93.
[77] G.S.D. Silva, et al., Coronary artery bypass graft surgery cost coverage by the Brazilian unified health system (SUS), Braz. J. Cardiovasc. Surg. 32 (2017) 253–259, https://doi.org/10.21470/1678-9741-2016-0069.
[78] A. Mostafa, et al., Atrial fibrillation post cardiac bypass surgery Avicenna, J. Med. 2 (2012) 65–70, https://doi.org/10.4103/2231-0770.102280.
[79] B.C. Gulack, et al., Secondary surgical-site infection after coronary artery bypass grafting: a multi-institutional prospective cohort study, J. Thorac. Cardiovasc. Surg. 155 (2018) 1555–1562 e1, https://doi.org/10.1016/j.jtcvs.2017.10.078.
[80] L. Ryden, et al., Acute kidney injury after coronary artery bypass grafting and long-term risk of end-stage renal disease, Circulation 130 (2014) 2005–2011, https://doi.org/10.1161/CIRCULATIONAHA.114.010622.
[81] A. Velayati, et al., Vitamin D and postoperative delirium after coronary artery bypass grafting: a prospective cohort study, J. Cardiothorac. Vasc. Anesth. 34 (2020) 1774–1779, https://doi.org/10.1053/j.jvca.2020.02.008.
[82] B. Lu, X. Lv, Y. Le, Chitosan-modified PLGA nanoparticles for control-released drug delivery polymers, Basel) 11 (2019) e304, https://doi.org/10.3390/polym11020304.
[83] S.N. dos Santos, et al., Anti-inflammatory/infection PLA nanoparticles labeled with technetium 99m for in vivo imaging, J. Nanoparticle Res. 19 (2017) 1–8, https://doi.org/10.1007/s11051-017-4037-x.
[84] N. Melnychuk, A.S. Klymchenko, DNA-functionalized dye-loaded polymeric nanoparticles: ultrabright FRET platform for amplified detection of, Nucleic Acids Journal of the American Chemical Society 140 (2018) 10856–10865, https://doi.org/10.1021/jacs.8b05840.
[85] A.A. Yetisgin, et al., Therapeutic nanoparticles and their targeted delivery applications, Molecules 25 (2020) e2193, https://doi.org/10.3390/molecules25092193.
[86] Y. Li, T. Thambi, D.S. Lee, Co-delivery of drugs and genes using polymeric nanoparticles for synergistic cancer therapeutic effects advanced, Healthcare Materials 7 (2018) e201700886, https://doi.org/10.1002/adhm.201700886.
[87] Mohammed Nadim, Sardoiwala Babita, K.S. Roy, Chapter 37 - development of engineered nanoparticles expediting diagnostic and therapeutic applications across blood–brain barrier, in: Handbook of Nanomaterials for Industrial Applications, 2018, pp. 696–709.
[88] Y.H. Wang, et al., Multi-responsive hollow nanospheres self-assembly by amphiphilic random copolymer and azobenzene, Polymer 175 (2019) 235–242, https://doi.org/10.1016/j.polymer.2019.04.071.
[89] J.P. Rao, K.E. Geckeler, Polymer nanoparticles: preparation techniques and size-control parameters, Prog. Polym. Sci. 36 (2011) 887–913, https://doi.org/10.1016/j.progpolymsci.2011.01.001.
[90] R.H. Prabhu, V.B. Patravale, M.D. Joshi, Polymeric nanoparticles for targeted treatment in oncology: current insights, Int. J. Nanomed. 10 (2015) 1001–1018, https://doi.org/10.2147/IJN.S56932.
[91] P.A. Lovell, F.J. Schork, Fundamentals of emulsion polymerization, Biomacromolecules 21 (2020) 4396–4441, https://doi.org/10.1021/acs.biomac.0c00769.
[92] Y.Q. Yang, et al., An overview of pickering emulsions: solid-particle materials, classification, morphology, and applications, Front. Pharmacol. 8 (2017) e287, https://doi.org/10.3389/fphar.2017.00287.
[93] N. Sharma, P. Madan, S.S. Lin, Effect of process and formulation variables on the preparation of parenteral paclitaxel-loaded biodegradable polymeric nanoparticles: a co-surfactant study, Asian J. Pharm. Sci. 11 (2016) 404–416, https://doi.org/10.1016/j.ajps.2015.09.004.
[94] Guangfeng Liu, P. Liu, Synthesis of monodispersed crosslinked nanoparticles decorated with surface carboxyl groups via soapless emulsion polymerization, Colloids Surf. A Physicochem. Eng. Asp. 354 (2010) 377–381, https://doi.org/10.1016/j.colsurfa.2009.05.016.
[95] S. Choudhury, S.K. Ray, Synthesis of polymer nanoparticles based highly selective membranes by mini-emulsion polymerization for dehydration of 1,4 dioxane and recovery of ethanol from water by pervaporation, J. Membr. Sci. 617 (2021) e118646, https://doi.org/10.1016/j.memsci.2020.118646.
[96] Satyajeet Sahoo, et al., Preparation of polymeric nanomaterials using emulsion polymerization, Adv. Mater. Sci. Eng. 2021 (2021) e1539230, https://doi.org/10.1155/2021/1539230.

[97] G.P.S. Ibrahim, et al., Integration of zwitterionic polymer nanoparticles in interfacial polymerization for ion separation, Appl. Polym. Mater. 2 (2020) 1508–1517, https://doi.org/10.1021/acsapm.9b01192.
[98] K. Parkatzidis, et al., Recent developments and future challenges in controlled radical polymerization: a 2020 update, Inside Chem. 6 (2020) 1575–1588, https://doi.org/10.1016/j.chempr.2020.06.014.
[99] C.I.C. Crucho, M.T. Barros, Polymeric nanoparticles: a study on the preparation variables and characterization methods, Mater. Sci. Eng. Mater. Biol. Appl. 80 (2017) 771–784, https://doi.org/10.1016/j.msec.2017.06.004.
[100] S. Salatin, et al., Development of a nanoprecipitation method for the entrapment of a very water soluble drug into Eudragit RL nanoparticles, Res. Pharm. Sci. 12 (2017) 1–14, https://doi.org/10.4103/1735-5362.199041.
[101] C.E. Mora-Huertas, H. Fessi, A. Elaissari, Polymer-based nanocapsules for drug delivery, Int. J. Pharm. (Amst.) 385 (2010) 113–142, https://doi.org/10.1016/j.ijpharm.2009.10.018.
[102] M. Kostog, et al., Pure cellulose nanoparticles from trimethylsilyl cellulose, Macromol. Symp. 294 (2010) 96–106, https://doi.org/10.1002/masy.200900095.
[103] P. Alzate, L. Gerschenson, S. Flores, Micro/nanoparticles containing potassium sorbate obtained by the dialysis technique: effect of starch concentration and starch ester type on the particle properties, Food Hydrocolloids 95 (2019) 540–550, https://doi.org/10.1016/j.foodhyd.2019.04.066.
[104] Paroma Chakravarty, et al., Using supercritical fluid technology as a green alternative during the preparation of drug delivery systems, Pharmaceutics 11 (2019) e629, https://doi.org/10.3390/pharmaceutics11120629.
[105] M.C. Paisana, et al., Production and stabilization of olanzapine nanoparticles by rapid expansion of supercritical solutions (RESS), J. Supercrit. Fluids 109 (2016) 124–133, https://doi.org/10.1016/j.supflu.2015.11.012.
[106] F. Razmimanesh, G. Sodeifian, S.A. Sajadian, An investigation into Sunitinib malate nanoparticle production by US- RESOLV method: effect of type of polymer on dissolution rate and particle size distribution, J. Supercrit. Fluids 170 (2021) e105163, https://doi.org/10.1016/j.supflu.2021.105163.
[107] Mary M. Nguyen, Nathan C. Gianneschi, K.L. Christman, Developing injectable nanomaterials to repair the heart, Curr. Opin. Biotechnol. 34 (2015) 225–231, https://doi.org/10.1016/j.copbio.2015.03.016.
[108] D.J. Lundy, et al., Distribution of systemically administered nanoparticles reveals a size-dependent effect immediately following cardiac ischaemia-reperfusion injury, Sci. Rep. 6 (2016) 25613, https://doi.org/10.1038/srep25613.
[109] K.-H. Chen, et al., Nanoparticle distribution during systemic inflammation is size-dependent and organ-specific, Nanoscale 7 (2015) 15863–15872, https://doi.org/10.1039/C5NR03626G.
[110] T. dos Santos, et al., Quantitative assessment of the comparative nanoparticle-uptake efficiency of a range of cell lines, Small 7 (2011) 3341–3349, https://doi.org/10.1002/smll.201101076.
[111] T. Avsievich, et al., Mutual interaction of red blood cells influenced by nanoparticles, Sci. Rep. 9 (2019) 5147–5153, https://doi.org/10.1038/s41598-019-41643-x.
[112] V.P. Vu, et al., Immunoglobulin deposition on biomolecule corona determines complement opsonization efficiency of preclinical and clinical nanoparticles, Nat. Nanotechnol. 14 (2019) 260–268, https://doi.org/10.1038/s41565-018-0344-3.
[113] J.M. de Lima, et al., Evaluation of hemagglutination activity of chitosan nanoparticles using human erythrocytes, Biomed. Res. Int. (2015) e247965, https://doi.org/10.1155/2015/247965.
[114] T.L. Hwang, et al., Cationic additives in nanosystems activate cytotoxicity and inflammatory response of human neutrophils: lipid nanoparticles versus polymeric nanoparticles, Int. J. Nanomed. 10 (2015) 371–385, https://doi.org/10.2147/IJN.S73017.
[115] Y.W. Yang, W.H. Luo, Cellular biodistribution of polymeric nanoparticles in the immune system, J. Contr. Release 227 (2016) 82–93, https://doi.org/10.1016/j.jconrel.2016.02.011.
[116] D. Chenthamara, et al., Therapeutic efficacy of nanoparticles and routes of administration, Biomater. Res. 23 (2019) e166, https://doi.org/10.1186/s40824-019-0166-x.
[117] M. Adabi, et al., Biocompatibility and nanostructured materials: applications in nanomedicine, Artif. Cell Nanomed. Biotechnol. 45 (2017) 833–842, https://doi.org/10.1080/21691401.2016.1178134.
[118] H. Xu, et al., Lyophilization of self-assembled polymeric nanoparticles without compromising their microstructure and their in vivo evaluation: pharmacokinetics, tissue distribution and toxicity, J. Biomater. Tissue Eng. 5 (2015) 919–929, https://doi.org/10.1166/jbt.2015.1405.
[119] S. Xiong, et al., Size influences the cytotoxicity of poly (lactic-co-glycolic acid) (PLGA) and titanium dioxide (TiO(2)) nanoparticles, Arch. Toxicol. 87 (2013) 1075–1086, https://doi.org/10.1007/s00204-012-0938-8.
[120] B. Zhang, et al., Shape dependent cytotoxicity of PLGA-PEG nanoparticles on human cells, Sci. Rep. 7 (2017) 7315, https://doi.org/10.1038/s41598-017-07588-9.
[121] G. Romero, et al., Surface engineered Poly(lactide-co-glycolide) nanoparticles for intracellular delivery: uptake and cytotoxicity–a confocal Raman microscopic study, Biomacromolecules 11 (2010) 2993–2999, https://doi.org/10.1021/bm1007822.
[122] J.J. Rennick, A.P.R. Johnston, R.G. Parton, Key principles and methods for studying the endocytosis of biological and nanoparticle therapeutics, Nat. Nanotechnol. 16 (2021) 266–276, https://doi.org/10.1038/s41565-021-00858-8.
[123] Parisa Foroozandeh, A.A. Aziz, Insight into cellular uptake and intracellular trafficking of nanoparticles, Nanoscale Res. Lett. 13 (2018) 2728–2736, https://doi.org/10.1186/s11671-018-2728-6.
[124] A. Gallud, et al., Cationic gold nanoparticles elicit mitochondrial dysfunction: a multi-omics study, Sci. Rep. 9 (2019) 4366, https://doi.org/10.1038/s41598-019-40579-6.
[125] H. Eidi, et al., Drug delivery by polymeric nanoparticles induces autophagy in macrophages, Int. J. Pharm. 422 (2012) 495–503, https://doi.org/10.1016/j.ijpharm.2011.11.020.
[126] M.E. Grady, et al., Intracellular nanoparticle dynamics affected by cytoskeletal integrity, Soft Matter 13 (2017) 1873–1880, https://doi.org/10.1039/c6sm02464e.
[127] S. Barua, S. Mitragotri, Challenges associated with penetration of nanoparticles across cell and tissue barriers: a review of current status and future prospects, Nano Today 9 (2014) 223–243, https://doi.org/10.1016/j.nantod.2014.04.008.
[128] Li-Juan Feng, Short-term exposure to positively charged polystyrene nanoparticles causes oxidative stress and membrane destruction in cyanobacteria Environmental Science, Nano 6 (2019) 3072–3079, https://doi.org/10.1039/C9EN00807A.
[129] A. Beyerle, et al., Toxicity pathway focused gene expression profiling of PEI-based polymers for pulmonary applications, Mol. Pharm. 7 (2010) 727–737, https://doi.org/10.1021/mp900278x.
[130] L. Wang, C. Hu, L. Shao, The antimicrobial activity of nanoparticles: present situation and prospects for the future, Int. J. Nanomed. 12 (2017) 1227–1249, https://doi.org/10.2147/IJN.S121956.
[131] X. Gong, et al., High sensitive and multiple detection of acute myocardial infarction biomarkers based on a dual-readout immunochromatography test strip, Nanomedicine 14 (2018) 1257–1266, https://doi.org/10.1016/j.nano.2018.02.013.
[132] Juthi Adhikari, et al., An ultra-sensitive label-free electrochemiluminescence CKMB immunosensor using a novel nanocomposite-modified printed electrode, RSC Adv. 9 (2019) 34283–34292, https://doi.org/10.1039/C9RA05016G.
[133] Y.W. Wu, et al., Clinical feasibility of biofunctionalized magnetic nanoparticles for detecting multiple cardiac biomarkers in emergency chest pain patients, Acta Cardiol. Sin. 36 (2020) 649–659, https://doi.org/10.6515/ACS.202011_36(6).20200414A.
[134] S. Lahtinen, et al., Improving the sensitivity of immunoassays by reducing non-specific binding of poly(acrylic acid) coated upconverting nanoparticles by adding free poly(acrylic acid), Mikrochim. Acta 185 (2018) 220, https://doi.org/10.1007/s00604-018-2756-z.
[135] H. Korkusuz, et al., Transferrin-coated gadolinium nanoparticles as MRI contrast agent, Mol. Imag. Biol. 15 (2013) 148–154, https://doi.org/10.1007/s11307-012-0579-6.
[136] F. Wang, et al., Albumin nanocomposites with MnO2/Gd2O3 motifs for precise MR imaging of acute myocardial infarction in rabbit models, Biomaterials 230 (2020) 119614, https://doi.org/10.1016/j.biomaterials.2019.119614.
[137] Pavel Broz, et al., Nano Imaging Technologies: polymer vesicles loaded with precipitated gadolinium nanoparticles: a novel target-specific contrast agent for magnetic resonance imaging, Eur. J. Nanomed. 2 (2009), https://doi.org/10.1515/EJNM.2009.2.2.43.
[138] G.S. Heo, et al., Molecular imaging visualizes recruitment of inflammatory monocytes and macrophages to the injured heart, Circ. Res. 124 (2019) 881–890, https://doi.org/10.1161/CIRCRESAHA.118.314030.
[139] F. Hyafil, et al., Noninvasive detection of macrophages using a nanoparticulate contrast agent for computed tomography, Nat. Med. 13 (2007) 636–641, https://doi.org/10.1038/nm1571.
[140] D. Pan, et al., Detecting vascular biosignatures with a colloidal, Radio-Opaque Polymeric Nanoparticle Journal of the American Chemical Society 131 (2009) 15522–15527, https://doi.org/10.1021/ja906797z.
[141] Y.J. Fu, et al., Dendritic iodinated contrast agents with PEG-cores for CT imaging: synthesis and preliminary characterization, Bioconjugate Chem. 17 (2006) 1043–1056, https://doi.org/10.1021/bc060019c.
[142] S. Sawall, et al., In vivo quantification of myocardial infarction in mice using micro-CT and a novel blood pool agent, Contrast Media Mol. Imaging (2017) e2617047, https://doi.org/10.1155/2017/2617047.
[143] E.J. Keliher, et al., 89Zr-labeled dextran nanoparticles allow in vivo macrophage imaging, Bioconjugate Chem. 22 (2011) 2383–2389, https://doi.org/10.1021/bc200405d.
[144] M. Fairclough, et al., A new technique for the radiolabelling of mixed leukocytes with zirconium-89 for inflammation imaging with positron emission tomography, J. Label. Compd. Radiopharm. 59 (2016) 270–276, https://doi.org/10.1002/jlcr.3392.
[145] P.K. Woodard, et al., Design and modular construction of a polymeric nanoparticle for targeted atherosclerosis positron emission tomography imaging: a story of 25% (64)Cu-CANF-Comb, Pharm. Res. (N. Y.) 33 (2016) 2400–2410, https://doi.org/10.1007/s11095-016-1963-8.
[146] Y. Liu, et al., Targeting angiogenesis using a C-type atrial natriuretic factor-conjugated nanoprobe and PET, J. Nucl. Med. 52 (2011) 1956–1963, https://doi.org/10.2967/jnumed.111.089581.
[147] A. Almutairi, et al., Biodegradable dendritic positron-emitting nanoprobes for the noninvasive imaging of angiogenesis, Proc. Natl. Acad. Sci. U. S. A. 106 (2009) 685–690, https://doi.org/10.1073/pnas.0811757106.
[148] Edmund J. Keliher, et al., Polyglucose nanoparticles with renal elimination and macrophage avidity facilitate PET imaging in ischaemic heart disease, Nat. Commun. 8 (2017) e14064, https://doi.org/10.1038/ncomms14064.
[149] N.C. Ni, et al., Non-invasive macrophage tracking using novel porphysome nanoparticles in the post-myocardial infarction murine heart, Mol. Imag. Biol. 18 (2016) 557–568, https://doi.org/10.1007/s11307-015-0922-9.
[150] Leon Shargel, A.B.C. Yu, Applied Biopharmaceutics & Pharmacokinetics, sixth ed., 2012.

[151] Flavio Dormont, Mariana Varna, P. Couvreur, Nanoplumbers: biomaterials to fight cardiovascular diseases Materials, Today Off. 21 (2018) 122–143, https://doi.org/10.1016/j.mattod.2017.07.008.
[152] L. Saludas, et al., Heart tissue repair and cardioprotection using drug delivery systems, Maturitas 110 (2018) 1–9, https://doi.org/10.1016/j.maturitas.2018.01.011.
[153] R.P. Prajnamitra, et al., Nanotechnology Approaches in Tackling Cardiovascular Diseases Molecules 24 (2019) e24102017, https://doi.org/10.3390/molecules24102017.
[154] S. Khodayari, et al., Inflammatory microenvironment of acute myocardial infarction prevents regeneration of heart with stem cells therapy, Cell. Physiol. Biochem. 53 (2019) 887–909, https://doi.org/10.33594/000000180.
[155] F. Bagheri, et al., Reactive oxygen species-mediated cardiac-reperfusion injury: mechanisms and therapies Life, Sci 165 (2016) 43–55, https://doi.org/10.1016/j.lfs.2016.09.013.
[156] M. Faghihi, et al., The role of nitric oxide, reactive oxygen species, and protein kinase C in oxytocin-induced cardioprotection in ischemic rat heart, Peptides 37 (2012) 314–319, https://doi.org/10.1016/j.peptides.2012.08.001.
[157] C.J. Cheng, et al., A holistic approach to targeting disease with polymeric nanoparticles, Nat. Rev. Drug Discov. 14 (2015) 239–247, https://doi.org/10.1038/nrd4503.
[158] M.Y. Chang, et al., Functionalized nanoparticles provide early cardioprotection after acute myocardial infarction, J. Contr. Release 170 (2013) 287–294, https://doi.org/10.1016/j.jconrel.2013.04.022.
[159] J. Rodness, et al., VEGF-loaded microsphere patch for local protein delivery to the ischemic heart, Acta Biomater. 45 (2016) 169–181, https://doi.org/10.1016/j.actbio.2016.09.009.
[160] Y. Oduk, et al., VEGF nanoparticles repair the heart after myocardial infarction, Am. J. Physiol. Heart Circ. Physiol. 314 (2018) H278–H284, https://doi.org/10.1152/ajpheart.00471.2017.
[161] H.C. Quadros, et al., Development and in vitro characterization of polymeric nanoparticles containing recombinant adrenomedullin-2 intended for therapeutic angiogenesis, Int. J. Pharm. 576 (2020) 118997, https://doi.org/10.1016/j.ijpharm.2019.118997.
[162] K. Ichimura, et al., A translational study of a new therapeutic approach for acute myocardial infarction: nanoparticle-mediated delivery of pitavastatin into reperfused myocardium reduces ischemia-reperfusion injury in a preclinical porcine model, PLoS One 11 (2016) e0162425, https://doi.org/10.1371/journal.pone.0162425.
[163] K. Nagaoka, et al., A new therapeutic modality for acute myocardial infarction: nanoparticle-mediated delivery of pitavastatin induces cardioprotection from ischemia-reperfusion injury via activation of PI3K/Akt pathway and anti-inflammation in a rat, Model PLoS One 10 (2015) e0132451, https://doi.org/10.1371/journal.pone.0132451.
[164] X. Xue, et al., Delivery of microRNA-1 inhibitor by dendrimer-based nanovector: an early targeting therapy for myocardial infarction in mice, Nanomedicine 14 (2018) 619–631, https://doi.org/10.1016/j.nano.2017.12.004.
[165] J.T. Magruder, et al., Selective localization of a novel dendrimer nanoparticle in myocardial ischemia-reperfusion injury, Ann. Thorac. Surg. 104 (2017) 891–898, https://doi.org/10.1016/j.athoracsur.2016.12.051.
[166] G. Seshadri, et al., The delivery of superoxide dismutase encapsulated in polyketal microparticles to rat myocardium and protection from myocardial ischemia-reperfusion injury, Biomaterials 31 (2010) 1372–1379, https://doi.org/10.1016/j.biomaterials.2009.10.045.
[167] J.M. Li, et al., Local arterial nanoparticle delivery of siRNA for NOX2 knockdown to prevent restenosis in an atherosclerotic rat model, Gene Ther. 17 (2010) 1279–1287, https://doi.org/10.1038/gt.2010.69.
[168] Z.M. Binsalamah, et al., Intramyocardial sustained delivery of placental growth factor using nanoparticles as a vehicle for delivery in the rat infarct model, Int. J. Nanomed. 6 (2011) 2667–2678, https://doi.org/10.2147/IJN.S25175.
[169] J. Liu, et al., Functionalized dendrimer-based delivery of angiotensin type 1 receptor siRNA for preserving cardiac function following infarction, Biomaterials 34 (2013) 3729–3736, https://doi.org/10.1016/j.biomaterials.2013.02.008.
[170] T. Bejerano, et al., Nanoparticle delivery of miRNA-21 mimic to cardiac macrophages improves myocardial remodeling after myocardial infarction, Nano Lett. 18 (2018) 5885–5891, https://doi.org/10.1021/acs.nanolett.8b02578.
[171] D. Kim, et al., Anti-apoptotic cardioprotective effects of SHP-1 gene silencing against ischemia-reperfusion injury: use of deoxycholic acid-modified low molecular weight polyethyleneimine as a cardiac siRNA-carrier, J. Contr. Release 168 (2013) 125–134, https://doi.org/10.1016/j.jconrel.2013.02.031.
[172] N. Hardy, et al., Nanoparticle-mediated dual delivery of an antioxidant and a peptide against the L-Type Ca2+ channel enables simultaneous reduction of cardiac ischemia-reperfusion injury, ACS Nano 9 (2015) 279–289, https://doi.org/10.1021/nn5061404.
[173] M. Alsaggar, D. Liu, Organ-based drug delivery, J. Drug Target. 26 (2018) 385–397, https://doi.org/10.1080/1061186X.2018.1437919.
[174] R. Yang, et al., Getting drugs across biological barriers, Adv. Mater. 29 (2017) e6596, https://doi.org/10.1002/adma.201606596.
[175] V. Kumar Khanna, Targeted delivery of nanomedicines, ISRN Pharmacol 2012 (2012) 571394, https://doi.org/10.5402/2012/571394.
[176] M.F. Attia, et al., An overview of active and passive targeting strategies to improve the nanocarriers efficiency to tumour sites, J. Pharm. Pharmacol. 71 (2019) 1185–1198, https://doi.org/10.1111/jphp.13098.
[177] S.T. Jahan, et al., Targeted therapeutic nanoparticles: an immense promise to fight against cancer, J Drug Deliv 2017 (2017) 9090325, https://doi.org/10.1155/2017/9090325.
[178] Z. Huang, et al., Targeted delivery of thymosin beta 4 to the injured myocardium using CREKA-conjugated nanoparticles, Int. J. Nanomed. 12 (2017) 3023–3036, https://doi.org/10.2147/IJN.S131949.
[179] Z. Huang, et al., Fibrin-targeting delivery: a novel platform for cardiac regenerative medicine, J. Cell Mol. Med. 20 (2016) 2410–2413, https://doi.org/10.1111/jcmm.12912.
[180] B. Zhang, et al., Fibrin-targeting peptide CREKA-conjugated multi-walled carbon nanotubes for self-amplified photothermal therapy of tumor, Biomaterials 79 (2016) 46–55, https://doi.org/10.1016/j.biomaterials.2015.11.061.
[181] Wael Sumaya, et al., Fibrin clot properties independently predict adverse clinical outcome following acute coronary European Heart, Journal 39 (2018) 1078–1085, https://doi.org/10.1093/eurheartj/ehy013.
[182] M.P. Ferreira, et al., In vitro and in vivo assessment of heart-homing porous silicon nanoparticles, Biomaterials 94 (2016) 93–104, https://doi.org/10.1016/j.biomaterials.2016.03.046.
[183] L.M. Bimbo, et al., Biocompatibility of thermally hydrocarbonized porous silicon nanoparticles and their biodistribution in rats, ACS Nano 4 (2010) 3023–3032, https://doi.org/10.1021/nn901657w.
[184] M.P.A. Ferreira, et al., Drug-loaded multifunctional nanoparticles targeted to the endocardial Layer of the injured heart modulate hypertrophic signaling, Small 13 (2017) e1276, https://doi.org/10.1002/smll.201701276.
[185] W.L.A. Brooks, et al., Triple responsive block copolymers combining pH-responsive, thermoresponsive, and glucose-responsive behaviors, J. Polym. Sci. Polym. Chem. 55 (2017) 2309–2317, https://doi.org/10.1002/pola.28615.
[186] S. Mura, J. Nicolas, P. Couvreur, Stimuli-responsive nanocarriers for drug delivery, Nat. Mater. 12 (2013) 991–1003, https://doi.org/10.1038/nmat3776.
[187] A. Sirker, et al., Cell-specific effects of Nox2 on the acute and chronic response to myocardial infarction, J. Mol. Cell. Cardiol. 98 (2016) 11–17, https://doi.org/10.1016/j.yjmcc.2016.07.003.
[188] I. Somasuntharam, et al., Delivery of Nox2-NADPH oxidase siRNA with polyketal nanoparticles for improving cardiac function following myocardial infarction, Biomaterials 34 (2013) 7790–7798, https://doi.org/10.1016/j.biomaterials.2013.06.051.
[189] M.M. Nguyen, et al., Enzyme-responsive nanoparticles for targeted accumulation and prolonged retention in heart tissue after myocardial infarction, Adv. Mater. 27 (2015) 5547–5552, https://doi.org/10.1002/adma.201502003.
[190] W.D. Gray, et al., N-acetylglucosamine conjugated to nanoparticles enhances myocyte uptake and improves delivery of a small molecule p38 inhibitor for post-infarct healing, J Cardiovasc Transl Res 4 (2011) 631–643, https://doi.org/10.1007/s12265-011-9292-0.
[191] H.Y. Nam, et al., Primary cardiomyocyte-targeted bioreducible polymer for efficient gene delivery to the myocardium, Biomaterials 31 (2010) 8081–8087, https://doi.org/10.1016/j.biomaterials.2010.07.025.
[192] D. Lee, et al., H2O2-responsive molecularly engineered polymer nanoparticles as ischemia/reperfusion-targeted nanotherapeutic agents, Sci. Rep. 3 (2013) 2233, https://doi.org/10.1038/srep02233.
[193] K.A. Krishna, et al., Myocardial infarction and stem cells, J. Pharm. BioAllied Sci. 3 (2011) 182–188, https://doi.org/10.4103/0975-7406.80761.
[194] R. Yokoyama, et al., Cardiac regeneration by statin-polymer nanoparticle-loaded adipose-derived stem cell therapy in myocardial infarction, Stem Cells Transl Med 8 (2019) 1055–1067, https://doi.org/10.1002/sctm.18-0244.
[195] K.S. Oh, et al., Temperature-induced gel formation of core/shell nanoparticles for the regeneration of ischemic heart, J. Contr. Release 146 (2010) 207–211, https://doi.org/10.1016/j.jconrel.2010.04.014.
[196] Mónica P.A. Ferreira, et al., Dual-drug delivery using dextran-functionalized nanoparticles targeting cardiac fibroblasts for cellular reprogramming advanced, Funct. Mater. 28 (2018) e1705134, https://doi.org/10.1002/adfm.201705134.
[197] Hye Jin Kim, et al., Direct conversion of human dermal fibroblasts into cardiomyocyte-like cells using CiCMC nanogels coupled with cardiac transcription factors and a nucleoside drug, Adv. Sci. (2020) e1901818, https://doi.org/10.1002/advs.201901818.
[198] X. Yao, et al., Nitric oxide releasing hydrogel enhances the therapeutic efficacy of mesenchymal stem cells for myocardial infarction, Biomaterials 60 (2015) 130–140, https://doi.org/10.1016/j.biomaterials.2015.04.046.
[199] R. Waters, et al., Stem cell secretome-rich nanoclay hydrogel: a dual action therapy for cardiovascular regeneration, Nanoscale 8 (2016) 7371–7376, https://doi.org/10.1039/c5nr07806g.
[200] Audrey E. Mayfield, et al., The effect of encapsulation of cardiac stem cells within matrixenriched hydrogel capsules on cell survival, post-ischemic cell retention and cardiac function, Biomaterials 35 (2013) 133–142, https://doi.org/10.1016/j.biomaterials.2013.09.085.
[201] Milad Fathi-Achachelouei, et al., Use of nanoparticles in tissue engineering and regenerative medicine, Front. Bioeng. Biotechnol. 7 (2019) e113, https://doi.org/10.3389/fbioe.2019.00113.

[202] Q. Tan, et al., Controlled release of chitosan/heparin nanoparticle-delivered VEGF enhances regeneration of decellularized tissue-engineered scaffolds, Int. J. Nanomed. 6 (2011) 929–942, https://doi.org/10.2147/IJN.S18753.
[203] M. Izadifar, M.E. Kelly, X. Chen, Regulation of sequential release of growth factors using bilayer polymeric nanoparticles for cardiac tissue engineering, Nanomedicine 11 (2016) 3237–3259, https://doi.org/10.2217/nnm-2016-0220.
[204] W. Wang, et al., Rebuilding postinfarcted cardiac functions by injecting TIIA@PDA nanoparticle-cross-linked ROS-sensitive hydrogels, ACS Appl. Mater. Interfaces 11 (2019) 2880–2890, https://doi.org/10.1021/acsami.8b20158.
[205] H. Yang, et al., An in vivo miRNA delivery system for restoring infarcted myocardium, ACS Nano 13 (2019) 9880–9894, https://doi.org/10.1021/acsnano.9b03343.
[206] Y. He, et al., Mussel-inspired conductive nanofibrous membranes repair myocardial infarction by enhancing cardiac function and revascularization, Theranostics 8 (2018) 5159–5177, https://doi.org/10.7150/thno.27760.
[207] Leyu Wang, et al., Mussel-inspired conductive cryogel as cardiac tissue patch to repair myocardial infarction by migration of conductive nanoparticles advanced, Funct. Mater. 26 (2016) 4293–4305, https://doi.org/10.1002/adfm.201505372.
[208] S. Indoria, V. Singh, M.F. Hsieh, Recent advances in theranostic polymeric nanoparticles for cancer treatment: a review, Int. J. Pharm. 582 (2020) 119314, https://doi.org/10.1016/j.ijpharm.2020.119314.
[209] Remedios Guadalupe Gomez-Mauricio, et al., A preliminary approach to the repair of myocardial infarction using adipose tissue-derived stem cells encapsulated in magnetic resonance-labeled alginate microspheres in a porcine model, Eur. J. Pharm. Biopharm. 84 (2013) 29–39, https://doi.org/10.1016/j.ejpb.2012.11.028.
[210] X. Qin, et al., Photoacoustic imaging of embryonic stem cell-derived cardiomyocytes in living hearts with ultrasensitive semiconducting polymer nanoparticles, Adv. Funct. Mater. 28 (2018) e1704939, https://doi.org/10.1002/adfm.201704939.
[211] Changsun Kang, et al., Fibrin-targeted and H2O2-responsive nanoparticles as a theranostics for thrombosed vessels, ACS Nano 11 (2017) 6194–6203, https://doi.org/10.1021/acsnano.7b02308.
[212] H. Hwang, et al., Peptide-loaded nanoparticles and radionuclide imaging for individualized treatment of myocardial ischemia, Radiology 273 (2014) 160–167, https://doi.org/10.1148/radiol.14132942.
[213] Kathrin Müller, Dmitry A. Fedosov, G. Gompper, Margination of micro- and nano-particle in blood flow and its effect on drug delivery, Sci. Rep. 4 (2014) e4871, https://doi.org/10.1038/srep04871.
[214] M. Forouzandehmehr, A. Shamloo, Margination and adhesion of micro- and nanoparticles in the coronary circulation: a step towards optimised drug carrier design, Biomech. Model. Mechanobiol. 17 (2018) 205–221, https://doi.org/10.1007/s10237-017-0955-x.
[215] W.B. Wince, P. Suranyi, U.J. Schoepf, Contemporary cardiovascular imaging methods for the assessment of at-risk, Myocardium J. Am. Heart Assoc. 3 (2014) e000473, https://doi.org/10.1161/JAHA.113.000473.
[216] S. Doppalapudi, et al., Biodegradable polymers for targeted delivery of anti-cancer drugs, Expet Opin. Drug Deliv. 13 (2016) 891–909, https://doi.org/10.1517/17425247.2016.1156671.
[217] Oladeji O. Ige, Lasisi E. Umoru, S. Aribo, Natural products: a minefield of biomaterials, ISRN Mater. Sci. (2012) e983062, https://doi.org/10.5402/2012/983062.
[218] J.J. Green, J.H. Elisseeff, Mimicking biological functionality with polymers for biomedical applications, Nature 540 (2016) 386–394, https://doi.org/10.1038/nature21005.
[219] W. Malaeb, et al., The sulfation of biomimetic glycosaminoglycan substrates controls binding of growth factors and subsequent neural and glial cell growth, Biomater Sci 7 (2019) 4283–4298, https://doi.org/10.1039/c9bm00964g.
[220] R.L. Wu, et al., Hyaluronic acid-CD44 interactions promote BMP4/7-dependent Id1/3 expression in melanoma cells, Sci. Rep. 8 (2018) 14913, https://doi.org/10.1038/s41598-018-33337-7.
[221] B. Noriega-Luna, et al., Applications of dendrimers in drug delivery agents, diagnosis, therapy, and detection, J. Nanomater. (2014) e507273, https://doi.org/10.1155/2014/507273.
[222] Mohd Athar, A.J. Das, Therapeutic nanoparticles: state-of-The-Art of nanomedicine, Advanced Materials Reviews 1 (2014) 25–37, https://doi.org/10.5185/amr.2014.1005.
[223] M. Kamimura, et al., Design of poly(ethylene glycol)/streptavidin coimmobilized upconversion nanophosphors and their application to fluorescence biolabeling, Langmuir 24 (2008) 8864–8870, https://doi.org/10.1021/la801056c.
[224] I.M. Pongrac, et al., Improved biocompatibility and efficient labeling of neural stem cells with poly(L-lysine)-coated maghemite nanoparticles, Beilstein J. Nanotechnol. 7 (2016) 926–936, https://doi.org/10.3762/bjnano.7.84.
[225] J. Hu, et al., A biodegradable polyethylenimine-based Vector modified by trifunctional peptide R18 for enhancing gene transfection efficiency in vivo, PLoS One 11 (2016) e0166673, https://doi.org/10.1371/journal.pone.0166673.
[226] R. Balint, N.J. Cassidy, S.H. Cartmell, Conductive polymers: towards a smart biomaterial for tissue engineering, Acta Biomater. 10 (2014) 2341–2353, https://doi.org/10.1016/j.actbio.2014.02.015.
[227] E. Song, J.W. Choi, Conducting polyaniline nanowire and its applications in chemiresistive sensing, Nanomaterials 3 (2013) 498–523, https://doi.org/10.3390/nano3030498.
[228] Yong Du, et al., Research progress on polymer–inorganic thermoelectric nanocomposite materials, Prog. Polym. Sci. 37 (2012) 820–841, https://doi.org/10.1016/j.progpolymsci.2011.11.003.
[229] H. Ragelle, et al., Nanoparticle-based drug delivery systems: a commercial and regulatory outlook as the field matures, Expet Opin. Drug Deliv. 14 (2017) 851–864, https://doi.org/10.1080/17425247.2016.1244187.
[230] F. Lebre, et al., The shape and size of hydroxyapatite particles dictate inflammatory responses following implantation, Sci. Rep. 7 (2017) 2922, https://doi.org/10.1038/s41598-017-03086-0.
[231] W.J. Sandberg, et al., Comparison of non-crystalline silica nanoparticles in IL-1beta release from macrophages Part Fibre, Toxicol 9 (2012) 32, https://doi.org/10.1186/1743-8977-9-32.
[232] R.P. Singh, P. Ramarao, Accumulated polymer degradation products as effector molecules in cytotoxicity of polymeric nanoparticles, Toxicol. Sci. 136 (2013) 131–143, https://doi.org/10.1093/toxsci/kft179.
[233] W. Lu, et al., Effect of surface coating on the toxicity of silver nanomaterials on human skin keratinocytes, Chem. Phys. Lett. 487 (2010) e27, https://doi.org/10.1016/j.cplett.2010.01.027.
[234] P.K. Woodard, et al., Design and modular construction of a polymeric nanoparticle for targeted atherosclerosis positron emission tomography imaging: a story of 25% (64)Cu-CANF-Comb, Pharm. Res. (N. Y.) 33 (2016) 2400–2410, https://doi.org/10.1007/s11095-016-1963-8.